Intrinsic Mechanisms Regulating T Cell Tolerance in Autoimmune Diabetes

by

Qianxia Zhang

B.Sc. Biological Science, Nankai University, 2012

Submitted to the Graduate Faculty of

The School of Medicine in partial fulfillment

of the requirements for the degree of

Doctor of Philosophy

University of Pittsburgh

2018

UNIVERSITY OF PITTSBURGH

SCHOOL OF MEDICINE

This dissertation was presented

by

Qianxia Zhang

It was defended on

January 11, 2018

and approved by

Sarah L. Gaffen, PhD, Gerald P. Rodnan Professor, Department of Medicine

Lawrence P. Kane, PhD, Professor, Department of Immunology

Peter C. Lucas, MD, PhD, Associate Professor, Department of Pathology

Jon D. Piganelli, PhD, Associate Professor, Department of Surgery

Mark J. Shlomchik, MD, PhD, UPMC Endowed Professor, Department of Immunology

Dissertation Advisor: **Dario AA. Vignali, PhD**, The Frank Dixon Chair in Cancer Immunology, Professor, Department of Immunology

Intrinsic Mechanisms Regulating T Cell Tolerance in Autoimmune Diabetes

Qianxia Zhang, PhD

University of Pittsburgh, 2018

Type 1 Diabetes (T1D) is a polygenic autoimmune disease characterized by immune cell infiltration into the islets of Langerhans, destruction of insulin-producing β cells, and uncontrolled hyperglycemia. Islet-antigen reactive $CD4^+$ and $CD8^+$ T cells, and regulatory T cells (Tregs) are the major players in T1D pathogenesis. Both cell-intrinsic and cell-extrinsic inhibitory mechanisms are required to maintain self-tolerance to islet-antigens.

Lymphocyte Activation Gene 3 (LAG3, CD223), a co-inhibitory receptor highly expressed on T cells, is one of these essential mechanisms that intrinsically regulate T cell tolerance in autoimmune diabetes. I evaluate the role of LAG3 on T cells versus non-T cells, $CD8^+$ T cells, and Tregs by generating mice in which LAG3 is specifically absent on these subsets in a murine model of T1D. In **Chapter 3**, I show that the predominant expression of LAG3 on insulitic $CD4^+$ and $CD8^+$ T cells is required to limit the pathogenesis of autoimmune diabetes in non-obese diabetic (NOD) mice. The loss of LAG3 on $CD8^+$ T cells alone is sufficient to promote early onset of autoimmune diabetes by promoting islet-specific glucose-6-phophatase catalytic subunit-related protein (IGRP)-reactive $CD8^+$ T cells to differentiate into effector T cells. In **Chapter 4**, I show that LAG3 is preferentially and constitutively expressed on a subset of insulitic Tregs, and loss of LAG3 on Tregs leads to delayed onset and reduced incidence of autoimmune diabetes. LAG3 may intrinsically limit Treg proliferation and functionality by repressing pathways that promote the maintenance of Tregs in the pancreas of NOD mice.

In addition to dissecting the role of LAG3 in regulating T cell tolerance, I also show that removal of programmed death protein 1 (PD1) or overexpression of Neuropilin 1 (Nrp1) on Tregs protect NOD mice from autoimmune diabetes in **Appendix A** and **Appendix B**, respectively. In summary, my findings have advanced our understanding of cell-intrinsic mechanisms that regulate T cell tolerance in autoimmune diabetes.

Table of Contents

Acknowledgement

The path to this PhD has been a wonderful experience, and I am deeply grateful to my family, mentor, friends, and colleagues for their immense support throughout this journey.

First and foremost, I would like to thank my thesis advisor, Dr. Dario Vignali. Dario's mentorship has been tremendously critical in the past five and a half years. His focus for well-crafted science, his creativity and openness to new ideas, and his scientific ethics have inspired me throughout my graduate study and will continue to inspire me in my future career. I am tremendously thankful for his guidance in constructing the whole body of my thesis, for his carefulness in technical details and data quality, and also for his trust and patience in every step of my research, my performance, and my capacity to tackle a problem. It has been an honor to be his student.

I want to thank Drs. Andrea Workman and Creg Workman. Andrea made the mutant mice that my entire thesis is dependent on, and Creg initiated all the LAG3 related projects in this lab. I also want to thank Dr. Maria Chikina and Dr. Sasikanth Manne, both of who have helped me enormously in bioinformatics analyses. I am thankful to Dr. William Horne for his help in next generation sequencing, and to Hongmei Shen for her help in sorting.

I am deeply grateful to my thesis committee (in alphabetical order) – Drs. Sarah Gaffen, Lawrence Kane, Peter Lucas, Jon Piganelli, and Mark Shlomchik for their kindness, openness, sharpness, and insightfulness. Their advice has not only impacted my thesis studies but also illuminated my development as a scientist. I also want to thank

Dr. Maria Bettini, my “half-advisor”, who introduced me to the scientific world of autoimmune diabetes and T cell tolerance. I am thankful to Dr. Christophe Benoist for his kindness in sharing reagents and for his insightful advice on my research and career development. I would also like to thank Drs. Arlene Sharpe and John Wherry for their great discussions and collaborations. I am also thankful to Drs. Amanda Poholek and Tim Hand for their valuable advice on my career development.

This thesis could not have been completed without help from the Vignali lab. Erin Brunazzi has been a fantastic friend and colleague and helped immensely with mouse maintenance. I have also enjoyed intense yet valuable conversations with Gracie Liu, Hiroshi Yano, Anabelle Visperas, and Sayali Onker. Kate Vignali has been so kind to teach me cloning, to provide me reagents and to share interesting stories outside the lab. Abby Overacre-Delgoffe has been a great companion during my graduate study. I also want to thank other former and present lab members for their tremendous support.

The importance of family and friends cannot be understated. I am so grateful to my parents for their enormous understanding. Their love and support has fueled this work. Last but not least, I would like to thank my best friend Mengyin for leading me into biological sciences even back in high school. I am also immensely thankful for my good friends Gracie, Erin, Yumei, Xizhi, Yinan, Agustin, Siyi, Jun, Qifan, and Wanting for sharing tremendous ideas of all aspects.

Abbreviations

4-1BB: tumor necrosis factor receptor superfamily member 9

Aire: autoimmune regulator

APC: antigen presenting cell

BrdU: 5-bromo-2’-deoxyuridine

cDC: classical dendritic cell

CNS: conserved non-coding DNA sequences

CTLA4: cytotoxic T lymphocyte associated protein 4

DNA: deoxyribonucleic acid

DTR: diphtheria toxin receptor

EAE: experimental autoimmune encephalomyelitis

Eomes: Eomesdermin

ES cell: embryonic stem cells

EV: empty vector

Foxp3: Forkhead box P3

GAD65: glutamic acid decarboxylase

GFP: green fluorescent protein

HLA: human leukocyte antigen

HSP60: heat shock protein 60

IA-2: tyrosine phosphatase-related islet antigen-2

IA-2β: phogrin

IAPP: islet amyloid polypeptide

ICOS: inducible T cell costimulator (CD278)

IDDM: Insulin Dependent Diabetes Mellitus

IDO: indoleamine 2,3-dioxygenase

IEL: intraepithelial lymphocyte

IFNγ: interferon-γ

Ig: immunoglobulin

IGRP: islet-specific glucose-6-phosphatase catalytic subunit-related protein

Ikzf4: Ikaros family zinc finger 4 (encodes gene product Eos)

IL2: interleukine-2

ILC: innate lymphoid cell

IPEX syndrome: immune dysregulation, polyendocrinopathy, enteropathy, X-linked syndrome

IR: inhibitory receptor

IRES: internal ribosomal entry site

IRF4: interferon regulator factor 4

Klrg1: killer cell lectin-like receptor subfamily G member 1

LAG3: lymphocyte activation gene-3 (CD223)

li-CTLA4: ligand-independent CTLA4

LESCtin: liver and lymph node sinusoidal endothelial cell C-type lectin

MDSC: myeloid-derived suppressor cell

MHC: major histocompatibility complex

ndLN: non-draining lymph nodes

Nrp1: neuropilin 1

NK cell: natural killer cell

NKT cell: natural killer T cell

NOD mouse: non-obese diabetic mouse

NTC: non-targeting control

OR: odds ratio

OX40: tumor necrosis factor receptor superfamily member 4 (CD134)

PBMC: peripheral blood mononuclear cell

pDC: plasmacytoid dendritic cell

PDX1: insulin promoter factor 1

PLN: pancreatic lymph nodes

PD1: programmed cell death protein 1 (CD279)

PKC: protein kinase C

pTreg: peripherally derived Treg

qPCR: quantitative polymerase chain reaction

SEM: standard error of the mean

sLAG3: soluble LAG3

SNP: single nucleotide polymorphism

Stat5: signal transducer and activator of transcription 5

T1D: type 1 diabetes

Tbx21: T-box transcriptional factor 21 (encodes gene product T-bet)

Tconv: conventional T cells

TCR: T cell receptor

Teffs: effector T cells

TGFβ: transforming growth factor β

Th: helper T cell

TIGIT: T cell immunoreceptor with Ig and ITIM domains

TIM3: T cell immunoglobulin and mucin-domain containing 3

TNFα: tumor necrosis factor-α

Tr1: type 1 regulatory T cells

Tregs: regulatory T cells

tTreg: thymus-derived Treg

UTR: untranslated region

vi-SNE: a visualization tool for high-dimensional single-cell data based on the t-distributed stochastic neighbor embedding algorithm

WT: wildtype

YFP: yellow fluorescent protein

ZNT8: zinc transporter 8

List of tables

List of figures

1.0 Chapter 1: Introduction

Type 1 Diabetes (T1D) is a polygenic autoimmune disease that is influenced by various genetic and environmental risk factors. Both innate and adaptive components have been implicated in the initiation and progression of T1D, with islet-antigen reactive T cells and regulatory T cells (Tregs) being the predominant players. The non-obese diabetic (NOD) mouse model has been a very useful tool to elucidate the pathology of autoimmune diabetes, in particular testing the "two-checkpoint hypothesis". Both cell-intrinsic and cell-extrinsic inhibitory mechanisms are required to maintain self-tolerance to islet-antigens. Lymphocyte Activation Gene 3 (LAG3, CD223), a co-inhibitory receptor highly expressed on T cells, is one of these essential mechanisms that regulate T cell tolerance in autoimmune diabetes.

1.1 Type 1 diabetes

T1D is a chronic autoimmune disease associated with immune cell infiltration into the islets of Langerhans, production of islet-targeting autoantibodies, destruction of insulin-producing β cells, and subsequent insulin inadequacy and uncontrolled hyperglycemia [1,8]. Although a very small proportion of T1D patients also suffer from insulinopenia

(diabetes mellitus with an inadequate secretion of insulin), there is a lack of evidence for β cell autoimmunity and Human Leukocyte Antigen (HLA) association in these patients, and therefore this form of T1D is referred to as idiopathic diabetes (also as type 1b diabetes); the vast majority (70-90%) of T1D patients lose pancreatic β cells as a consequence of cellular-mediated autoimmune destruction of β cells, and this form of T1D is referred to as type 1a diabetes (formerly juvenile-onset diabetes or insulin-dependent diabetes) [9]. This thesis will mainly focus on autoimmune-related T1D.

1.1.1 Epidemiology

Staging of T1D

The pathogenesis of T1D can be divided into three continuous stages (**Fig. 1**) [1-3]. Stage 1 is characterized by the loss of β cells, the presence of autoantibodies, but normal blood glucose level; whereas stage 2 is characterized by the presence of both autoantibodies and hyperglycemia. Stage 1 and 2 are considered as presymptomatic T1D. While the autoimmune processes that lead to diabetes can begin years before clinical onset, symptoms only present at stage 3.

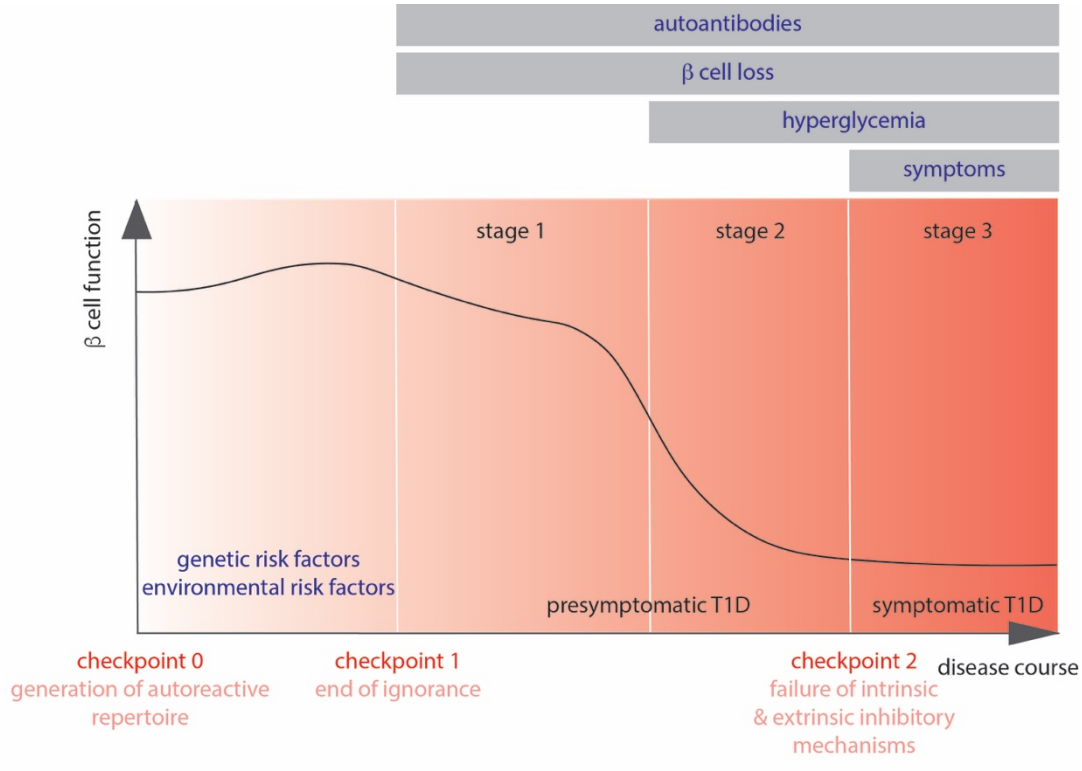

Figure 1. Three stages and two checkpoints of T1D.

T1D can be divided into three stages based on the presence or absence of autoantibodies, β cell loss, hyperglycemia, and diabetes symptoms [1-3]. These stages are affected by various genetic and environmental risk factors [4,5], and are tightly controlled by two checkpoints with both intrinsic and extrinsic inhibitory mechanisms [7].

Incidence and prevalence of T1D

T1D is the most common form of diabetes in children, with the peak incidence of disease onset occurring between 5 and 14 years of age [10,11]. More than a million children and adolescents (< 20 years of age) worldwide are currently living with this condition, and it is estimated that 130,000 children and adolescents are diagnosed annually (International Diabetes Federation). The risk of progression to stage 3 T1D is strongly

associated with the number of islet autoantibodies detected and the age of seroconversion. In the DAISY (Colorado Diabetes Autoimmunity Study in the Young), DIPP (Finnish Type 1 Diabetes Prediction and Prevention), and German BABYDIAB and BABYDIET studies, the average rate of progression to stage 3 T1D at 10 years of follow-up from seroconversion was 70% in children with multiple islet autoantibodies and 15% in children with a single autoantibody, while only 0.4% of children who had no islet autoantibodies developed T1D by 15 years of age [12]. In these same studies, children who had islet autoantibody seroconversion before 3 years of age were faster in progression to symptomatic T1D than those who had seroconversion at 3 years of age or older [12]. Although the incidence is similar between boys and girls, the peak of incidence for girls precedes that for boys, and the progression to symptomatic T1D is slightly faster in girls [12,13].

The incidence and prevalence of T1D vary remarkably among countries (International Diabetes Federation). The highest incidence rate is observed among Scandinavian countries (such as Finland, Sweden, Norway, and Denmark), and slightly lower in other European countries, North America, and Australia. Interestingly, T1D is a relatively rare disease in Asian countries. Such variations among different regions are possibly associated with the genetic susceptibility, environmental triggers, and lifestyle factors as well as the availability of diagnostic resources [2].

1.1.2 Etiology

T1D is a polygenic disease that is influenced by both genetic risk factors and environmental risk factors [4,5]. Even though the primary risk factor for β cell autoimmunity is genetic, an environmental trigger is often needed. On the other hand, environmental factors appear to have their effects mainly on the genetically predisposed individuals.

Genetic risk factors

Fifty-seven T1D-susceptibility regions have been genetically mapped thus far, some of which are also linked with the susceptibility to other autoimmune diseases (data were from T1DBase). The *MHC* (Chr6p21.32) has an odds ratio (OR) of approximately 5.6, which is the strongest association with T1D susceptibility. *HLA-DR3-DQ2* and *HLA-DR4-DQ8* are the two major risk haplotypes [4]. Besides *MHC*, more than fifteen prominent associations, including *PTPN22* (Chr1p13.2, OR 1.89), *CTLA4* (Chr2q33.2, OR 1.2), *IL2* (Chr4q27, OR 1.2), *NRP1* (Chr10p11.22, OR 1.1), *IL2RA* (Chr10p15.1, OR 1.6), *IKZF4* (Chr12q13.2, OR 1.3), are involved in T cell biology (T1DBase). *IL2*, *IL2RA*, *NRP1* and *IKZF4* are likely to affect Treg functions [14-22]. The *INS* locus (Chr11p15.5) has an OR of 2.38, which may affect insulin expression in thymus and negative selection [23-26].

Environmental risk factors

Many environmental factors have been reported as potential triggers for T1D, including infection, microbiota, diet (such as breastfeeding, cow milk, solid foods, vitamin D, polyunsaturated fatty acids, wheat), toxins and chemical compounds, birthweight and infant growth, and β cell stress [5]. Some of these factors have been shown to directly affect the immune system, such as microbiota and vitamin D. Toxins, chemical

compounds and β cell stress are thought to promote the generation of neoautoantigens. Even though studies using animal models have helped implicate the modes of action of those environmental factors, the causal effects of what has been observed in human T1D are yet to be established, and thus further investigation is warranted.

1.1.3 Pathology

B cells and autoantibodies

Even though most of the genetic risk factors for T1D are associated with T cells, B cells have also been implicated in breaking down tolerance to islet-antigens. Antibody-mediated depletion of B cells has been shown to prevent autoimmune diabetes in animal models [27]. Additionally, a clinical trial with rituximab (anti-CD20) has shown efficacy in preserving C-peptide levels for at least 1 year post treatment [28]. However, the ability of B cells to secret antibodies may not be required for the pathology of autoimmune diabetes [29]. A recent mouse study indicates that B-1a cells may activate plasmacytoid dendritic cells (pDCs) to initiate autoimmune diabetes, and depletion of B-1a cells reduced diabetes incidence [30].

Several targets of T1D-associated autoantibodies have been identified, including insulin, proinsulin, glutamic acid decarboxylase (GAD65), islet-specific glucose-6-phosphatase catalytic subunit-related protein (IGRP), tyrosine phosphatase-related islet antigen 2 (IA-2), phogrin (IA-2β), and zinc transporter 8 (ZNT8) [12,31]. There is little evidence that these autoantibodies are pathogenic. However, the presence of those autoantibodies may be used as biomarkers to identify progressing autoimmune

responses, as the risk of progression to stage three T1D is strongly associated with the number of islet autoantibodies detected and the age of seroconversion [12].

Innate immune cells

In addition to T cells and B cells, components of innate immunity have also been implicated in promoting β cell death using the NOD mouse model (which I will introduce in detail in **Chapter 1.2** "The non-obese diabetic mouse model"). Depletion of macrophages prevented autoimmune diabetes onset by converting cytotoxic T cells into regulatory-like cells [32,33]. The crosstalk between neutrophils, B-1a cells and pDCs has been shown to initiate autoimmune diabetes, and depletion of these populations reduced the incidence rate of autoimmune diabetes in the NOD mouse model [30]. Classical dendritic cells (cDCs) from NOD mice are equally capable of presenting autoantigens, regardless of diabetic and inflammatory status [34]. However, only intra-islet DCs can activate primary insulin B_{9-23}-reactive T cell lines, as the epitopes presented by DCs from other tissues are not recognized by insulin-reactive T cells [34].

While both innate and adaptive immune systems play intricate roles in T1D pathogenesis, T cells are considered one of the major players. My thesis is mainly focused on elucidating cell-intrinsic mechanisms that regulate T cell tolerance in autoimmune diabetes, and I will elaborate on this topic in the following chapters.

1.2 The non-obese diabetic mouse model

Several animal models, including the NOD mouse, the BioBreeding/Worcester rat, and autoimmune diabetes induced with streptozotocin or lymphocytic choriomeningitis virus, have been utilized to study T1D [35-39]. The NOD mouse model, first reported in 1980, has become the T1D model of choice because of the similarity between it and human T1D [39]. The NOD mouse model has been a valuable tool for our understanding of T1D disease mechanisms.

1.2.1 Advantages and limitations of the NOD mouse model

Advantages

The NOD mouse model shares many common features with T1D in humans (**Table 1**) [40]. First, NOD mice spontaneously develop chronic autoimmune diabetes, characterized by hyperglycemia and leukocytic infiltration, including DCs, macrophages, B cells, natural killer cells (NK cells), and $CD4^+$ and $CD8^+$ T cells, into the pancreatic islets. In female mice, insulitis starts at three to four weeks of age and subsequent diabetes onset occurs between twelve and twenty-five weeks of age, which resembles the early onset of T1D in humans during childhood. Male NOD mice exhibit slightly delayed onset and reduced incidence because of elevated testosterone in a commensal symbiosis dependent manner, which is not an evident feature of human T1D [41,42]. Second, > 40 insulin-dependent diabetes-susceptibility (*Idd*) regions and genes have been mapped in NOD mice, some of which are also implicated in human T1D (T1DBase)

[43-45]. Third, the same autoantigens have also been identified in both T1D patients and NOD mice (**Table 1**) [40,46].

Table 1. Comparison between human T1D and the NOD mouse model of autoimmune diabetes.

	Human T1D	the NOD mouse model
Age of onset	the incidence peak of onset is between 5 and 14 years of age	the incidence peak of onset is between 12 and 25 weeks of age
Gender effect	females and males are equally affected before puberty	lower incidence and delayed onset in males dependent on the husbandry
Genetic susceptibility	57 T1D-susceptibility regions have been mapped MHC is the primary risk factor	> 40 *Idd* regions have been mapped MHC is the primary risk factor
Autoantigens	insulin, insulin derivatives, IGRP, ZNT8, PDX1, carboxypeptidase H, IA-2, IA-2β, GAD65, IAAP, HSP60	insulin, insulin derivatives, IGRP, ZnT8, PDX1, IA-2, IA-2b, GAD65, IAAP, Chromogranin A
T cell repertoire bias	none	none
Insulitis	NK cells, macrophages, DCs, B cells, $CD4^+$ and $CD8^+$ T cells (including Tregs)	NK cells, macrophages, DCs, B cells, $CD4^+$ and $CD8^+$ T cells (including Tregs)

Limitations

There are some differences between the NOD mouse model and human T1D, in particular the frequency and timing of insulitic immune subsets [47]. The most prominent difference in human T1D is that the insulitis is primarily mediated by $CD8^+$ T cells and macrophages, whereas $CD4^+$ T cells and B cells are more frequent in NOD mice [48].

1.2.2 The two-checkpoint hypothesis of autoimmune diabetes

Early evaluation of the NOD mouse model and various T cell receptor (TCR) transgenic mice led to the initial "two-checkpoint hypothesis" for autoimmune diabetes development (**Fig. 1**) [7], which has formed the fundamental basis for numerous studies.

Checkpoint 0: generation of the islet-antigen reactive repertoire

An autoreactive repertoire must exist before the self-tolerance breaks down. I will introduce how the islet-antigen reactive T cell repertoire is selected in the thymus in **Chapter 1.3.2** "Generation of the islet-antigen-reactive T cell repertoire".

Checkpoint 1: the end of self-ignorance

The first checkpoint in autoimmune diabetes development is when clonal ignorance transitions to islet infiltration. However, it is less clear how the transition starts. The original hypothesis proposed that the presence of appropriate antigen presenting cells (APCs) and/or homing of autoreactive T cells to the islet might influence checkpoint 1 [7]. Although recent studies have provided some clues, further investigation on checkpoint 1 is merited, as such findings may benefit efforts to prevent disease initiation in genetically predisposed individuals.

Checkpoint 2: from controlled violence to chaos

Controlled insulitis before the onset of diabetes symptoms has been observed in both NOD mice and T1D patients [2,3,7]. The original hypothesis proposed that adaptive immune responses against islet autoantigens may be regulated through both cell-intrinsic and cell-extrinsic mechanisms in checkpoint 2 [7]. Cell-intrinsic mechanisms can be

affected by: (1) acquisition of new effector capabilities [i.e., perturbed type 1 helper T cells (Th1)/Th2 balance, production of inflammatory cytokines, and expression of Fas ligand], and (2) loss of sensitivity to negative signaling [i.e., regulation through cytotoxic T lymphocyte associated protein 4 (CTLA4), interleukin-2 (IL-2) receptors, and NK-like receptors]. Cell-extrinsic mechanisms can be affected by: (1) abrogation of negative controls [i.e., loss of regulatory cell populations, and defects in inhibitory cytokines such as transforming growth factor β (TGFβ) and IL-10], (2) perturbation of anti-idiotypic networks, and (3) recruitment of accessory cell types into the lesion.

In addition to these mechanisms proposed 20 years ago [7], numerous studies have expanded our knowledge on checkpoint 2. I will introduce cell-intrinsic mechanisms (in particular co-stimulatory and co-inhibitory pathways) and cell-extrinsic mechanisms (in particular Treg mediated self-tolerance) in **Chapter 1.3.3** "Co-stimulatory and co-inhibitory receptors in autoimmune diabetes" and **Chapter 1.3.4** "An essential role for Tregs in self-tolerance", respectively.

1.3 T cell tolerance in the context of autoimmune diabetes

Immunological self-tolerance is the unresponsiveness of the immune system to self-antigens. A breakdown in immune homeostasis and self-tolerance leads to autoimmunity, resulting in deleterious inflammation in, and destruction of, self-tissues mediated by autoreactive T cells and autoantibodies [49,50]. In order to prevent autoimmunity, an intricate series of cellular and molecular checks helps to ensure that the immune system produces a measured and appropriate response to foreign threats while avoiding host

tissue pathology and destruction. However, emerging observations suggest that these control mechanisms are defective in autoimmune diabetes, providing underlying mechanistic insight while also pointing to potential avenues for therapeutic intervention.

1.3.1 Recessive and dominant tolerance

The mammalian immune system utilizes two main mechanisms, "recessive" and "dominant" tolerance, to achieve self-tolerance and homeostasis [51]. Here, I will discuss these two types of mechanisms in the regulation of T cell tolerance.

Recessive tolerance mechanisms

Recessive tolerance consists of a series of cell-intrinsic mechanisms to determine the fate of autoreactive T cells. Firstly, immature T cells that strongly respond to self-antigens may undergo programed cell death during thymic development, a process called "negative selection" [52,53]. Secondly, while this mechanism is less understood, T cells that escape negative selection may re-express RAG recombinase and replace their autoreactive receptors in the periphery, a process called "TCR revision" [54]. Thirdly, mature T cells that escape both negative selection and TCR revision can be rendered functionally inactive when they are activated in the absence of a "proper" amount of co-stimulation, a state called "anergy" [55]. Lastly, clonal activation, expansion and/or survival thresholds of autoreactive T cells may be raised because of the upregulation of sustained co-inhibition, a state called "exhaustion" [56].

Dominant tolerance mechanisms

Dominant tolerance relies on a collection of immune regulatory cell populations, such as Tregs, myeloid-derived suppressor cells (MDSCs), and subsets of NKT cells, γδT cells, RORγt$^+$ innate lymphoid cells (ILCs), and CD8αα$^+$ intestinal epithelial cells (IELs), to keep aberrant T cell activation and expansion in check via cell-extrinsic mechanisms [6,51,57-61]. Disruption of the balance between immune regulatory populations and pro-inflammatory populations leads to either unresponsiveness to foreign antigens or catastrophic self-responsiveness.

1.3.2 Generation of the islet-antigen reactive T cell repertoire

Autoantigens

As summarized in **Table 1**, many islet-associated autoantigens have been identified, most of which overlap in both T1D patients and NOD mice. These autoantigens can be divided into three groups based on their tissue expression: first, β cell specific autoantigens, such as insulin, insulin derivatives, IGRP, ZnT8, and insulin promoter factor 1 (PDX1); second, neuroendocrine autoantigens, such as carboxypeptidase H, IA-2, IA-2β, GAD65, islet amyloid polypeptide (IAPP), and Chromogranin A; third, ubiquitously expressed autoantigens, such as heat shock protein 60 (HSP60). Although these autoantigens have been implicated to various degrees in the pathogenesis of autoimmune diabetes, a single primary autoantigen driving the development of T1D has not been identified.

Proinsulin or insulin may be very important in the initiation of autoimmune diabetes. Autoanbodies against proinsulin or insulin tend to appear before those against other

autoantigens in T1D patients during their early childhood [62]. Removal of proinsulin or insulin but not IGRP completely prevents insulitis and diabetes in NOD mice, suggesting the primacy of insulin in the development of autoimmune diabetes in the NOD mouse model [23,63]. However, it is not clear this is also the case in human T1D.

After the disease is initiated and islet damage is perpetuated, intramolecular and intermolecular epitope spreading may occur and promote the progression of autoimmune diabetes [64]. Besides those well characterized autoantigens, newly discovered autoantigens (including ZnT8, PDX1, Chromogranin A, IAPP, and hybrid insulin peptides) have also been implicated in the NOD mouse model and/or human T1D [46,65]. Understanding the kinetics of autoantibodies and autoreactive T cells will help to elucidate how and when the two checkpoints are broken down.

Selection of islet-antigen reactive T cell repertoire

T cell negative selection, a recessive tolerance mechanism, is crucial in preventing autoimmune diabetes. As aforementioned, insulin epitopes appear to be very important in the initiation of autoimmune diabetes. Defects in the elimination of insulin-reactive T cells from the repertoire are strongly associated with T1D susceptibility. In humans, a polymorphism in the *INS* promoter is associated with lower thymic *INS* expression compared to the diabetes resistant alleles, raising a potential mechanism by which the Insulin Dependent Diabetes Mellitus 2 (*IDDM2)* locus predisposes to T1D [24]. In mice, *Ins1* is predominantly expressed by β cells, whereas *Ins2* is expressed in thymus and β cells. While *Ins1*$^{-/-}$.NOD mice exhibit reduced diabetes incidence, *Ins2*$^{-/-}$.NOD mice develop remarkably accelerated autoimmune diabetes, likely due to defectivve negative selection [23,25,26].

Some insulin-reactive T cells can escape negative selection as certain epitopes may not be presented in the thymus. For instance, differential registers of insulin peptides on the major histocompatibility complex (MHC) in the thymus versus periphery have been implicated as an escape mechanism for insulin-reactive T cells [66-68]. Furthermore, hybrid insulin peptides have been identified as autoantigens in both NOD mice and T1D patients, but these neo-antigens are generated in β cell secretory granules and are not presented in the thymus [46].

Interestingly, although the gene *Aire* (autoimmune regulator) is essential in thymic selection, *Aire*$^{-/-}$.NOD mice are normoglycemic and die because of severe systemic autoimmune pathology, rather than insulitis and autoimmune diabetes [69], perhaps due to a differential effects on selection between the autoreactive effector T cell (Teff) and Treg repertoires.

1.3.3 Co-stimulatory and co-inhibitory receptors in autoimmune diabetes

Note: This part of the Introduction was taken from a part of my previously published review "Zhang Q, Vignali DAA. *Immunity.* (2016)" [70].

The immune system is guided by a series of checks and balances, a major component of which is a large array of co-stimulatory and co-inhibitory pathways that modulate the host response. While co-stimulation is essential to boost and shape the initial response following signaling through the antigen receptor, inhibitory pathways are also critical to modulate the immune response. Excessive co-stimulation and/or

insufficient co-inhibition can lead to a breakdown of self-tolerance, leading to autoimmunity.

The most prominent feature of co-stimulatory or co-inhibitory pathway utilization in autoimmune diabetes is the differential temporal utilization observed. CD28:B7 and CD40:CD40L co-stimulation, and CTLA4-mediated inhibition appear to be more important during disease onset and establishment of insulitis. In contrast, other co-stimulatory and co-inhibitory receptors are utilized more broadly or at later stages of disease progression after insulitis occurs. In addition, co-stimulation is also essential for the maintenance of Treg homeostasis in NOD mice, potentially complicating the therapeutic potential of some modalities.

Two signals in T cell activation

The Two-Signal model proposes that activation of naïve T cells requires both TCR stimulation by MHC:peptide complexes [Signal 1] and co-stimulation via co-stimulatory receptors and their corresponding ligands on APCs [Signal 2] [71,72]. For instance, one of the most prominent co-stimulatory pathways is the CD28:B7 axis, which amplifies TCR signaling and IL-2 production to promote T cell proliferation and survival. In order to provide a mechanism to turn off or turn down T cell activation, co-inhibitory receptors are induced by TCR stimulation and co-stimulation and subsequently transduce feedback signals that dampen the ascending co-stimulatory and TCR signals. Therefore, the net outcome of TCR stimulation is modified by both co-stimulatory and co-inhibitory receptors. Both sets of receptors are expressed by all T cell subsets, thereby helping to shape the overall immune response. For instance, co-stimulatory and co-inhibitory recpetors are also expressed by, and have a critical impact on, Tregs, an

immunosuppressive population that plays a pivotal role in self-tolerance [6,51]. Excessive co-stimulation and/or inadequate co-inhibition results in aberrant T cell activation, which can result in a breakdown of self-tolerance by activating and expanding autoreactive T cells. Similarly, B cells also require two signals for their activation, maturation and function [73]. Therefore, the immune response is fundamentally shaped and modulated by co-stimulatory and co-inhibitory receptors and their corresponding ligands. Disruption of the balance between co-stimulation and co-inhibition unleashes self-reactivity, leading to autoimmune disease.

Co-stimulatory pathways in autoimmune diabetes

Several co-stimulatory receptors are known to be critical for the development of autoimmune diabetes in NOD mice. Even though the CD28:B7 axis provides essential co-stimulation for autoreactive T cell priming, it is also critical for Treg development and homeostasis in autoimmune diabetes. Both *Cd28*$^{-/-}$ and B7.1-B7.2 (CD80-CD86) double-deficient NOD mice had a profoundly reduced number of $CD4^+CD25^+$ Tregs, and thus exhibited accelerated autoimmune diabetes [74]. The protective effect of CD28:B7 co-stimulation seems to be mainly provided by B7.1, since B7.2-deficient NOD mice were free of autoimmune diabetes [74-76]. However, the protective effect of anti-B7.2 treatment was abolished if it was administered in older NOD mice [75]. Thus, B7.1 and B7.2 may have different functions depending on the timing and context of their involvement [77,78].

Other co-stimulatory pathways independent of the CD28:B7 axis have been implicated in T1D pathogenesis. Inducible T cell costimulatory (ICOS, CD278):ICOSL co-stimulation is also used by both autoreactive T cells and Tregs in autoimmune diabetes. Blockade with anti-ICOS resulted in delayed autoimmune diabetes in NOD

mice, and *Icos*$^{-/-}$ NOD mice were free of autoimmune diabetes, with reduced IFNγ production [79,80]. Conversely, other studies using the BDC2.5 TCR transgenic NOD model demonstrated that ICOS is preferentially expressed on Tregs and mediates enhanced suppressive capacity of Tregs [81-83], with ICOS blockade in BDC2.5 NOD mice resulting in rapid diabetes onset [79,81].

Unlike the CD28:B7.1 and ICOS:ICOSL co-stimulatory pathways, CD40:CD40L co-stimulation appears to have less impact on Tregs and is required for the initiation of insulitis and autoreactive T cell priming in autoimmune diabetes. Blockade with anti-CD40L in neonates or deficiency of CD40L (CD154) prevented autoimmune diabetes in NOD mice, but the protective effect of anti-CD40L treatment was abolished in older mice [76,84-86].

In contrast to the CD40:CD40L axis, tumor necrosis factor receptor superfamily member 4 (OX40, Tnfrsf4, CD134):OX40L co-stimulation appears to be more important at later stages of autoimmune diabetes. OX40 is expressed on primed (CD44^{hi}) T cells and OX40L (Tnfsf4, CD252) is upregulated on DCs after insulitis initiation but prior to islet destruction (11-13 weeks of age). Thus, interruption of OX40:OX40L interactions had no effect on diabetes onset in young NOD mice but exhibited the most significant delay in diabetes onset in NOD mice at 12 weeks of age [87]. Interestingly, *Tnfsf4*$^{-/-}$ NOD mice exhibited normal (or even accelerated) insulitis but did not develop autoimmune diabetes [88], supporting the idea that different co-stimulatory axes participate at different stages to promote autoimmune diabetes.

Another TNFRSF member, 4-1BB (Tnfrsf9), has also been studied in autoimmune diabetes. *Tnfrsf9* has been mapped to *Idd9.3*, which modulates susceptibility to

autoimmune diabetes in NOD mice. Interestingly, while treatment with 4-1BB agonist autoantibody prevented autoimmune diabetes in NOD mice by inducing Tregs, overexpression of a 4-1BB agonist induced severe autoimmune diabetes [89-91]. 4-1BB is constitutively expressed on Tregs, but transiently upregulated on effector T cells after activation. Therefore, there might be functionally and/or temporally distinct usage of 4-1BB on Tregs versus autoreactive T cells in autoimmune diabetes.

Collectively, these studies highlight the importance of multiple co-stimulatory receptors in modulating autoimmune diabetes via their differential impact on diabetogenic T cell function and Treg homeostasis.

Co-inhibitory pathways in autoimmune diabetes

In addition to Treg-mediated suppression, co-inhibitory receptors also provide cell-intrinsic regulation of autoreactive T cells in NOD mice. For instance, CTLA4 is critical for controlling autoimmune diabetes. Identified polymorphisms within the *CTLA4* locus appear to associate with susceptibility to T1D and map to *Idd5.1* in NOD mice [92,93]. NOD mice are genetically deficient in expression of a CTLA4 splice variant that cannot bind to its B7 ligand (ligand-independent CTLA4; li-CTLA4) [94,95]. Curiously, restoration of li-CTLA4 expression in NOD mice limits insulitis and autoimmune diabetes in full-length CTLA4-dependent manner [96,97]. Genetic deletion or blockade of CTLA4 showed dramatic acceleration of diabetes onset in NOD mice [98,99], whereas APC-directed CTLA4 engagement delayed autoimmune diabetes onset by inhibition of B cell maturation [100]. CTLA4 engagement dampens diabetogenic T cell activity but in a very restricted time window that coincides with islet Ag re-encounter [98,99]. Interestingly, CTLA4 upregulation is prevented by low CD86 expression and impaired T cell priming in NOD mice [101],

suggesting that optimal T cell priming is also required to induce cell-intrinsic negative signals.

Programmed death protein 1 (PD1, CD279):PD-L1 or :PD-L2 interactions mediate co-inhibitory effects that appear to be distinct from CTLA4. Polymorphisms at the *PDCD1* locus are associated with susceptibility to T1D [102]. *Pdcd1*$^{-/-}$.NOD mice developed autoimmune diabetes by 11 weeks of age with 100% penetrance in both females and males [103]. In contrast to CTLA4 blockade, treatment with anti-PD1 or anti-PD-L1, but not anti-PD-L2, precipitated insulitis and autoimmune diabetes onset in NOD mice regardless of when the mice were treated [1-10 weeks of age] [104], suggesting PD1:PD-L1 interactions may impact all stages of autoimmune diabetes onset and progression. PD1 appears to prevent stable interactions between T cells and DCs in pancreatic lymph nodes [105]. Interestingly, PD-L1 may also be expressed on pancreatic islets [104,106], providing a regulatory signal before autoreactive T cells enter the islets. Interaction between PD-L1 and another of its known ligands, B7.1, induces negative signals in diabetogenic T cells at the late phase of autoimmune diabetes [78]. Curiously, while PD-L1 overexpression on β-cells protected NOD mice from autoimmune diabetes [107], its overexpression on β-cells in B6 mice provoked autoreactive T cells [108]. The basis for these contradictory observations remains to be defined. Besides its regulation on peripheral autoreactive T cells, it is noteworthy that PD1 may also impacts thymic selection of diabetogenic T cells [109].

Co-inhibitory receptors T cell immunoglobulin and mucin-domain containing 3 (TIM3) and B7-H4 may function to dampen β-cell destruction at a later stage. Treatment with either anti-TIM3 or TIM3Ig, which blocks interactions between endogenous TIM3 and

its ligands, augmented autoimmune diabetes but did not impact insulitis [110]. Likewise, early treatment with B7-H4Ig, which provides a co-inhibitory signal via an unknown ligand on T cells, did not block insulitis but delayed aggressive β-cell destruction at the later stage [111]. Thus, the analyses of co-inhibitory receptors in NOD mice suggest that these pathways are broadly utilized but at different stages during the pathogenesis of autoimmune diabetes.

Like PD1, LAG3 is also required to restrain the expansion of diabetogenic T cells in the islets [112,113]. I will introduce the basic biology of LAG3 in **Chapter 1.4** "LAG3 in T cell tolerance".

1.3.4 An essential role for Tregs in self-tolerance

Identification of Tregs

The concept of Tregs originated in experiments with which neonatal thymectomy led to multi-organ damage, while transfer of normal $CD4^+$ T cells or $CD4^+CD8^-$ thymocytes ameliorated the development of autoimmunity in sub-lethally irradiated mice [114,115]. These results indicated that central tolerance may sometimes neglect autoreactive T cells, and also that thymic development may positively select $CD4^+$ T cells that can suppress autoimmunity. These immuno-suppressive $CD4^+$ T cells are now known to be generated during thymic selection and are called "thymus-derived Tregs" (tTregs) [116]. Later experiments that identified Treg markers, such as receptors CD25 (IL-2 receptor alpha), Neuropilin 1 (Nrp1), and transcription factor Foxp3, have not only provided the

opportunity to distinguish Tregs from other T cell subsets but also shed light on Treg development and function [19,117-125].

Some Tregs differentiate from naïve T cells in the periphery ("peripherally derived Tregs", pTregs), most frequently at mucosal barriers [116]. Foxp3 expression is induced in pTregs by TGFβ, retinoic acid, or other microbial metabolites [126-128]. Some pTregs do not express Foxp3, but regulate immune responses through suppressive cytokines such as IL10 and IL35 ("Tr1" and "iTr35", respectively) [129,130].

Mechanisms of Treg suppression

The various suppressive mechanisms utilized by Tregs can be grouped into four types based on their modes of action (**Fig. 2**) [6]. First, Tregs can function through the secretion of suppressive cytokines, such as IL-10, TGFβ, and IL-35 [129,131-134]. Second, Tregs can kill Teffs through granzyme-dependent and/or perforin-dependent cytolysis, or through death receptor-induced cell death [135-138]. Third, Tregs can disrupt Teff metabolism by depriving IL2 through high affinity CD25, transferring cAMP into Teffs through gap junctions, or generating adenosine through ectoenzymes CD39 and CD73 [139-141]. Last, Tregs can indirectly regulate Teffs by targeting DCs [142,143]. For instance, Tregs constitutively express CTLA4, which has a higher affinity for binding to B7.1/B7.2 than CD28, and therefore competes with Teffs engaging DCs [144]. Tregs have been shown to condition DCs to express the inhibitory molecule indoleamine 2,3-dioxygenase (IDO) [144,145]. The co-inhibitory receptor LAG3 has also been implicated in mediating Treg suppression through interactions with DCs [146].

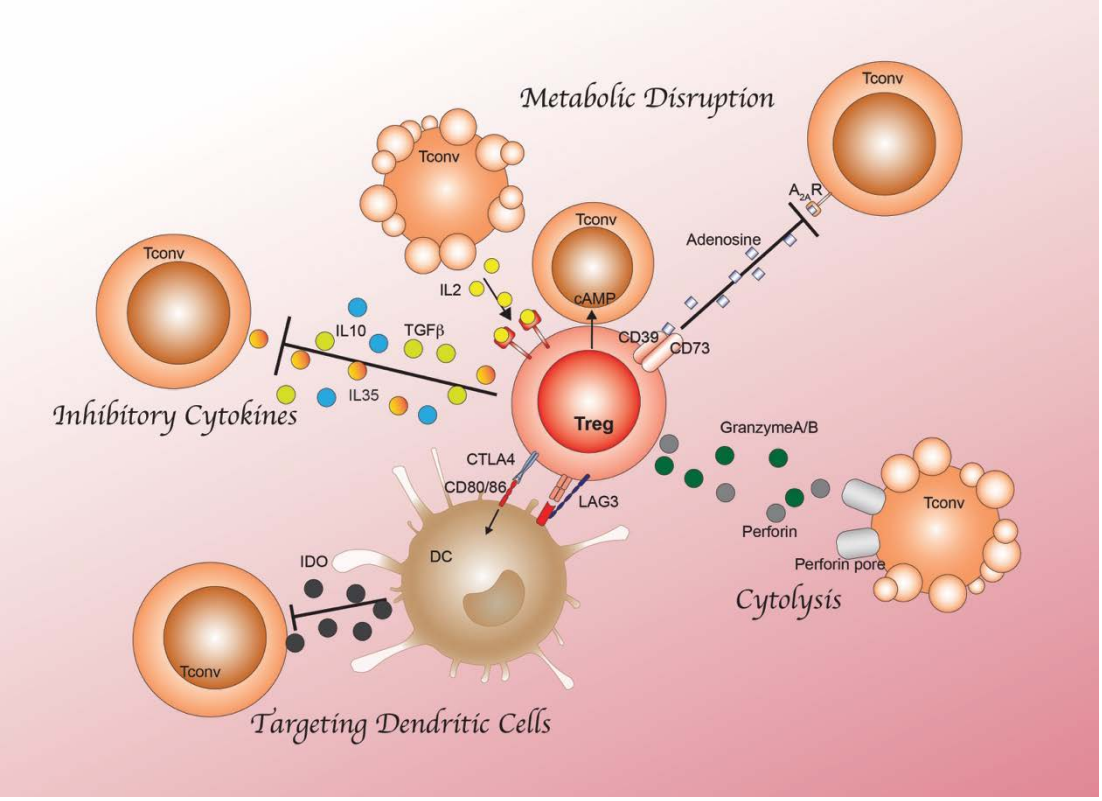

Figure 2. Mechanisms of Treg suppression.

The various suppressive mechanisms utilized by Tregs can be grouped into four types based on their modes of action: inhibitory cytokines, cytolysis, metabolic disruption, and targeting dendritic cells [6].

Foxp3: the master coordinator in tTregs

Foxp3 is a transcription factor that is expressed in tTregs during thymic development and also induced in pTregs in the periphery. *Foxp3* was originally identified in a mouse strain exhibiting an X-linked recessive "scurfy" phenotype [124]. Scurfy mice exhibit extensive multi-organ infiltration and over-activation of lymphocytes, and die by 20 days old. Subsequent functional analyses verified that Foxp3 is essential in Treg development and function. Mice that are deficient in *Foxp3* expression or are depleted

of *Foxp3*-expressing cells develop a phenotype similar to that of Scurfy mice, and overexpression of *Foxp3* is sufficient to confer the suppressive capacity in $CD4^+$ naïve T cells [122,123,125,147].

Some humans develop immunodysregulation polyendocrinopathy enteropathy X-linked (IPEX) syndrome as a consequence of mutations in the *FOXP3* gene [148-150]. Affected individuals usually exhibit neonatal onset of autoimmune diabetes, enteropathy, thrombocytopenia, anemia and other endocrinopathy, and die within the first two years. However, FOXP3 may not be a bona fide marker for human Tregs. Activated human conventional T cells (Tconvs) transiently upregulate FOXP3, but do not possess regulatory functions [151]. Additionally, virally transduced or TGFβ induced FOXP3 expression in human T cells is not sufficient to confer them with an immuno-suppressive phenotype [148,152].

Foxp3 governs Treg phenotypes through cooperation with many other key transcription factors, including GATA3, GATA1, Eos, IRF4, Runx1, Helios, Lef1, Satb1, Aiolos, EZH2, and Rel [153-155]. Foxp3 acts as a transcriptional activator or repressor depending on the context and binding partner, and thus switches or reinforces the transcriptional and epigenic landscapes in developing or established Tregs [156,157]. Of note, the Ikaros family member Eos (encoded by gene Ikaros family zinc finger 4, *Ikzf4*) coordinates with Foxp3 to silence Tconv genes in Tregs, and loss of Eos expression leads to rapid conversion of $CD4^+Foxp3^+$ Tregs into helper-like cells [21,22,157]. An N-terminal mutation of *Foxp3* leads to Treg insufficiency in autoimmune diabetes due to reduced interactions with Tip60, HDAC7 and Eos, whereas the same mutation increases its interaction with interferon factor 4 (IRF4) and thus results in alleviated arthritis [15,16]. In

humans, *IKZF4* (Chr12q13.2, OR 1.3) has also been genetically mapped to the T1D-susceptibility region (T1DBase).

Treg stability and homeostasis

Many cell-intrinsic and cell-extrinsic factors can affect Treg homeostasis and function. The composition, size and maintenance of Foxp3$^+$ Tregs are intrinsically controlled by *Foxp3* conserved non-coding DNA sequences (CNS) elements [158-160]. IL-2 signaling is critically required for the development and maintenance of Tregs [14,17,120,121]. Although Nrp1 does not seem to be essential under homeostatic conditions, it may be required to maximize the competitive fitness of Tregs under inflammatory conditions *in vivo* [18-20]. Treg homeostasis is also extrinsically modulated by microbial metabolites (i.e., short chain fatty acids) [161,162]. A diet containing the short chain fatty acids acetate and butyrate boosted the number and function of Tregs in NOD mice and provided protection against autoimmune diabetes [163].

Tregs in autoimmune diabetes

Tregs are perhaps the most crucial controller of autoimmune diabetes. Most IPEX patients exhibit neonatal onset of T1D [148-150]. Scurfy mice that are deficient of Tregs and on a NOD background develop fulminant diabetes and die as early as three weeks of age [164]. Similarly, ablation of Tregs using the *Foxp3*^{DTR}.NOD mouse model (these NOD mice express human diphtheria toxin receptor in Foxp3$^+$ cells, so diphtheria toxin administration results in ablation of all Foxp3$^+$ Tregs) rapidly unleashed autoimmune lesions within the pancreatic islets [165]. Conversely, transfer of Tregs can protect mice from autoimmune diabetes [74,81,166-168]. Furthermore, in a recent phase 1 trial, *ex vivo*-

expanded polyclonal Treg therapy showed safety and was well tolerated in recent-onset T1D patients [169].

Crucial as they are, Tregs appear to be very “fragile” in an autoimmune diabetes-prone environment. For instance, a substantial percentage of Tregs in NOD mice lose Foxp3 expression, and transfer of these ex-Foxp3^{+} T cells led to rapid onset of diabetes [170]. Additionally, a mutation at Foxp3 N-terminus resulted in dramatically accelerated autoimmune diabetes in NOD mice, whereas B6 mice with the same mutation did not exhibit any confounding disease phenotypes [15,16]. Defects in co-stimulatory signaling (i.e., CD28:CD80/CD86) or IL-2 signaling also disrupted the balance between Tregs and autoreactive T cells, leading to accelerated autoimmune diabetes in NOD mice [14,17,74,171]. Collectively, these studies highlight the importance of Treg-mediated tolerance in controlling β cell autoimmunity.

1.4 LAG3 in T cell tolerance

The gene encoding LAG3 is located on human Chromosome 12 (mouse Chromosome 6) and the protein is a surface receptor expressed on activated T and NK cells [172]. Studies have suggested that LAG3 may possess unique features different from other co-inhibitory receptors, in terms of its structure, signaling, expressional regulation and physiological functions.

1.4.1 LAG3 structure, ligands, and signaling

Structure

LAG3 and CD4 genes are adjacent to each other on mouse Chromosome 6 (human Chromosome 12) and share high structural homology within the four-extracellular immunoglobulin (Ig)-like domains (D1 to D4) [173]. However, LAG3 and CD4 share less than 20% amino acid sequence homology, which results in a ~100-fold increase in LAG3 binding affinity to MHC-II compared with CD4 [172-175]. Furthermore, LAG3 and CD4 vary greatly in the transmembrane and cytoplasmic domains, which may result in very distinct cellular functions and signaling pathways between these two receptors [176,177].

The cytoplasmic tail of LAG3 contains three conserved regions and is unique among all known immune receptors [176,178]. The first region is a potential serine phosphorylation site, which may act as a protein kinase C (PKC) substrate. The second is a KIEELE motif with a single "lysine" residue that is conserved across all species sequenced, but this region is not homologous with any other known proteins. The third is a glutamic acid-proline (EP) repetitive sequence, which is found in a wide variety of functionally distinct proteins. Interestingly, the intracellular tail of LAG3 does not contain any ITIMs (immunoreceptor tyrosine-based inhibition motifs) or ITSMs (immunoreceptor tyrosine-based switch motifs), which are often used by other co-inhibitory receptors to limit TCR signaling [179]. In comparison to CD4, LAG3 lacks the binding site for tyrosine kinase $p56^{Lck}$ [173]. There is also a connecting peptide between the D4 and transmembrane domains that can be cleaved by metalloproteinases [177].

Ligands

LAG3 binds to MHC-II through the D1 domain with an additional 30-amino acid-loop that is not present in CD4 [173]. Alternative ligands of LAG3 other than MHC-II have been identified. Liver and lymph node sinusoidal endothelial cell C-type lectin (LSECtin), a member of the DC-SIGN family and expressed on human melanoma tissues, has been shown to be a ligand for LAG3 [180]. It was suggested that LSECtin may promote tumor growth by inhibiting IFNγ production of LAG3$^+$ effector T cells [180]. It was also shown that the LAG3:galectin-3 interaction suppressed IFNγ secretion by CD8$^+$ T cells [181]. A more recent study showed that LAG3 facilitated the pathogenesis of a murine Parkinson's disease model through the binding to α-synuclein preformed fibrils in the central nervous system [182].

Signaling

The signaling pathway downstream of LAG3 is still unknown. It has been shown that the unique conserved KIEELE motif, in particular the "lysine" residue (mouse K468), is essential for the inhibitory function of LAG3 in CD4$^+$ Tconvs [183]. However, it is not clear what are the downstream binding proteins for this motif, and whether this motif mediates similar or distinct signaling in Tregs. The EP motif does not seem to be required for the inhibitory activity of LAG3, but it may possess some modulatory effects on the LAG3 signaling transduction [183,184].

LAG3 may also mediate signaling into its ligand-expressing cells. It was suggested that LAG3-expressing Tregs may inhibit DC maturation via binding to MHC-II [146]. This process is mainly mediated through the extracellular domain of LAG3, as tailless LAG3 was sufficient to suppress DC function [146].

1.4.2 Regulation of LAG3 expression

LAG3 expression

LAG3 is highly expressed on $CD4^+$ and $CD8^+$ Tconvs 24-48 hours post-stimulation *in vitro*, with expression declining by day eight [185]. Chronic antigen stimulation also leads to sustained co-expression of LAG3 with other co-inhibitory receptors on T cells *in vivo* [56]. Similarly, LAG3 is expressed on activated human T and NK cells [172].

LAG3 expression in Tregs is different from that in Tconvs. tTregs constitutively express low levels of *Lag3* message and readily upregulate expression of LAG3 on the cell surface following TCR stimulation [186]. Moreover, co-expression of LAG3 and CD49b defines $Foxp3^-$ IL-10-producing Tr1 cells in both humans and mice [187]. While it has been suggested that LAG3 may contribute to suppressive activities of Tregs [146,186-188], one needs to be cautious when partitioning the cell-intrinsic and cell-extrinsic impact of LAG3 on Tregs, as the signaling mediated by LAG3 can be bidirectional.

LAG3 is constitutively expressed on pDCs and $CD8\alpha\alpha^+$ IELs, and induced on NK cells, although its biological significance on these cell types is to be determined [185,189]. LAG3 was also detected in cerebellum and was shown to facilitate the pathogenesis of Parkinson's disease, suggesting a role for LAG3 outside the immune system [182,185].

sLAG3, LAG3 shedding and intracellular storage

LAG3 expression is regulated through different mechanisms, which may help to ensure optimal immunoregulation. One mode of regulation is cleavage at the connecting peptide region between the D4 and transmembrane domains by metalloproteinases

ADAM10 and ADMA17, releasing soluble LAG3 (sLAG3) [177,190]. While ADAM10 constitutively cleaves LAG3 on resting T cells, cleavage by both ADAM10 and ADAM17 is enhanced upon T cell activation [177].

Soluble LAG3 has been suggested as a prognostic biomarker in breast cancer patients who express estrogen or progesterone receptors, active tuberculosis patients and T1D patients [191-193]. Our group did not observe any biological function of natural murine sLAG3, as T cell homeostasis was not affected in mice that express ~1000-fold higher levels of sLAG3 than normal serum concentrations [177]. A separate group suggested that a human LAG3-Ig fusion protein induces DC maturation and migration [194-197]. However, clinical grade hLAG3-Ig (IMP321), designed as an APC activator, has exhibited minimal activity as a monotherapy [176].

Another way to regulate cell surface expression of LAG3 on previously activated resting T cells is through its intracellular storage in lysosomal compartments [198,199]. While LAG3 can be degraded in lysosomes, it can also rapidly translocate to the cell surface upon TCR re-stimulation. Understanding how LAG3 expression is regulated may provide additional avenues to target LAG3 in the clinic, other than antibody-mediated blockade.

1.4.3 Role of LAG3 in disease

Infection

Exhausted T cells are marked by the upregulation of co-inhibitory receptors and defects in proliferation, cytokine production and cytotoxicity [56]. LAG3 is co-expressed with PD1 on exhausted $CD8^+$ T cells in the Clone 13 LCMV chronic infection model, and

its expression is correlated with virus load [200,201]. Although LAG3 single blockade had little effect, it synergistically improved the anti-viral response with PD-L1 blockade [200,201]. A similar synergistic effect was also observed in exhausted $CD4^+$ T cells during malaria infection [202].

Cancer

Similar to exhausted T cells in chronic infections, tumor-infiltrating T cells also co-express PD1 and LAG3 and display impaired proliferation and IFNγ/TNFα production [203,204]. The synergistic interplay between LAG3 and PD1 was observed in multiple murine cancer models, as demonstrated using anti-LAG3 and anti-PD1 or *Lag3*$^{-/-}$*Pdcd1*$^{-/-}$ mutant mice [203]. For instance, LAG3/PD1 dual-blockade resulted in MC38 tumor clearance in 80% of mice, compared to 40% remission in PD1 mono-blockade, but almost no effect in LAG3 mono-blockade [203]. Furthermore, LAG3 and PD1 dual blockade during T cell priming efficiently augmented proliferation and cytokine production by NY-ESO-1-specific $CD8^+$ T cells from ovarian cancer patients [204]. All these data provide a rationale for clinical trials of combinatorial checkpoint blockade regimens including LAG3 targeting [205].

LAG3 is expressed on both Tregs and Tconvs as aforementioned, and it is unclear which T cell subset is predominantly impacted by LAG3 blockade in the current studies. $LAG3^+Foxp3^+$ Tregs have been seen in peripheral blood mononuclear cells (PBMC), lymph nodes (LNs), and tumor tissues of melanoma and colorectal cancer patients [206]. $LAG3^+CD49b^+$ Tr1 cells were shown to be associated with poor prognosis of colorectal cancer [207]. These data indicate an immuno-suppressive role for LAG3 in Tregs. Interestingly, a study has suggested that combining LAG3 blockade with specific anti-

tumor vaccination resulted in enhanced tumor-specific $CD8^+$ T cell activation, and this effect was independent of LAG3 expression on $CD4^+$ T cells, therefore supporting a direct role for LAG3 in regulating $CD8^+$ T cells [208]. Taken together, these previous findings dissecting the role of LAG3 and its modes of action in different T cell subsets may be the key to efficiently targeting LAG3 in the clinic.

Autoimmunity

Unlike *Ctla4*$^{-/-}$ mice, *Lag3*$^{-/-}$.B6 mice do not develop spontaneous autoimmune disease, indicating that LAG3 may not be required under a homeostatic state [113,209-211]. However, *Lag3* deficiency on the NOD background results in accelerated autoimmune diabetes with 100% penetrance even before WT littermates start to develop hyperglycemia [112,113]. LAG3 blockade at 7 weeks of age also accelerated disease onset in NOD mice [112]. Similarly, genetic ablation or blockade of LAG3 on the B6.SJL background resulted in increased susceptibility to mercury-induced autoimmunity [212]. The synergistic cooperation between LAG3 and PD1 has also been observed in maintaining immune homeostasis and preventing autoimmunity. *Lag3*$^{-/-}$*Pdcd1*$^{-/-}$ B6 mice succumb to lethal systemic autoimmunity, which is not evident in either *Pdcd1*$^{-/-}$ or *Lag3*$^{-/-}$ B6 mice [113,203].

Together, these data suggest that LAG3 is essential in maintaining self-tolerance when other tolerance mechanisms are compromised, and that LAG3 may mediate distinct functions in different immune subsets. However, many questions remain unclear: (1) On which immune population(s) does LAG3 play a dominant role in regulating self-tolerance? (2) What is the relative contribution of LAG3 expressed on autoreactive T cells vs. Tregs? (3) What is the cell-intrinsic vs. cell-extrinsic impact of LAG3 on T cell subsets? (4) What

are the transcriptional and functional differences between LAG3^{+} vs. LAG3^{-}, and *Lag3*-deficient T cells? Therefore, *Lag3* conditional knockout mice that could also report *Lag3* promoter activity in combination with immune subset-specific CRE mice were developed to address these questions.

2.0 Chapter 2: Materials and methods

Note: Most of the following methods were published in my previous publication "Zhang Q *et. al. Sci. Imm.* (2017)"

2.1 Mice and study design

NOD/ShiLtJ (stock# 001976), Thy1.1.NOD (stock# 004483), BDC2.5.NOD (stock# 004460), and *Foxp3*^{GFP}.NOD (stock# 025097) mice were purchased from Jackson Laboratories. Foxp3$^{CRE-GFP}$.NOD mice were obtained from J.A. Bluestone [213]. Cd4^{CRE}.NOD mice were obtained from A. Chervonsky. *Lag3*$^{-/-}$ C57BL/6 mice were obtained from Y.H. Chen with permission from C. Benoist and D. Mathis [112,214], and E8i$^{CRE-GFP}$ C57BL/6 mice were obtained from I. Taniuchi, and both mice were bred onto an NOD background with 100% NOD as determined by single nucleotide polymorphism microsatellite analysis.

All animal experiments were performed in American Association for the Accreditation of Laboratory Animal Care-accredited, specific-pathogen-free facilities in Animal Resource Center [St Jude Children's Research Hospital (SJCRH)] and Division of Laboratory Animal Resources [University of Pittsburgh School of Medicine (UPSOM)]. Animal protocols were approved by the Institutional Animal Care and Use Committees (IACUC) of SJCRH and UPSOM. Mice of different groups were co-housed and randomly assigned to any analyses. Ten to twenty mice per group were used in diabetes incidence

studies and followed up to 30wk-of-age. Three to five age-matched female mice per group were used in each analytical experiment, and two to four independent experiments were repeated. Three female mice at indicated age were pooled per group and used in RNAseq analyses, and two to three independent experiments were repeated. The genotypes were not blinded, except for the insulitis scoring. All data points were presented.

2.2 Generation of *Lag3*$^{L/L\text{-}YFP}$ mice

A 5.7 kb *Xba*I-*Sal*I fragment (5' arm of homology) corresponding to exon 6 and the intronic region between exon 5 and 6 and a 4.1 kb *Cla*I-*Eco*RI fragment (3' arm of homology) containing the polyA site (pA) were generated by PCR from C57BL/6J genomic DNA and cloned into pSP73. A fragment corresponding to exon 7 (containing the CP cleavage site and flanked by loxP sites) and exon 8 was inserted between the two homologous arms. An IRES-YFP fragment was inserted between *Lag3* stop codon and the pA. Just after the pA, a frt-flanked neomycin positive selection cassette (Frt-Neo) was inserted. To increase the frequency of homologous recombination and reduce non-specific integration, a diphtheria toxin cassette (DT-A) was cloned upstream of the 5' homologous arm. The resulting plasmid was linearized with *Ssp*I and electroporated into E14 ES cells. Following selection with G418, resistant clones were screened by Southern blot analysis, sequenced, injected into blastocycts and the resulting chimeras bred to C57BL/6J for germline transmission. The mice were backcrossed 12 generations onto the NOD background and tested by microsatellite analysis. All 20 *Idd* loci were covered by 144

single nucleotide polymorphisms (SNPs) in the microsatellite test [43], and all the tested SNPs were NOD. The *Lag3*$^{L/L\text{-}YFP}$ mouse was generated by **Dr. Andrea Szymczak-Workman**.

Primers 5'-GCA GGT CTC AGC AGC TCC GC-3' and 5'-GTC AGA AGT GAG GGC TCT TTG GAG C-3' were used for detecting WT *Lag3* 3'UTR, and primers 5'-GAC TTC AAG GAG GAC GGC AAC ATC C-3' and 5'-GTC AGA AGT GAG GGC TCT TTG GAG C-3' were used for detecting IRES-YFP inserted into the 3'UTR. Primers 5'-CGC CTA GAC AAC CCG CAC-3' and 5'-GGT ACT CGC CCG CAT CG-3' were used for detecting *Lag3* Exon3, and primers 5'-AGG CCA TCT CGT TCT CGT TC-3' and 5'-CCA CCA GTG AAA GCC AAA GG-3' were used for detecting *Lag3* Exon7.

2.3 Measurement of diabetes and insulitis

Diabetes and insulitis were assessed as previously described [112,215]. Briefly, diabetes incidence was monitored weekly by testing for the presence of glucose in the urine by Diastix (Bayer). Mice positive by Diastix were then bled and tested with a Breeze2 glucometer (Bayer). Mice were considered diabetic if the blood glucose level was ≥ 400 mg/dl.

Pancreata were embedded in paraffin block and cut at 4μm-thick sections at 150μm step sections and stained with H&E. Pancreata collected at SJCRH were processed at the Veterinary Pathology Core of SJCRH, and pancreata collected at UPSOM were repeated in the same way at HISTO-SCIENTIFIC Research Laboratories (HSRL Inc.) for the histology shown in Chapter 4. An average of 60-80 islets per mouse

were scored in a blinded manner. Two methods of insulitis measurement were used as previously [215].

2.4 Islet isolation and lymphocyte preparation

Islets were isolated as described previously [216]. Briefly, the pancreata were perfused with 3mL of collagenase type 4 (Worthington) through the pancreas duct and incubated in 3mL of collagenase (600 U/mL in HBSS with 10% FBS) at 37°C water bath for 30min. The pancreata were then distributed and washed twice with HBSS (Corning) with 10% FBS. The islets were picked under a dissecting microscope, distributed with 1mL of cell dissociation buffer (life technology) and incubated at 37°C for 15min with vortexing every 5min. Following a final wash, the cells were resuspended, counted and used.

2.5 Antibodies and flow cytometry

Single cell suspensions were stained with antibodies against CD4 (clone# GK1.5, Biolegend), CD8β (clone# YTS156.7.7, Biolegend; clone# H35-17.2, eBioscience), TCRβ (clone# H57-597, Biolegend), Vβ4 (clone# KT4, BD Biosciences), Thy1.1 (clone# OX-7, Biolegend), Thy1.2 (clone# 30-H12, Biolegend), CD45RB (clone# C363-16A, Biolegend), CD44 (clone# IM7, Biolegend), CD62L (clone# MEL-14, Biolegend), CD25 (clone# PC61, Biolegend), LAG3 (clone# 4-10-C9, made in house), Foxp3 (clone# FJK-16s, eBioscience; clone# 150D, Biolegend), Eos (clone# ESB7C2, eBioscience), Helios

(clone# 22F6, Biolegend), Ki67 (clone# B56, BD Biosciences), BrdU (clone# Bu20a, Biolegend), Bcl2 (clone# BCL/10C4, Biolegend), TNFα (clone# MP6-XT22, Biolegend), IFNγ (clone# XMG1.2, Biolegend), IL2 (clone# JES6-5H4, Biolegend), IL4 (clone# 11B11, eBioscience), IL17A (clone# TC11-18H10.1, Biolegend), GATA3 (clone# TWAJ, eBioscience), RORγt (clone# B2D, eBioscience), PD1 (clone# RMP1-30, Biolegend), TIM3 (clone# RMT3-23, Biolegend), TIGIT (clone# GIGD7, eBioscience), KLRG1 (clone# 2F1, eBioscience), ICOS (clone# C398.4A, Biolegend), phospho-Stat5 (Clone# C71E5, Cell Signaling), CD127 (clone# A7R34, Biolegend), Eomes (clone# Dan11mag, eBioscience), CD28 (clone 37.51, Biolegend).

Surface staining was performed on ice for 15min.

For cytokine expression analysis, cells were activated with 0.1μg/mL PMA (Sigma) and 0.5μg/mL Ionomycin (Sigma) in RPMI containing 10% FBS and Monensin (eBioscience) for 5hr. For intracellular staining of cytokines and transcription factors, cells were stained with surface markers, fixed in Fix/Perm buffer (eBioscience) for 0.5-2hr, washed in permeabilization buffer (eBioscience) twice and stained intracellular factors in permeabilization buffer for 30min on ice.

For phosphoprotein staining, cells were fixed with 1.6% PFA (Alfa Aesar) at 37°C for 15min, permeablized with ice-cold Methanol for 1hr, and stained on ice for 1hr.

For BrdU incorporation analysis, mice were injected with 2mg BrdU (Sigma) in PBS intraperitoneally 8hr ahead of sacrifice. After transcription factor staining, cells were incubated in Cytofix/Cytoperm buffer (BD Biosciences) at room temperature for 10min, washed with PermWash buffer (BD Biosciences), treated with 650U/mL DNase I (Sigma)

at 37°C for 30min, and stained with anti-BrdU antibody in PermWash buffer for 30min at room temperature.

Chromogranin $A_{29\text{-}42}$ (BDC2.5 mimotope, AHHPIWARMDA/A^{g7}) tetramer, insulin $B_{9\text{-}23}$ (InsB p8E mimotope, HLVERLYLVCGEEG/ A^{g7}; InsB p8G mimotope, HLVERLYLVCGGEG/ A^{g7}) tetramers, insulin $B_{15\text{-}23}$ (InsB G9L mimotope, LYLVCGERL/ H-$2K^{d}$; InsB G9V mimotope, LYLVCGERV/ H-$2K^{d}$) tetramers, and $IGRP_{206\text{-}214}$ (NRP-v7 mimotope, KYNKANVFL/H-$2K^{d}$) tetramer were obtained from NIH Tetramer Core Facility, and cells were stained in RPMI containing 10% FBS at room temperature for 40min.

Cells were sorted on Aria II (BD Biosciences) or analyzed on Fortessa (BD Biosciences), and data analysis was performed on FlowJo Version 9 or 10 (Tree Star).

2.6 Micro-suppression assay

Splenic TCRβ^{+}CD4^{+}CD45RB^{+}GFP^{-} cells were sorted from Foxp3$^{CRE\text{-}GFP}$.NOD mice as responder cells and labeled with CellTrace Violet (life technology). T cell-depleted whole splenocytes were treated with 2μg/ml mytomycin C (Sigma) at 37°C for 30min, washed three times with PBS, and then used as antigen presenting cells (APCs). Responder cells ($4x10^3$), APCs ($8x10^3$), and different concentrations of Treg cells were activated with 2μg/ml anti-CD3 (Biolegend) in a 96-well round bottom plate with 100ul RPMI for 3 days. Suppression was calculated as previously described [217]. Briefly, cells were acquired by BD Fortessa, and the division index (DI) of responder cells was analyzed using FlowJo based on the division of CellTrace Violet. Suppression was then calculated with the formula %Suppression = (1-DI_{Treg}/DI_{Ctrl}) x 100% (DI_{Treg} stands for the division index of

responder cells with Treg cells, and DI_{Ctrl} stands for the division index of responder cells activated without Treg cells).

2.7 Treg expansion and adoptive transfer

Splenic TCRβ^+CD4$^+$GFP$^+$CD45RB^{low} cells (Treg cells) were sorted and activated with 0.1μg/mL PMA (Sigma) and 0.5μg/mL Ionomycin (Sigma) with 500U/mL hIL2 (Prometheus) for 2 days, and then expanded for another 3 days with hIL2. WT and *Lag3*-deficient Treg cells were mixed at equal ratio and $2x10^6$ total Treg cells were co-transferred into 6-8 wk-of-age WT NODs. Treg recipients were sacrificed and analyzed 4 days post-transfer.

2.8 *Ikzf4* overexpression and knockdown in Tregs

Human *IKZF4* ORF was amplified from *IKZF4*-pMIG construct (obtained from C. Benoist [157]) using primers (forward: 5'-CGC GGC TCT AGA TCT GCC AGC ATG CAT ACA CCA CCC GCA CTC C, reverse: 5'-CCT TCC ATC CCT CGA GCT AGC CCA CCT TAT GCT CCC CC), cut with *BglII* and *XhoI* restriction enzymes, and ligated into the pMI-Ametrine retroviral vector. Murine *Ikzf4* targeting shRNA (3'-TCC AGA AAG AGG ATG CGG CAG T, 5'-CCT GCC GCA TCC TCT TTC TGG A, loop-TAG TGA AGC CAC AGA TGT A) and non-targeting control (3'-TAA CCT ATA AGA ACC ATT ACC A, 5'- CGG TAA TGG TTC TTA TAG GTT A, loop-TAG TGA AGC CAC AGA TGT A) retroviral constructs (transOMIC

technologies) were cut with *BglII and MluI* restriction enzymes, and inserted with the IRES-Ametrine cassette as a fluorescence reporter.

Sorted splenic Treg cells were activated with αCD3/αCD28 dynabeads (Invitrogen) and 500U/mL IL2 for 48hr. Plat-E cells (obtained from H. Chi) were transiently transfected by retroviral vector along with pCL-Eco helper plasmid (obtained from H. Chi). Viral supernatant was harvested 36hr after transfection of Plat-E cells, and then used for spin transduction of activated Treg cells with 6μg/mL polybrene (Sigma) at 2000rpm for 1hr. Transduced Treg cells were sorted 48hr post transduction, rested for 72hr, and then re-stimulated with 0.1μg/mL PMA and 0.5μg/mL Ionomycin with 500U/mL hIL2 for another 48hr. 10μg/mL BrdU was pulsed into Treg culture media 2hr prior to the staining.

2.9 vi-SNE clustering

Flow cytometric data were initially analyzed and processed using FlowJo Version 9 (Tree Star). Samples were downsampled to 20,000 total cells per sample. Processed .fsc files were then imported into MATLAB platform (MathWorks), and vi-SNE plots were generated using cyt (Dana Pe'er Laboratory) [218].

2.10 Statistical analyses

Experiments were pooled for statistical analyses using Prism Version 7 (GraphPad). The log-rank test was applied to Kaplan-Meier survival function estimates to determine the

statistical significance of differences in diabetes incidence between experimental groups. The Fisher's LSD test was applied to one-way ANOVA to determine the statistical significance in the *Ikzf4* overexpression or knockdown experiments. The Spearman r was calculated to determine the correlation between any give two parameters. The nonparametric Mann-Whitney test was used in all other instances.

The statistical analyses were guided and overseen by **Dr. Daniel Normolle** at Department of Biostatistics, University of Pittsburgh.

2.11 Low cell number T cell repertoire sequencing

Tregs were sorted from either the ndLN or islet of individual mice. Treg gDNAs were isolated using the QIAamp DNA Micro kit (QIAGEN). TCR sequencing libraries were prepared using the mmTCRB immunoSEQ kit (Adaptive biotechnologies), pooled, diluted, and natured to a final concentration of 1pM with 20% PhiX spike-in control (Illumina). Cluster generation and 156x15bp paired-end single-indexed sequencing was performed on Illumina NextSeq 500 system. Data were analyzed on the immunoSEQ Analyzer platform (Adaptive biotechnologies).

Clonality is calculated as (1-normalized entropy), where normalized entropy is entropy/$\log_2$(productive unique β chain). Clonality ranges from 0 to 1. A low clonality indicates a relative diverse sample, while a high clonality number indicates that the sample is dominated by a few high-frequent clones.

Repertoire overlap between samples was calculated as Morisita Index $C_D = \frac{2\sum_{i=1}^{S} x_i y_i}{(D_x + D_y)XY}$ [219]. x_i is the number of times that clone *i* is represented in the total productive TCRs *X* sequenced from sample *x*, and y_i is the number of times that clone *i* is represented in the total productive TCRs *Y* sequenced from sample *y*. D_x and D_y are the Simpson's index values for the *x* and *y* samples, respectively. *S* is the number of unique clones. C_D = 1 if the two samples do not have any shared clones, and C_D = 1 if the same clones occur in the same frequencies in both samples.

2.12 Low cell number RNA sequencing

2.12.1 RNA-seq in Chapter 4.1

Tregs ($5x10^3$) were sorted from three pooled mice of each group and cDNAs were prepared using the SMATer® Ultra™ Low Input RNA Kit for Sequencing - v3 following the user manual (Clontech Laboratories). Sequencing libraries were prepared using Nextera XT DNA Library Preparation kit (Illumina), normalized at 2nM using Tris-HCl (10mM, pH 8.5) with 0.1% Tween20, diluted and denatured to a final concentration of 1.8pM using the Illumina Denaturing and Diluting libraries for the NextSeq 500 protocol Revision D (Illumina). Cluster generation and 75x75bp paired-end dual-indexed sequencing was performed on Illumina NextSeq 500 system.

2.12.2 RNA-seq in Chapter 3.2 and 4.2

Cell-of-interest (500 cells in total) were double-sorted from three pooled mice of each group directly into lysis buffer, and cDNAs were prepared based on the Smart-seq2 technique with a few steps modified [220]. Sequencing libraries were prepared using Nextera XT DNA Library Preparation kit (Illumina), normalized at 2nM using Tris-HCl (10mM, pH 8.5) with 0.1% Tween20, diluted and denatured to a final concentration of 1.8pM using the Illumina Denaturing and Diluting libraries for the NextSeq 500 protocol Revision D (Illumina). Cluster generation and 75bp single-end dual-indexed sequencing was performed on Illumina NextSeq 500 system.

I have put some effort on setting up the protocol to sequence a small number of cells ($\leq$ 500 cells) in the lab. For a detailed step-by-step protocol, please see the **Appendix C**.

2.13 Bioinformatics

2.13.1 Analyses in Chapter 4.1

The raw reads of RNA sequencing were aligned to the mm10 genome using TopHat and counts were computed relative to the RefSeq transcript annotation file provided in the cufflinks suite [221,222]. Genes whose mean count value (computed in $\log_2$ space) was below 32 (5 in $\log_2$ space) were removed from further processing leaving 10371 total

genes. The counts were analyzed for differential expression using DESeq2 with a GC content and length dependent offset computed by cqn R package [223,224].

We performed geneset analysis using the Wilcoxon rank-sum test on the differential expression statistic (Wald statistic for the Negative Binomial coefficient) computed from with the DESeq2 package. Significance was assessed with a parametric *p*-value calculation followed by multiple hypothesis correction as well as sample permutation tests. Since there are three replicates of islet Treg samples of each genotype, there are ten possible ways to divide those into two equal groups, and one of these corresponds to the correct grouping leaving 9 remaining permutations. Pathways that were significant at FDR of 0.2 but were not significant in any of the possible permutation tests were reported. Principle component analysis was performed using the "prcomp" R function on the $\log_2$ transformed normalized counts produced by the DESeq2 "counts" function with "normalized=T".

We retrieved processed data from the GEO accession GSE17166. As this dataset had no replicates we used fold change between the Eos siRNA and control siRNA as a reference. Genes that had expression levels less than $\log_2$ (intensity) of 5 as well as genes that were affected more than 2-fold by the control siRNA were excluded from the analysis. The significance of the association between the two transcriptional signatures was assessed using a Chi-squared test on the contingency table summarizing the number of up- or down-regulated genes in si-*Ikzf4* Treg cells and intra-islet Treg cells.

The bioinformatics analysis was performed by **Dr. Maria Chikina** at Department of Computational and Systems Biology, University of Pittsburgh School of Medicine.

2.13.2 Analyses in Chapters 3.2 and 4.2

The initial quality of raw sequence reads was checked using FastQC. After adaptor sequences were removed, and reads of low quality were trimmed using Trimmomatic, the quality of trimmed reads was checked again using FastQC. Filtered fastq files were aligned to the mm10 genome using STAR, and counts were computed and normalized using the PROT suite. Downstream analysis was carried out using limma and voom packages. (PORT: Pipeline of RNA-seq Transformations)

The bioinformatics analysis was performed by **Dr. Sasikanth Manne** at Department of Microbiology and Institute for Immunology, Perelman School of Medicine, University of Pennsylvania.

3.0 Chapter 3: Role of LAG3 in regulating diabetogenic T cells

Preface:

Co-inhibition is critical to modulate T cell activation and immune responses. Insufficient co-inhibition can lead to a breakdown of self-tolerance, leading to autoimmunity [70]. The co-inhibitory receptor LAG3 may not be required under a homeostatic state, but is critical to maintain self-tolerance when other tolerance mechanisms are compromised [113,203,209]. *Lag3* deficiency on the NOD background results in accelerated autoimmune diabetes with 100% penetrance, indicating an essential role for LAG3 in regulating autoimmune diabetes [112,113]. As LAG3 is expressed on activated $CD4^+$ and $CD8^+$ T cells, Tregs, pDCs and NK cells [172,185,186,189], it remains to be determined which immune subset(s) that LAG3 is expressed on predominantly mediate the immune suppression on autoimmune diabetes.

In this Chapter, two main questions will be addressed: (1) Which immune subset(s) that LAG3 is expressed on play a dominant role in regulating autoimmune diabetes? (2) What is the impact of LAG3 on diabetogenic $CD8^+$ T cells?

To dissect the role of LAG3 on different immune subsets, *Lag3*$^{L/L\text{-}YFP}$ conditional knockout-reporter mice [225] are crossed with several T cell subset-specific CRE mice (*Lag3*$^{L/L\text{-}YFP}$Cd4^{CRE}.NOD [226], *Lag3*$^{L/L\text{-}YFP}$E8i$^{CRE\text{-}GFP}$.NOD [227], and *Lag3*$^{L/L\text{-}YFP}$Foxp3$^{CRE\text{-}GFP}$.NOD [213] in comparison to *Lag3*$^{-/-}$.NOD mice [112]). The *Lag3*$^{L/L\text{-}YFP}$ mouse was generated by generated by Dr. Andrea Szymczak-Workman (University of Pittsburgh), a former research scientist in our lab.

This project is a part of the PO1 project “Synergies among inhibitory receptors in tolerance, cancer and antiviral immunity” in collaboration with Dr. Arlene Sharpe’s laboratory (Harvard Medical School) and Dr. John Wherry’s laboratory (University of Pennsylvania). The bioinformatics analysis (Fig. 11) was done by Dr. Sasikanth Manne (University of Pennsylvania).

Some figures in this chapter are taken from the publication “Zhang Q *et. al. Sci. Imm.* (2017)” [225] under the journal’s copyright permission. These figures include Fig. 3, Fig. 5, and Fig. 6 corresponding to Fig. 1 (and fig. S1), fig. S2, and Fig. 2B of the manuscript “Zhang Q *et. al. Sci. Imm.* (2017)”, respectively [225]. All other figures in this chapter are unpublished data.

3.1 A predominant role for LAG3 on T cells in autoimmune diabetes

3.1.1 LAG3 is highly upregulated on T cells at inflammatory sites

To evaluate the relative contribution of LAG3 on T cells versus non-T cells, we first assessed LAG3 expression pattern on different immune subsets at various ages of NOD mice. While non-T cells consisted only 6-12% of intra-islet $LAG3^+$ cells, a substantial fraction of insulitic $CD8^+$ T cells and Tregs upregulated surface expression of LAG3 compared to peripheral T cells (**Fig. 3**).

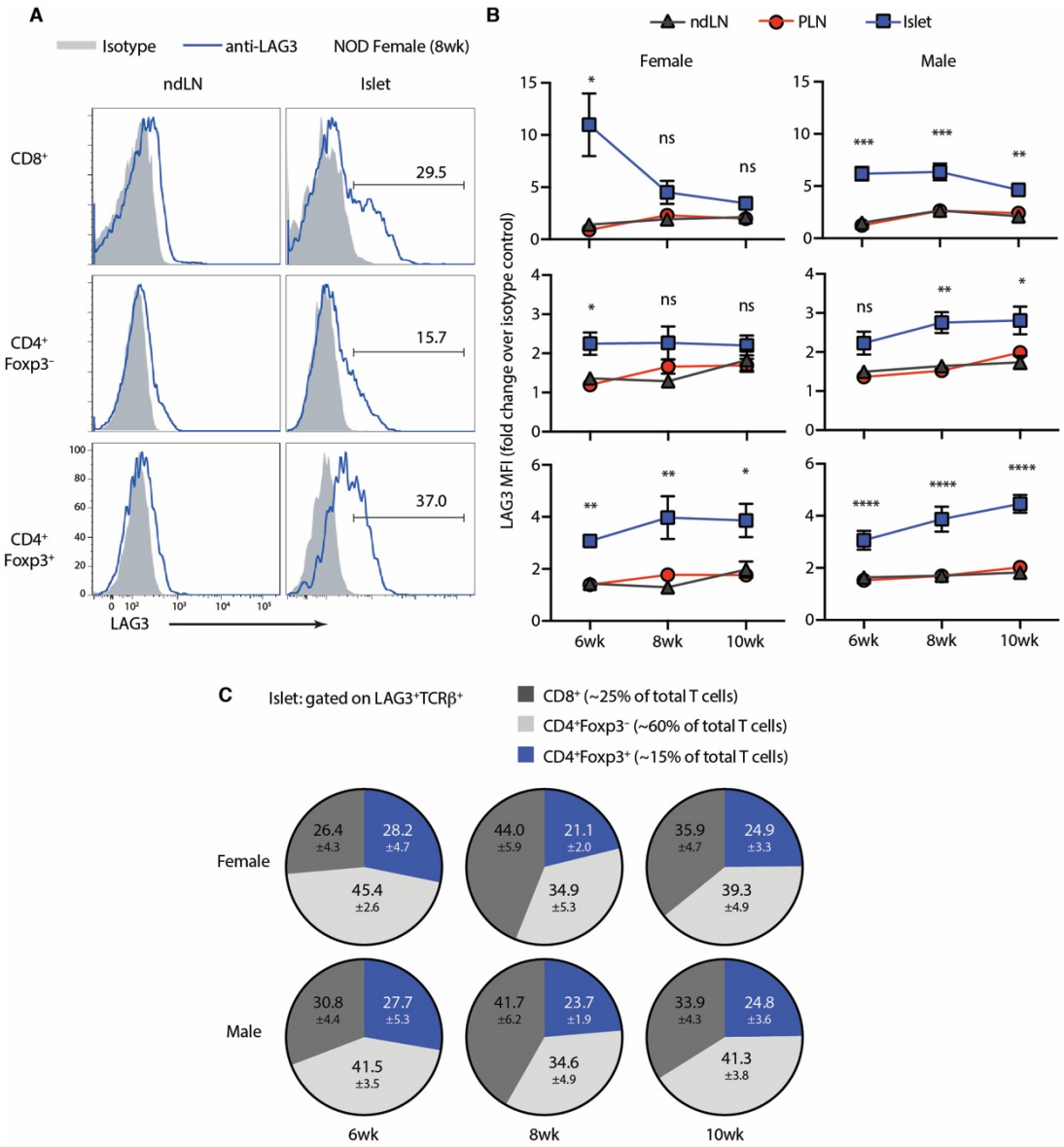

Figure 3. LAG3 is upregulated on intra-islet T cells.

(**A**) Representative histograms of LAG3 expression on the cell surface of CD8$^+$, CD4$^+$Foxp3$^-$, and CD4$^+$Foxp3$^+$ T cells in female WT NODs at 8 weeks of age. (**B**) Expression of LAG3 on CD8$^+$, CD4$^+$Foxp3$^-$, and CD4$^+$Foxp3$^+$ T cells of WT NODs at different ages (female, n = 5-6; male, n = 5-9). Statistical significance was determined by comparison of Islet and ndLN at each time point. (**C**) Proportion of CD8$^+$, CD4$^+$Foxp3$^-$, and CD4$^+$Foxp3$^+$ T cells in intra-islet LAG3$^+$ T cells. Data were presented as mean ± SEM. Nonparametric Mann-Whitney test was used in (B). ns, not significant; *p < 0.05, **p < 0.01, ***p < 0.001, ****p < 0.0001. This figure is taken from Fig. 1 and fig. S1 of the manuscript "Zhang Q, et al. *Sci. Immuno.* (2017)".

Unlike PD1, which is readily detected on peripheral T cells, in particular Tregs, in diseased mice, LAG3 expression appeared to be limited to pancreata of NOD mice or tumors of tumor-bearing B6 mice (**Fig. 4**). This suggests that the impact of LAG3 may be more restricted to tissue-specific tolerance.

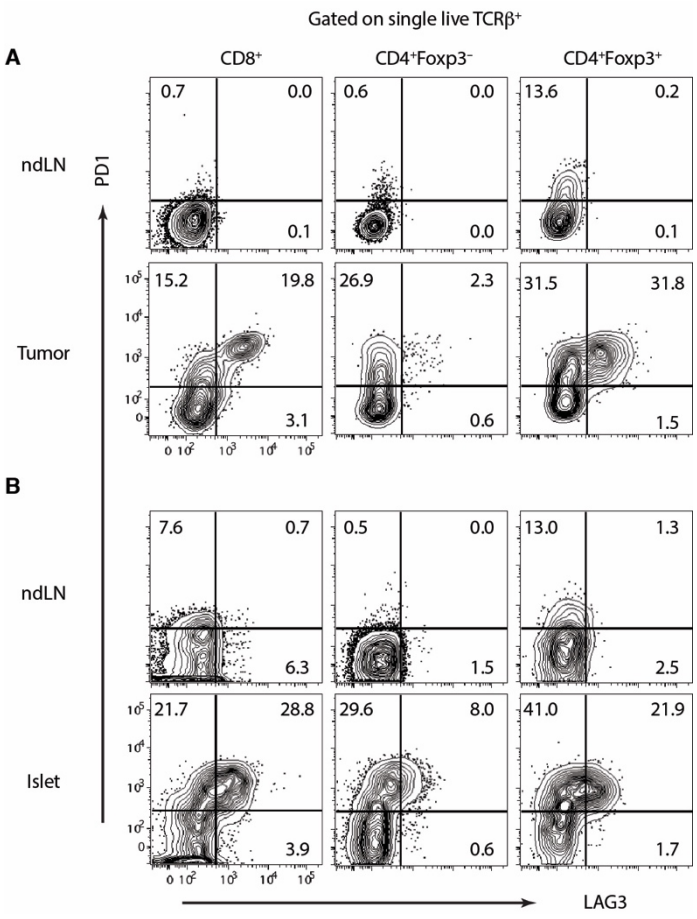

Figure 4. LAG3 expression is limited to inflamed tissues.

Representative flow plots of PD1 and LAG3 expression on the cell surface of $CD8^+$, $CD4^+Foxp3^-$, and $CD4^+Foxp3^+$ T cells from ndLN, and tumor of B16 tumor-bearing B6 mice (**A**) or islets of NOD mice (**B**). Female B6 mice were intradermally injected with 1.25 $x10^5$ B16.F10 melanoma cells, and tumors were harvested on day 12 post injection. The female NOD mice were analyzed at 8 weeks of age.

3.1.2 The predominant function of LAG3 in autoimmune diabetes is limited to $CD4^+$ and $CD8^+$ T cells

To assess the importance of LAG3 expression on different immune subsets in controlling autoimmune diabetes, we generated *Lag3*$^{L/L\text{-}YFP}$ conditional knockout-reporter mice (backcrossed to NOD/ShiLtJ for 12 generations – see Materials and methods) that lack cell surface expression of LAG3[177,190], and thus cannot mediate signaling but continue to release sLAG3, specifically on CRE^+ cells when crossed with cell-type specific CRE NOD mice (**Fig. 5**). Although there is no evidence that sLAG3 affects T cell function [177,190], we took this approach to avoid this complication. This mutant mouse also incorporated an IRES-YFP cassette inserted into the 3' UTR as a reporter of *Lag3* promoter activity (**Fig. 5**).

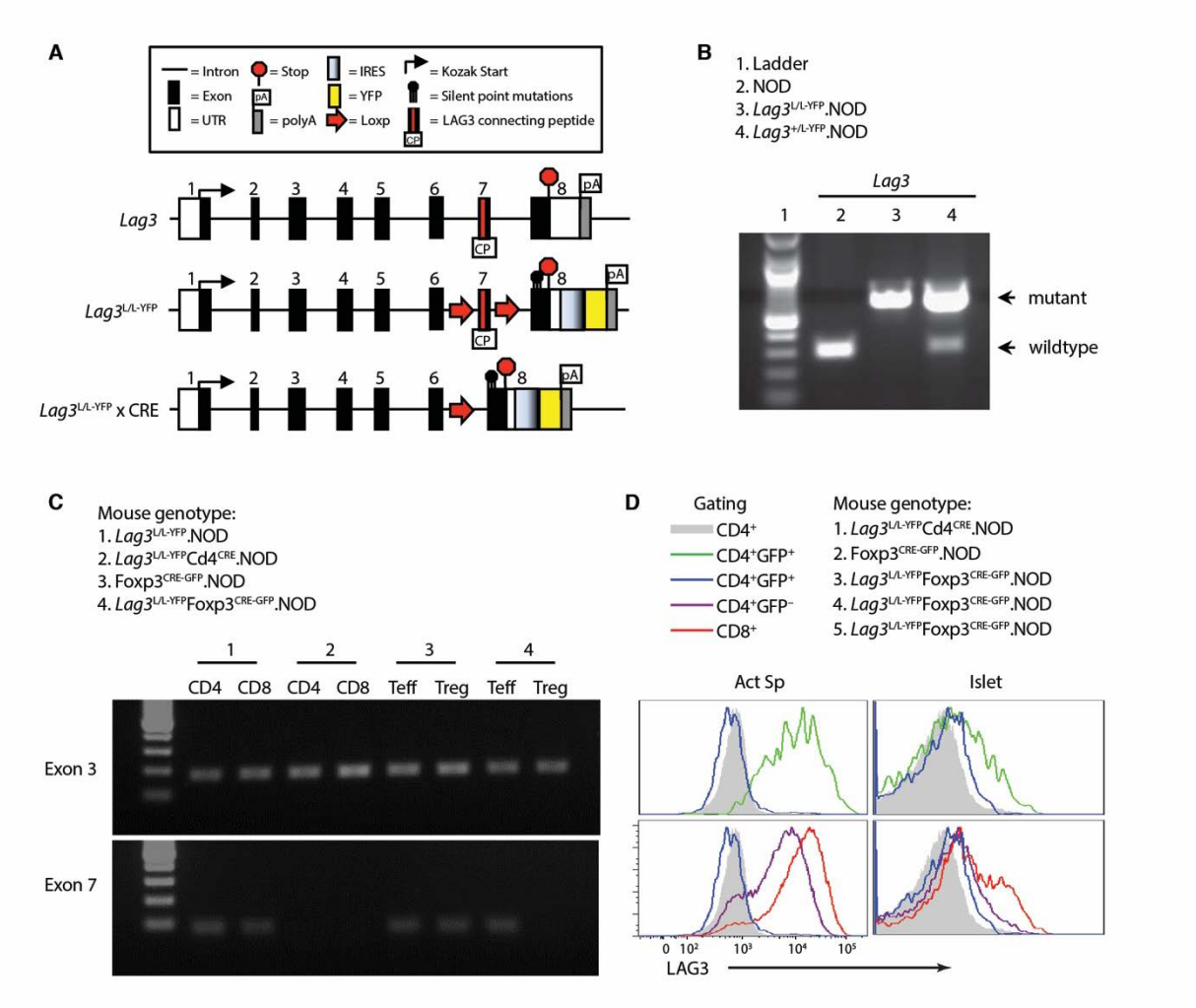

Figure 5. Generation and validation of *Lag3* conditional knockout-reporter mouse.

(A) Schematic of WT and *Lag3*$^{L/L\text{-}YFP}$ loci. (**B**) PCR products of the IRES-YFP cassette in genomic DNAs from mice shown. (**C**) PCR products of *Lag3* Exon3 and Exon7 in genomic DNAs from sorted cells shown. (**D**) Surface LAG3 expression assessed by flow cytometry. Act Sp, activated splenocytes. Splenocytes were activated with plate-bound αCD3 and αCD28 for 28 hours. This figure is taken from fig. S2 of the manuscript "Zhang Q, et al. *Sci. Immuno.* (2017)".

As LAG3 is mainly expressed on αβT cells among all the islet-infiltrating immune cells, we initially crossed *Lag3*$^{L/L\text{-}YFP}$.NOD with Cd4^{Cre}.NOD to assess the phenotype following global loss of surface LAG3 on all CD4^{+} and CD8^{+} T cells (**Fig. 5**). Loss of LAG3 surface expression on all CD4^{+} and CD8^{+} T cells (*Lag3*$^{L/L\text{-}YFP}$Cd4^{Cre}.NOD) resulted in dramatically accelerated onset of autoimmune diabetes with 100% penetrance by 12 weeks of age, which phenocopied our observations with *Lag3*$^{-/-}$.NOD mice and suggested that the dominant function of LAG3 was indeed limited to αβT cell populations (**Fig. 6**) [112].

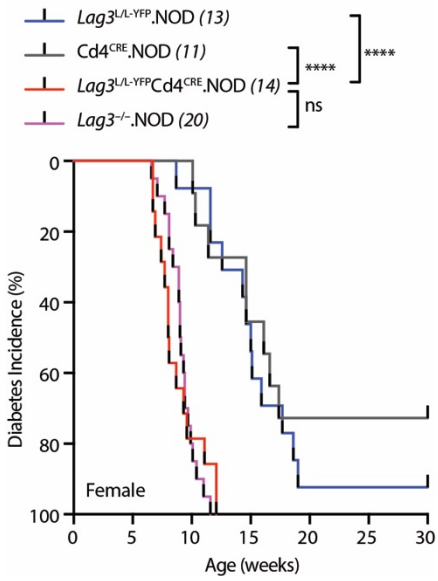

Figure 6. Loss of LAG3 on T cells results in accelerated autoimmune diabetes.

Diabetes onset and incidence monitored in *Lag3*$^{L/L\text{-}YFP}$Cd4^{CRE}.NOD females and co-caged littermate controls. The log-rank test was applied to Kaplan-Meier survival function estimates to determine the statistical significance. ns, not significant; ****$p < 0.0001$. This figure is taken from Fig. 2B of the manuscript "Zhang Q, et al. *Sci. Immuno.* (2017)".

3.2 Impact of LAG3 on selecting diabetogenic CD8$^+$ T cells

3.2.1 The absence of LAG3 on CD8$^+$ T cells results in accelerated autoimmune diabetes

Even though CD4$^+$Foxp3$^-$ T cells comprised ~60% of islet-infiltrating T cells, CD8$^+$ and CD4$^+$Foxp3$^+$ T cells expressed a much higher level of LAG3 than CD4$^+$Foxp3$^-$ T cells (**Fig. 3** and **4**), possibly due to differential regulation of LAG3 cleavage among T cell subsets. LAG3 was highly upregulated on intra-islet CD8$^+$ T cells, with a broad range of expression intensity (**Fig. 3, 4** and **7**), suggesting that heterogeneity of LAG3 expression exists within insulitic CD8$^+$ T cells. LAG3 was also co-expressed with other co-stimulatory and co-inhibitory receptors, consistent with an "exhausted" state in the pre-diabetic islets (**Fig. 7**). I reasoned that the expression of LAG3 on CD8$^+$ T cells might drive T cell exhaustion as seen in some of those teplizumab (anti-CD3) treated T1D patients and other diseases [56,228], and thus limit the pathogenesis of autoimmune diabetes.

To evaluate the impact of LAG3 on CD8$^+$ T cells, I crossed *Lag3*$^{L/L\text{-}YFP}$.NOD with E8i$^{CRE\text{-}GFP}$.NOD [227] mice carrying a CD8$^+$ T cell-specific CRE that is driven by CD8α enhancer (**Fig. 8**). Loss of LAG3 surface expression on CD8$^+$ T cells (*Lag3*$^{L/L\text{-}YFP}$E8i$^{CRE/CRE\text{-}GFP}$.NOD) resulted in accelerated autoimmune diabetes (**Fig. 9**), suggesting that LAG3 is required to limit the diabetogenicity of CD8$^+$ T cells.

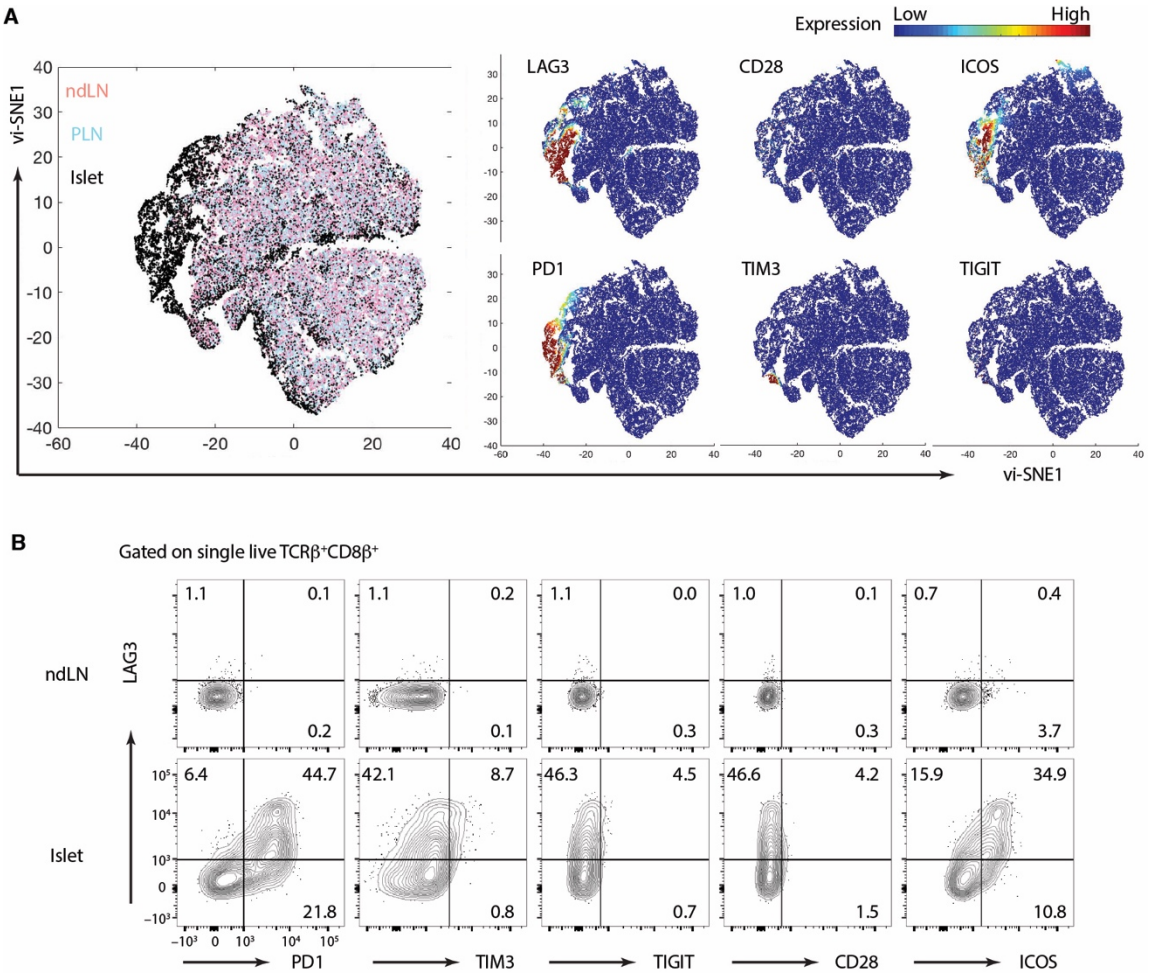

Figure 7. LAG3 is upregulated on insulitic CD8⁺ T cells.

(**A**) vi-SNE clustering of ndLN, PLN, and Islet CD8⁺ T cells of WT females NODs based on the expression of markers shown (8 weeks of age, n = 11). Expression of markers indicated were assessed using flow cytometry. Processed flow cytometric data were used for vi-SNE clustering, which allows mapping of high-dimensional cytometry data onto two dimensions. Each dot indicates a single CD8⁺ T cell. The heat map (left) indicates expression levels of markers shown. (**B**) Representative plots of receptor expression on CD8⁺ T cells.

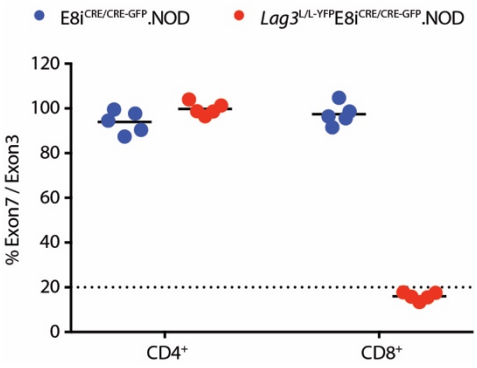

Figure 8. Deletion of *Lag3* Exon7 by E8i-CRE is specific to CD8$^+$ T cells.

qPCR quantification of *Lag3* Exon7 (targeted region) relative to Exon3 (non-targeted region) in genomic DNAs of sorted naïve splenic CD4$^+$ and CD8$^+$ T cells (n = 5 individual mice).

Consistent with accelerated diabetes, there was increased percentage of CD8$^+$ T cells but decreased percentage of Tregs in the islets of *Lag3*$^{L/L-YFP}$E8i$^{CRE/CRE-GFP}$.NOD mice (**Fig. 10A** and **B**). As LAG3-mediated signaling can be bidirectional, I reasoned that the increased CD8$^+$ to Treg ratio in the absence of LAG3 on CD8$^+$ T cells could result from the loss of extrinsic impact on Tregs, or the removal of an intrinsic effect on CD8$^+$ T cells. There was a trend, albeit not reaching significance, toward a higher number of intra-islet Tregs in the absence of LAG3 on CD8$^+$ T cells (**Fig. 10C**). There was no significant difference in the expression of CD73, CD39, CD25 (effector molecules for Treg function) [6] or Bcl2 (an anti-apoptotic factor) [229] in Tregs, either (data not shown). This indicates that the percentage of insulitic Tregs was relatively reduced because of an increased number of CD8$^+$ T cells in the absence of LAG3 on CD8$^+$ T cells.

Next, I assessed differences in WT vs. *Lag3*-deficient CD8$^+$ T cells. IGRP is one of the predominant β cell-specific autoantigens, and the NRP-v7 MHC-I tetramer contains an IGRP$_{206\text{-}214}$ mimotope that can be recognized by IGRP$_{206\text{-}214}$-reactive CD8$^+$ T cells [230]. The number of CD8$^+$ T cells and IGRP$_{206\text{-}214}$-reactive (NRP-v7$^+$) CD8$^+$ T cells were both substantially increased in the islets of *Lag3*$^{L/L\text{-}YFP}$E8i$^{CRE/CRE\text{-}GFP}$.NOD mice (**Fig. 10C**), indicating that the accelerated autoimmune diabetes observed in *Lag3*$^{L/L\text{-}YFP}$E8i$^{CRE/CRE\text{-}GFP}$.NOD mice was perhaps a consequence of uncontrolled autoimmune responses mediated by CD8$^+$ T cells. An increased number of CD4$^+$Foxp3$^-$ T cells was also observed in the pancreas of *Lag3*$^{L/L\text{-}YFP}$E8i$^{CRE/CRE\text{-}GFP}$.NOD mice perhaps because of

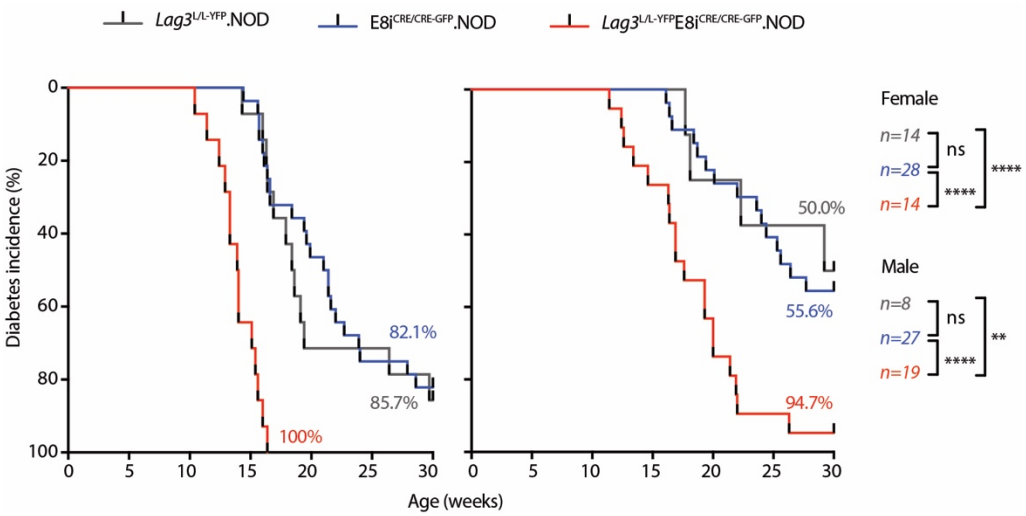

Figure 9. Loss of LAG3 on CD8$^+$ T cells results in accelerated autoimmune diabetes.

Diabetes onset and incidence monitored in *Lag3*$^{L/L\text{-}YFP}$E8i$^{CRE/CRE\text{-}GFP}$.NOD and co-caged littermate controls. The log-rank test was applied to Kaplan-Meier survival function estimates to determine the statistical significance. ns, not significant; $^{**}p < 0.01$, $^{****}p < 0.0001$.

enhanced inflammation in the islet (**Fig. 10C**), which may also contribute to the accelerated autoimmune diabetes of these mutant mice.

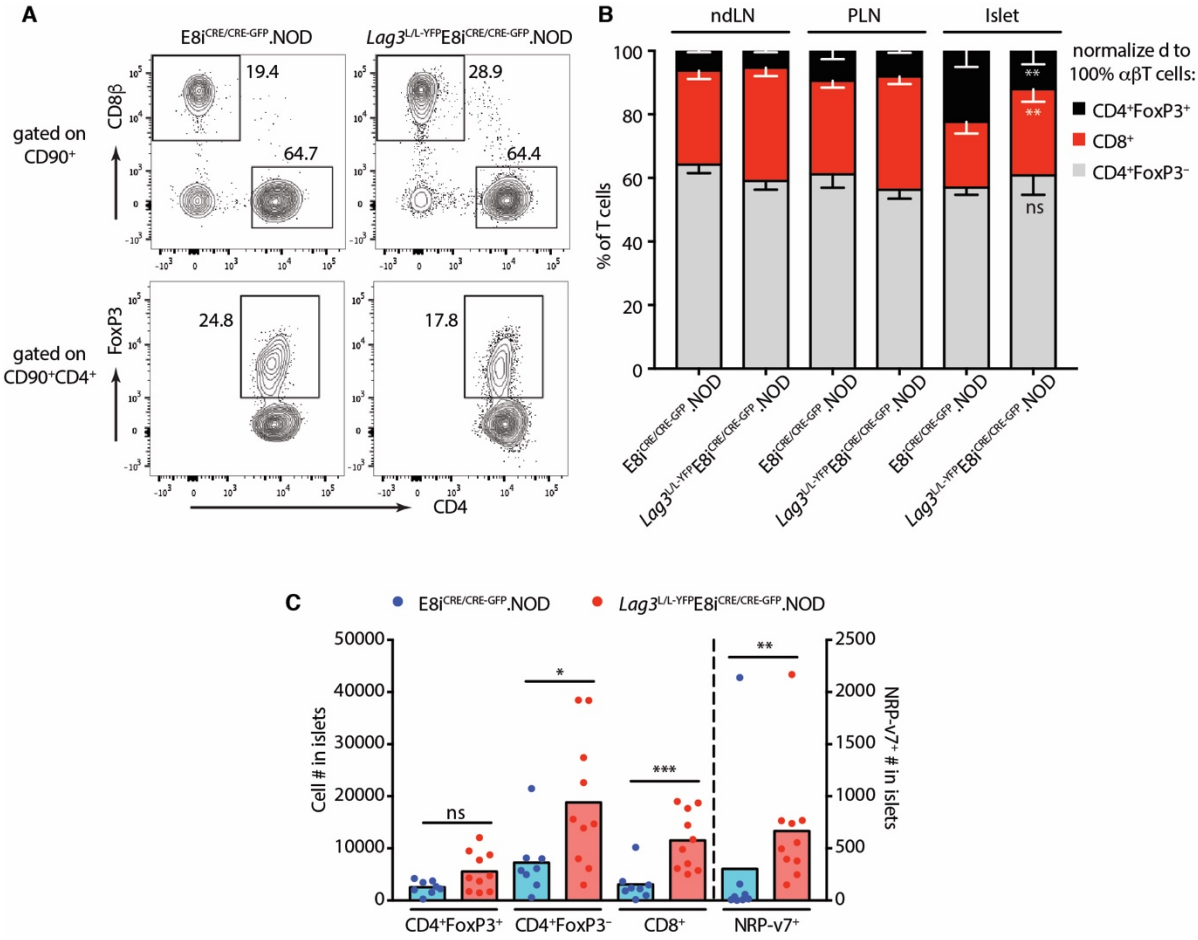

Figure 10. LAG3 limits insulitic CD8⁺ T cell number.

Representative flow plots (**A**), percent (**B**), and absolute number (**C**) of islet-infiltrating CD8⁺, CD4⁺Foxp3⁻, CD4⁺Foxp3⁺ T cells and NRP-v7⁺CD8⁺ T cells in *Lag3*$^{L/L\text{-}YFP}$E8i$^{CRE/CRE\text{-}GFP}$.NOD mice compared with cohoused controls (females, 8 weeks of age, n = 8 to 10, three independent experiments). Error bars indicate SEM. Horizontal black bars indicate means. Nonparametric Mann-Whitney test was used. ns, not significant; *p < 0.05, **p < 0.01, ***p < 0.001.

3.2.2 LAG3 intrinsically limits IGRP-reactive CD8$^+$ T cells to differentiate into pathogenic effector T cells

Next, I assessed the impact of LAG3 on CD8$^+$ T cell transcriptome and functionality. Since the *Lag3*$^{L/L\text{-}YFP}$ mouse incorporated the IRES-YFP cassette as a reporter for *Lag3* promoter activity (**Fig. 5**), I was able to partition insulitic CD8$^+$ T cells into *Lag3*$^–$ vs. *Lag3*$^+$ and "*Lag3*-wannbe" subsets based on YFP expression. *Lag3*-YFP$^+$CD8$^+$ T cells from *Lag3*$^{L/L\text{-}YFP}$E8i$^{CRE/CRE\text{-}GFP}$.NOD mice had a transcriptionally active *Lag3* promoter as indicated by the YFP expression but did not express LAG3 due to the genetic deficiency, so we refer these cells as "*Lag3*-wannabe" CD8$^+$ T cells.

I sorted *Lag3*-YFP$^+$ and *Lag3*-YFP$^–$ CD8$^+$ T cells from the islets of *Lag3*$^{L/L\text{-}YFP}$E8i$^{CRE/CRE\text{-}GFP}$.NOD and *Lag3*$^{L/L\text{-}YFP}$.NOD mice, as well as bulk CD8$^+$ T cells from ndLN and PLN as LAG3 expression was not evident in the periphery (**Fig. 3** and **7**), and subjected these samples to RNA sequencing analyses. CD8$^+$ T cell transcriptional profiles were substantially affected by the islet microenvironment, as insulitic CD8$^+$ T cells (square and circle) exhibited distinct transcriptomes compared to ndLN and PLN CD8$^+$ T cells (triangle and diamond, respectively). Furthermore, *Lag3*$^+$ and *Lag3*-wannabe CD8$^+$ T cells (circle) were also very different from the *Lag3*$^–$ cells (square) as indicated in the principle component analysis (PCA) plot (**Fig. 11**). However, the differences between WT (grey) and *Lag3*-deficient (red) CD8$^+$ T cells were not evident (**Fig 11**). Some variability was also observed among the WT and mutant intra-islet *Lag3*$^–$ subsets (**Fig 11**), probably because this subset consisted of cells that had never expressed *Lag3*-YFP and cells that

had once expressed *Lag3*-YFP but downregulated its expression at the moment when the transcriptome was captured.

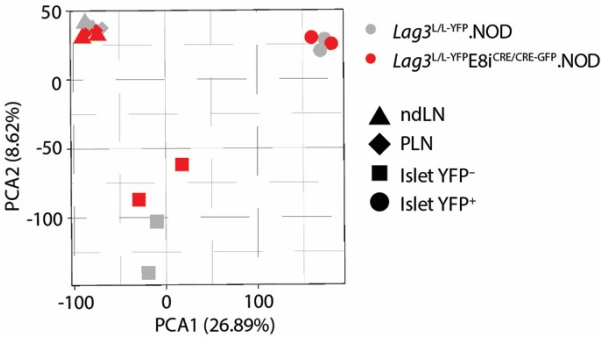

Figure 11. The effect of *Lag3* deletion on CD8⁺ T cell transriptome is not evident.

Principle component analysis of CD8⁺ T cell RNAseq profiles shown (females, 8 weeks of age, two independent experiments). Principal components PCA1 and PCA2, which explain 35.51% of the total variance observed, discriminate insulitic from peripheral CD8⁺ T cells and discriminate *Lag3*-YFP⁺ (either wildtype or *Lag3*-deficient) from *Lag3*-YFP⁻ CD8⁺ T cells.

Consistent with the transcriptional analysis, there were no significant differences in cytotoxic cytokine production [231] (IFNγ, TNFα, Granzyme B, **Fig. 12**), proliferation [232] (Ki67, **Fig. 13A**), effector vs. memory phenotypes [233] (Klrg1 vs. CD127, **Fig. 13C**) or expression of key CD8⁺ T cell transcription factors [233] (T-bet and Eomes, **Fig. 13B**) in the absence of LAG3 on CD8⁺ T cells. Both flow cytometric analyses and RNA sequencing analyses indicate that LAG3 may have very limited impact on CD8⁺ T cells at the bulk population level.

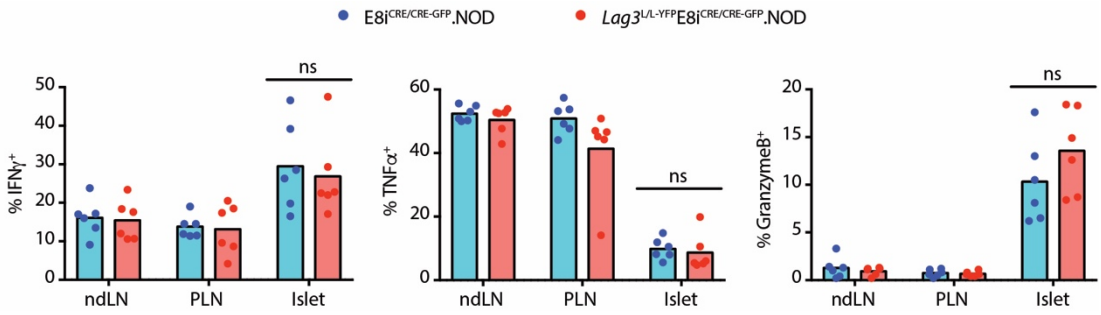

Figure 12. The absence of LAG3 does not affect cytokine production by CD8$^+$ T cells.

Percent of IFNγ$^+$, TNFα$^+$ and GranzymeB$^+$ cells in CD8$^+$T cells from *Lag3*$^{L/L-YFP}$E8i$^{CRE/CRE-GFP}$.NOD mice compared with cohoused controls (females, 8 weeks of age, n = 6, two independent experiments). Intracellular expression of IFNγ, TNFα and GranzymeB in CD8$^+$ T cells was assessed in the organs indicated after 5 hour *ex vivo* stimulation with PMA and ionomycin. Horizontal black bars indicate means. Nonparametric Mann-Whitney test was used. ns, not significant.

The lack of evident differences between WT and *Lag3*-deficient CD8$^+$ T cells suggested by RNA sequencing PCA and flow cytometric analyses was very surprising, as the accelerated autoimmune diabetes was quite dramatic in the absence of LAG3 on CD8$^+$ T cells (**Fig. 9**). Interestingly, slightly enhanced apoptosis (as indicated by Bcl2$^-$ aCasp3$^+$ staining) [229] was observed in insulitic *Lag3*-deficient CD8$^+$ T cells compared to WT CD8$^+$ T cells (**Fig. 14**), indicating that the absence of LAG3 expression may promote CD8$^+$ T cell death. I reasoned that the absence of LAG3 expression may lead to certain pathogenic CD8$^+$ T cell clones outcompeting others and contributing to the accelerated autoimmune diabetes observed in *Lag3*$^{L/L-YFP}$E8i$^{CRE/CRE-GFP}$.NOD mice.

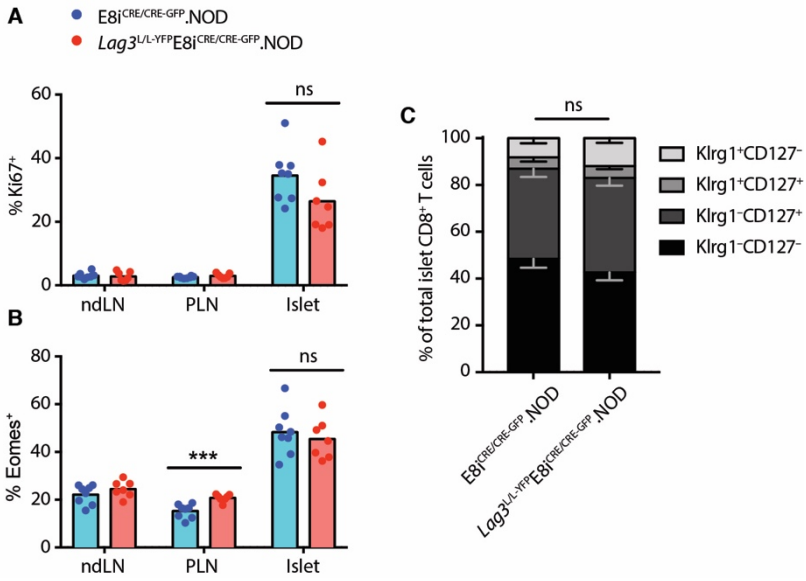

Figure 13. Phenotypic analysis of *Lag3*-deficient CD8⁺ T cells.

Flow cytometric analysis of markers shown in CD8⁺ T cells in *Lag3*$^{L/L\text{-}YFP}$E8i$^{CRE/CRE\text{-}GFP}$.NOD mice compared with cohoused controls (females, 8 weeks of age, n = 7 to 8, three independent experiments). Error bars indicate SEM. Horizontal black bars indicate means. Nonparametric Mann-Whitney test was used. ns, not significant.

Next, I questioned whether the impact of LAG3 was limited to a small subset of pathogenic CD8⁺ T cells, which might be correlated with the heterogeneous LAG3 expression in insulitic CD8⁺ T cells (**Fig. 3, 4,** and **7**). IGRP$_{206\text{-}214}$-reactive CD8⁺ T cells have been identified as a prevalent population of pathogenic CD8⁺ T cells in autoimmune diabetes, and it has been shown that autoimmune diabetes development is associated with the frequency of IGRP$_{206\text{-}214}$-reactive CD8⁺ T cells [230,234]. The absolute number and percentage of IGRP$_{206\text{-}214}$-reactive (NRP-v7⁺) CD8⁺ T cells were significantly increased in the absence of LAG3 on CD8⁺ T cells (**Fig. 10C, 15A** and **15B**). The increased

percentage of IGRP$_{206-214}$-reactive CD8$^+$ T cells in the absence of LAG3 expression was also positively correlated with enhanced Klrg1 expression [231,233], a marker of antigen-experienced effector cells (**Fig. 15C** and **15D**). Interestingly, we did not see similar differences in insulin B$_{15-23}$-reactive CD8$^+$ T cells [235] (**Fig. 15**), or at the whole population level (**Fig. 13C**), highlighting a potential role for LAG3 in the selection of certain pathogenic islet-antigen-reactive CD8$^+$ T cell clones. Taken together, these data suggest that LAG3 may selectively limit the ability of IGRP$_{206-214}$-reactive CD8$^+$ T cells to differentiate into pathogenic effectors.

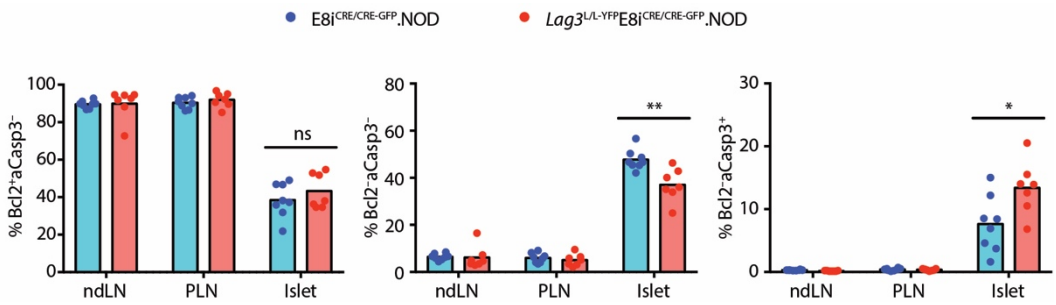

Figure 14. CD8$^+$ T cell apoptosis is enhanced in the absence of LAG3.

Flow cytometric analysis of markers shown in CD8$^+$ T cells in *Lag3*$^{L/L-YFP}$E8i$^{CRE/CRE-GFP}$.NOD mice compared with cohoused controls (females, 8 weeks of age, n = 7 to 8, three independent experiments). aCasp3: active Caspase-3. Horizontal black bars indicate means. Nonparametric Mann-Whitney test was used. ns, not significant; *p < 0.05, **p < 0.01.

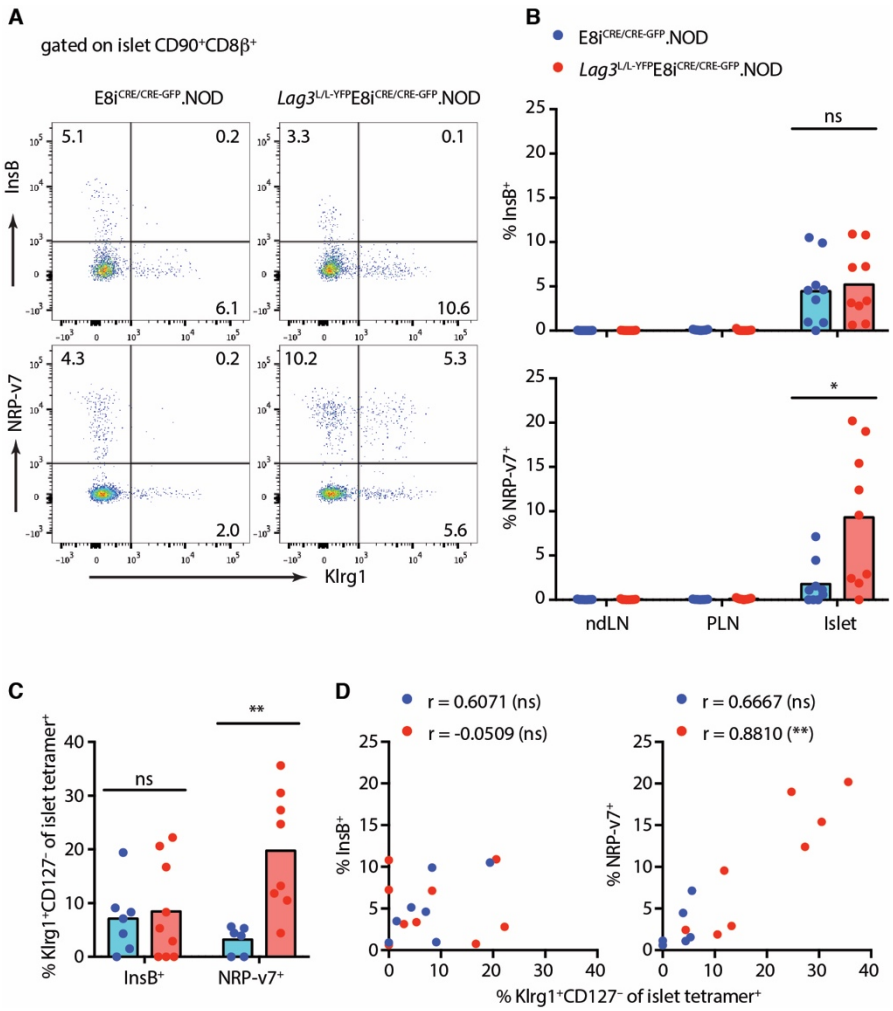

Figure 15. LAG3 limits IGRP-reactive CD8⁺ T cells differentiate into effector cells.

Representative flow plots (**A**) and percent (**B**) of tetramer⁺ cells in *Lag3*$^{L/L\text{-}YFP}$E8i$^{CRE/CRE\text{-}GFP}$.NOD mice compared with cohoused controls (females, 8 weeks of age, n = 9, three independent experiments). (**C**) Percent of Klrg1⁺CD127⁻ cells in tetramer⁺ cells as shown in (B), but only with the ones that have > 100 tetramer⁺ cells. (**D**) Correlation between the percent of tetramer⁺ cells and Klrg1 expression on tetramer⁺ cells. InsB: a cocktail of insulin $B_{15\text{-}23}$ mimotope H-2K^d tetramers; NRP-v7: $IGRP_{206\text{-}214}$ mimotope H-2K^d tetramer. Horizontal black bars indicate means. Nonparametric Mann-Whitney test was used in (B) and (C). Spearman r was calculated in (D). ns, not significant; *p < 0.05, **p < 0.01.

3.3 Summary and discussion

Previous work revealed that LAG3 is required to maintain self-tolerance in NOD mice [112,113]. Using *Lag3*$^{L/L\text{-}YFP}$ conditional knockout-reporter mice [225] in combination with T cell subset-specific CREs (*Lag3*$^{L/L\text{-}YFP}$Cd4^{CRE}.NOD [226] and *Lag3*$^{L/L\text{-}YFP}$E8i$^{CRE\text{-}GFP}$.NOD [227]) and in comparison to the *Lag3*-global knockout mouse [112], I was able to determine the relative contribution of LAG3 expressed on CD4$^+$ and CD8$^+$ T cells vs. non-T cells. LAG3 is highly upregulated on insulitic T cells, and its predominant expression on CD4$^+$ and CD8$^+$ T cells is necessary to limit the pathogenesis of autoimmune diabetes in NOD mice.

The loss of LAG3 on CD8$^+$ T cells alone is sufficient to promote early onset of autoimmune diabetes. LAG3 may function by selectively limiting IGRP-reactive CD8$^+$ T cells to differentiate into effector T cells. Even though LAG3 is expressed at a lower level on insulitic CD4$^+$Foxp3$^-$ T cells than CD8$^+$ T cells, it may also limit the pathogenicity of CD4$^+$Foxp3$^-$ T cells. Currently, there are no CD4$^+$ Teff-specific CRE mice, which limits our understanding of LAG3 function in regulating autoreactive CD4$^+$ T cells. However, a previous study has shown that transferring splenocytes that were reconstituted with *Lag3*-deficient CD4$^+$ Teffs was sufficient to promote accelerated autoimmune diabetes [112], indicating that LAG3 is also required to limit autoreactivity of CD4$^+$ T cells.

Notably, LAG3 expression is limited to the islet of NOD mice or the tumor of tumor-bearing mice (**Fig. 3** and **4**), indicating that it may have a more important role in tissue-specific tolerance than in systemic tolerance. This is in line with early findings that *Lag3*$^{-/-}$ mice on the B6 background do not develop spontaneous autoimmune disease, in contrast to *Ctla4*$^{-/-}$.B6 mice [209-211]. This may provide a good rationale to target LAG3 in

the clinic particularly when systematic effect needs to be avoided. However, it remains to be determined whether LAG3 is also expressed in other tissues. A recent finding suggests that LAG3 is also expressed in cerebellum and facilitates the pathogenesis of Parkinson's disease, indicating a role for LAG3 outside [182,185]. Additionally, LAG3 is also expressed on CD8$\alpha\alpha^+$ IELs (**Fig. 16**), although its function on these cells remains to be determined.

It is interesting and surprising that RNAseq analysis and flow cytometric analysis revealed a relatively minimal difference between WT and Lag3-deficient CD8$^+$ T cells at the whole population level, whereas the impact of LAG3 is predominantly seen on IGRP$_{206\text{-}214}$-reactive clones but not on insulin B$_{15\text{-}23}$-reactive clones (**Fig. 15**). There are two possible explanations. First, the expression of LAG3 on the cell surface may intrinsically affect the magnitude of TCR signaling, therefore limiting the avidity maturation of IGRP$_{206\text{-}214}$-reactive CD8$^+$ T cells. It was reported that CD8$^+$ T cell clones reactive to IGRP$_{206\text{-}214}$ but not those reactive to insulin undergo functional avidity maturation during the progression of autoimmune diabetes, and that naïve high-avidity IGRP$_{206\text{-}214}$-specific T cells are more diabetogenic than their low-avidity counterparts [236,237]. One could test this possibility using the following approaches: (1) Compare the frequency of high-avidity vs. low-avidity IGRP$_{206\text{-}214}$-specific T cells between *Lag3*$^{L/L\text{-}YFP}$E8i$^{CRE/CRE\text{-}GFP}$.NOD and WT control mice using NRP (low-avidity), NRP-a7 (intermediate-avidity), and NRP-v7 (high-avidity) tetramers [230]. (2) Compare the tetramer association and dissociation kinetics of insulitic WT vs. *Lag3*-deficient CD8$^+$ T cells at different ages. (3) Compare the diabetes onset and incidence of NRP-v7, or irrelevant peptide-treated *Lag3*$^{L/L\text{-}YFP}$E8i$^{CRE/CRE\text{-}GFP}$.NOD and WT control mice. Avidity maturation of IGRP$_{206\text{-}214}$-reactive T cells in NOD

mice can be abrogated by repeated treatment with soluble NRP-v7 peptide [236]. If the absence of LAG3 promotes avidity maturation of $IGRP_{206-214}$-reactive T cells, one would expect to see delayed diabetes onset in *Lag3*$^{L/L\text{-}YFP}$E8i$^{CRE/CRE\text{-}GFP}$.NOD mice treated with NRP-v7 compared to those treated with irrelevant peptide.

Another possibility is that these intra-islet $IGRP_{206-214}$-reactive $CD8^+$ T cells are expanded from intestinal cross-activated $CD8^+$ T cells. Two separate studies have suggested that these $IGRP_{206-214}$-reactive T cells can be cross-activated in the intestine [238,239]. $CD8\alpha\alpha^+$ IELs are immuno-suppressive [61], and express high level of LAG3 compared to other IEL subsets (**Fig. 16**). The E8i-CRE appears to also delete *Lag3* in these $CD8\alpha\alpha^+$ IELs (**Fig. 16**). However, to test this possibility, one needs to determine that (1) whether $CD8\alpha\alpha^+$ IELs lose suppressive capacity when they are deficient of LAG3 expression, (2) whether there is a cross-activation and expansion of $IGRP_{206-214}$-reactive T cells in the intestine of *Lag3*$^{L/L\text{-}YFP}$E8i$^{CRE/CRE\text{-}GFP}$.NOD, and (3) whether this clonal expansion is a cell-intrinsic effect of LAG3 on $IGRP_{206-214}$-reactive T cells or cell-extrinsic effect through $LAG3^+CD8\alpha\alpha^+$ IELs. Reconstitute of either WT or *Lag3*$^{L/L\text{-}YFP}$E8i$^{CRE/CRE\text{-}GFP}$.NOD hosts with equally mixed congenic marker-mismatched bone marrows from WT and *Lag3*$^{L/L\text{-}YFP}$E8i$^{CRE/CRE\text{-}GFP}$.NOD donors will help to elucidate the cell-intrinsic vs. cell-extrinsic effects.

My findings may be relevant to clinical medicine. It has been shown that $CD8^+$ T cells are the most abundant population during insulitis in T1D patients, and the frequency of $IGRP_{265-273}$-reactive $CD8^+$ T cells increases after clinical diagnosis and insulin treatment [48,240-242]. Studies in NOD mice suggest that the pathogenesis of autoimmune diabetes is initiated by reactivity to insulin epitopes, and that functional epitope spreading

to $IGRP_{206-214}$ or other epitopes promotes the development of ongoing autoimmune diabetes [63,235]. The differential impact of LAG3 on $IGRP_{206-214}$-reactive and insulin B_{15-23}-reactive $CD8^+$ T cells indicates that LAG3 may participate in pathogenic epitope spreading of autoimmune diabetes. Understanding how LAG3 selectively limits differentiation of $IGRP_{206-214}$-reactive $CD8^+$ T cells into pathogenic effector cells may help to elucidate the mode-of-action of LAG3 in regulating autoimmune diabetes and self-tolerance. Future studies should focus on comparing phenotype and functionality of $IGRP_{206-214}$-reactive and insulin B_{15-23}-reactive WT and *Lag3*-deficient $CD8^+$ T cells.

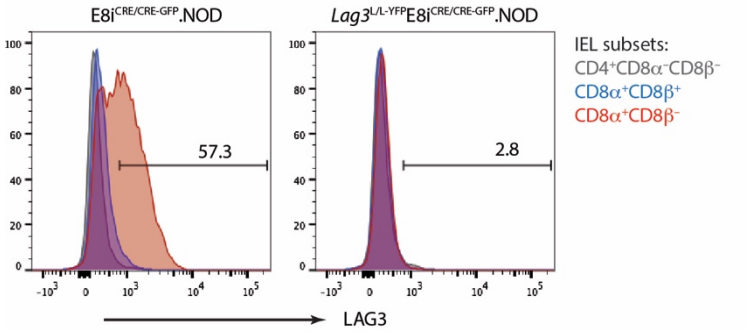

Figure 16. Intestinal CD8αα$^+$ IELs express high level of LAG3.

Representative histograms of surface LAG3 expression on small intestinal IELs in *Lag3*$^{L/L\text{-}YFP}$E8i$^{CRE/CRE\text{-}GFP}$.NOD mice compared with cohoused controls. Numbers shown in the plots indicate the frequency of LAG3$^+$ cells among CD8αα$^+$ IELs.

4.0 Chapter 4: Role of LAG3 in Treg-mediated self-tolerance

Preface:

Co-inhibitory receptors are pivotal in controlling T cell homeostasis because of their cell-intrinsic regulation of Tconv proliferation, viability, and function [70]. However, the role of co-inhibitory receptors on Tregs remains more obscure because they could be required for suppressive activity and/or limit Treg function [6]. LAG3 is required for maintaining self-tolerance in NOD mice, and deletion of *Lag3* in either all $CD4^+$ and $CD8^+$ T cells or just $CD8^+$ T cells leads to accelerated autoimmune diabetes (Chapter 3) [112,113]. LAG3 is also highly expressed on Tregs, a critical suppressive subpopulation of T cells that prevents autoimmunity but limits antitumor immunity [6,51]. Previous studies have suggested that LAG3 is used as a mechanism for Treg suppression [146,186,187]. However, it is also possible that LAG3 may intrinsically limit Treg function in a manner commensurate to its role on other T cell subsets.

In this Chapter, two main questions will be addressed: (1) What is the cell-extrinsic vs. cell-intrinsic impact of LAG3 on Tregs? (2) What are the differences between $LAG3^+$ and $LAG3^-$ Treg transcriptomes or clonotypes?

To assess the cell-extrinsic and cell-intrinsic impact of LAG3 on Tregs in regulating autoimmune diabetes, *Lag3*$^{L/L\text{-}YFP}$ conditional knockout-reporter mice [225] were crossed with Treg-specific CRE mice (*Lag3*$^{L/L\text{-}YFP}$Foxp3$^{CRE\text{-}GFP}$.NOD [213]). Additionally, the *Lag3*-YFP and Foxp3-GFP reporters (*Lag3*$^{L/L\text{-}YFP}$*Foxp3*^{GFP}.NOD [243] and *Lag3*$^{L/L\text{-}YFP}$Foxp3$^{CRE\text{-}GFP}$.NOD [213]) allowed me to compare transcription and clonotype differences of $LAG3^+$

and LAG3^{-} Treg subsets, and assess what changes are the cause vs. consequence of *Lag3* expression in Tregs.

The bioinformatics analysis in Chapter 4.1 (Fig. 25 and 26) was done by Dr. Maria Chikina (University of Pittsburgh), and analysis in Chapter 4.2 (Fig. 32) was done by Dr. Sasikanth Manne (University of Pennsylvania).

Figures in Chapter 4.1 (Fig. 17 to 30) are taken from the publication "Zhang Q *et. al. Sci. Imm.* (2017)" [225] under the journal's copyright permission. All figures in Chapter 4.2 are unpublished data.

4.1 Extrinsic and intrinsic impacts of LAG3 on Tregs

4.1.1 The absence of LAG3 on Tregs results in reduced autoimmune diabetes

Note: this sub-chapter is taken from the publication "Zhang Q *et. al. Sci. Imm.* (2017)" [225].

As LAG3 has been shown to be required for optimal Treg function [6,146,186,187], we reasoned that the accelerated autoimmune diabetes observed in the *Lag3*$^{-/-}$.NOD and *Lag3*$^{L/L\text{-}YFP}$Cd4^{CRE}.NOD mice might be partially due to the loss of LAG3 expression on Tregs. I then assessed the impact of the loss of LAG3 surface expression on Tregs by analyzing *Lag3*$^{L/L\text{-}YFP}$Foxp3$^{CRE\text{-}GFP}$.NOD mice (**Fig. 5**). Unexpectedly, female *Lag3*$^{L/L\text{-}YFP}$Foxp3$^{CRE\text{-}GFP}$.NOD mice had significantly delayed onset of autoimmune diabetes, decreased diabetes incidence (48% vs. 84%) by 30 weeks of age, while male *Lag3*$^{L/L\text{-}YFP}$Foxp3$^{CRE\text{-}GFP}$.NOD mice were completely protected from autoimmune diabetes (**Fig. 17A**). Although we only assessed a small number of co-housed female *Lag3*$^{+/L\text{-}YFP}$Foxp3$^{CRE\text{-}GFP}$.NOD littermates, their diabetes incidence was 60%, suggesting that LAG3 exhibits haploinsufficiency. While the absence of LAG3 on Tregs did not impact the degree of insulitis at 6 weeks of age, it did lead to a significant reduction at 10 weeks of age in female and male *Lag3*$^{L/L\text{-}YFP}$Foxp3$^{CRE\text{-}GFP}$.NOD mice (**Fig. 17B**), suggesting that the expression of LAG3 on Tregs had little impact on the initiation of islet infiltration but was critical to limit Treg-mediated self-tolerance and the onset of autoimmune diabetes. Taken together, these data suggest that LAG3 may limit Treg-mediated suppression of autoimmunity.

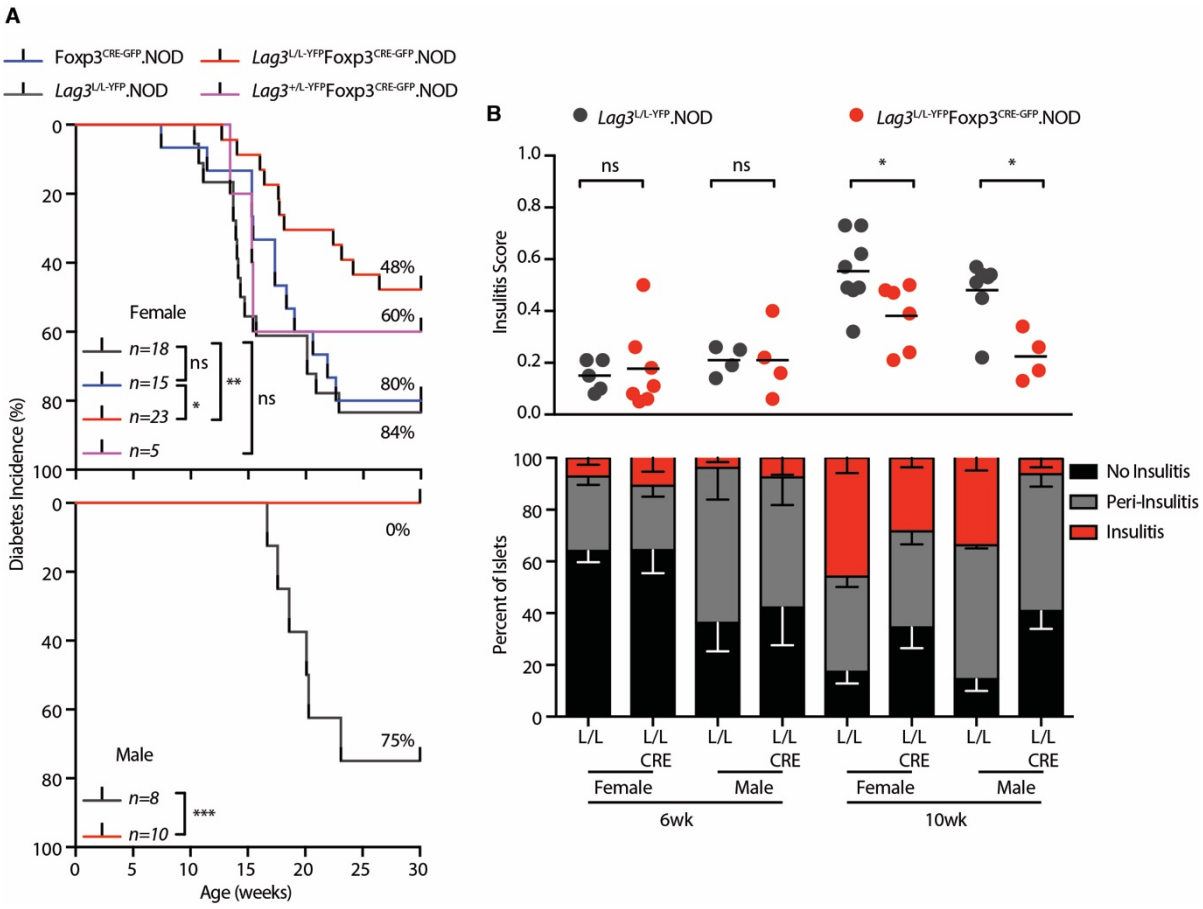

Figure 17. Loss of LAG3 on Tregs results in reduced autoimmune diabetes and insulitis.

(**A**) Diabetes onset and incidence monitored in *Lag3*$^{L/L\text{-}YFP}$Foxp3$^{CRE\text{-}GFP}$.NOD females (top) and males (bottom) together with cohoused littermate controls. (**B**) Histological assessment of insulitis performed in female and male *Lag3*$^{L/L\text{-}YFP}$Foxp3$^{CRE\text{-}GFP}$.NOD together with cohoused controls at 6 and 10 weeks of age (n = 4 to 7). Horizontal black bars indicate the mean. Error bars indicate SEM. The log-rank was applied to Kaplan-Meier survival function estimates to determine the statistical significance in (A), and nonparametric Mann-Whitney test was used in (B). ns, not significant; *$p < 0.05$, **$p < 0.01$, ***$p < 0.001$.

Consistent with the reduced insulitis and diabetes observed, there were reduced numbers of CD4$^+$Foxp3$^-$ and CD8$^+$ T cells in the islets of *Lag3*$^{L/L\text{-}YFP}$Foxp3$^{CRE\text{-}GFP}$.NOD mice (**Fig. 18**). Although the number of Tregs in the islets of *Lag3*$^{L/L\text{-}YFP}$Foxp3$^{CRE\text{-}GFP}$.NOD mice was decreased as a result of the reduced insulitis and inflammation, there

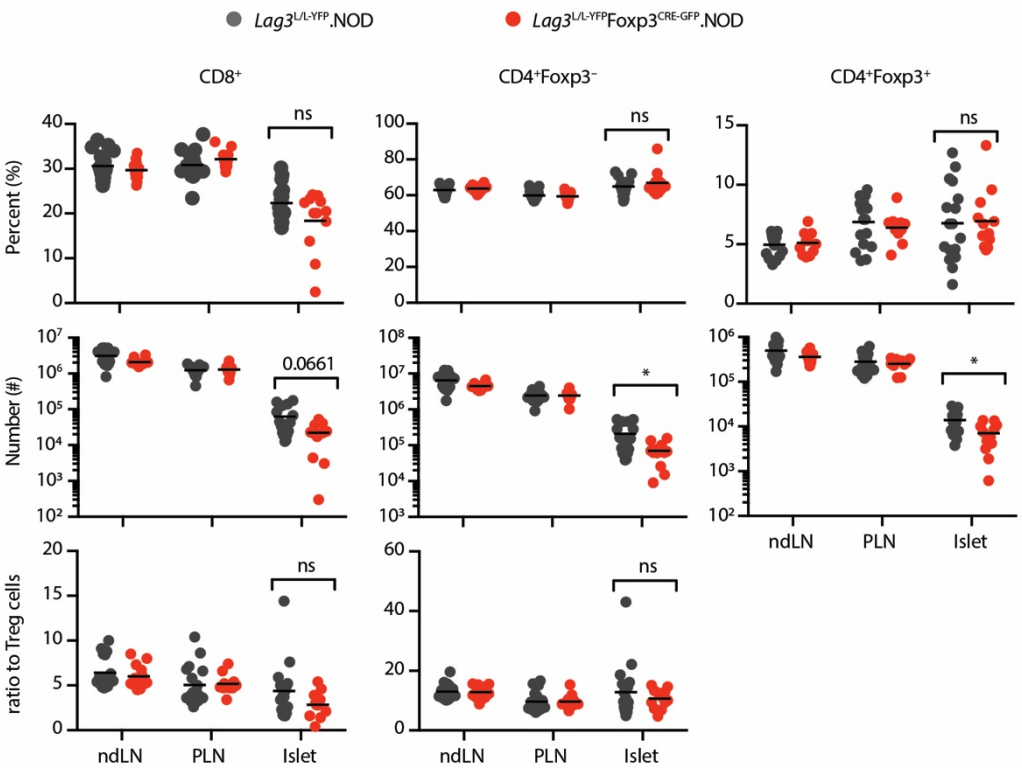

Figure 18. Reduced lymphocyte infiltration into islets in the absence of LAG3 on Tregs.

The frequency (top) and absolute number (middle) of CD8$^+$, CD4$^+$Foxp3$^-$, and CD4$^+$Foxp3$^+$ in TCRβ^+ cells, and the ratio (bottom) of CD8$^+$ and CD4$^+$Foxp3$^-$ T cells to CD4$^+$Foxp3$^+$ T cells in *Lag3*$^{L/L\text{-}YFP}$Foxp3$^{CRE\text{-}GFP}$.NOD mice compared with cohoused littermates (females, 10 weeks of age, n = 12 to 17, five independent experiments). Horizontal black bars indicate means. Nonparametric Mann-Whitney test was used. ns, not significant; *$p < 0.05$.

was a trend, albeit not reaching significance, toward a lower ratio of Tconv cells to Tregs (**Fig. 18**). The proportion of Chromogranin A-reactive (BDC2.5mi$^+$) CD4$^+$ T cells and IGRP-reactive (NRP-v7$^+$) CD8$^+$ T cells was not altered in the islets of *Lag3*$^{L/L\text{-}YFP}$Foxp3$^{CRE\text{-}GFP}$.NOD mice compared with controls, suggesting that *Lag3*-deficient Tregs may not selectively suppress specific sub-populations of diabetogenic T cells but rather globally impact all islet-infiltrating cells (**Fig. 19**). This observation may have been anticipated

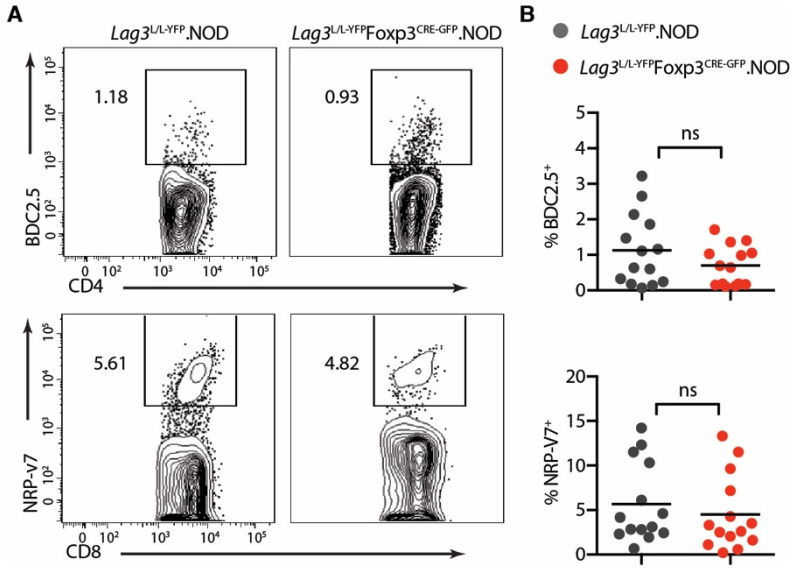

Figure 19. The frequency of islet-Ag specific T cells are not affected by the loss of LAG3 on Tregs.

Frequency of (top) chromogranin A mimotope (BDC2.5) tetramer$^+$ in CD4+ T cells and (bottom) IGRP mimotope (NRP-v7) tetramer$^+$ in CD8$^+$ T cells in the islets of *Lag3*$^{L/L\text{-}YFP}$Foxp3$^{CRE\text{-}GFP}$.NODs compared with cohoused littermates (females, 10 weeks of age, n = 14, five independent experiments). Representative plots were shown on the left. Horizontal black bars indicate means. Nonparametric Mann-Whitney test was used. ns, not significant.

given that we have previously shown that only islet-antigen reactive T cells can enter the islets [216]. The reduced number of Tconvs in the islets of *Lag3*$^{L/L\text{-}YFP}$Foxp3$^{CRE\text{-}GFP}$.NOD mice was due to decreased CD8$^+$ T cell proliferation (assessed by Ki67 expression and BrdU incorporation) and reduced expression of anti-apoptotic factor Bcl2 [229] in CD4$^+$Foxp3$^-$ T cells in islets (**Fig. 20** and **21**). Both CD4$^+$Foxp3$^-$ and CD8$^+$ T cells in the islets of *Lag3*$^{L/L\text{-}YFP}$Foxp3$^{CRE\text{-}GFP}$.NOD mice had significantly reduced expression of TNFα but not IFNγ (**Fig. 22**). A significant reduction in IL-2 production was also observed in CD4$^+$Foxp3$^-$ T cells in the islets of *Lag3*$^{L/L\text{-}YFP}$Foxp3$^{Cre\text{-}GFP}$.NOD mice (**Fig. 22**). There was a trend, albeit not reaching significance, toward an increased percentage of Th2 and Th17 cells (**Fig. 22**). Although the activation, terminal differentiation [as marked by KLRG1 expression [244]], and proliferation of *Lag3*-deficient and WT Tregs were comparable, *Lag3*-deficient Tregs expressed higher levels of the anti-apoptotic factor Bcl2 in the islets (**Fig. 20**, **21**, and **23**). ICOS, which has been shown to be critical for Treg homeostasis and functional stability in NOD mice [82], was also up-regulated on intra-islet Tregs in the absence of LAG3 (**Fig. 23**). The expression of multiple co-inhibitory receptors (PD1, TIGIT, and TIM3) was slightly enhanced on *Lag3*-deficient Tregs (**Fig. 23**), implying a cell intrinsic process in Tregs to compensate for the loss of LAG3. However, the suppressive capacity of intra-islet and peripheral WT and *Lag3*-deficient Tregs in an *in vitro* micro-suppression assay was comparable on a per-cell level (**Fig. 24**). Overall, these data suggest that *Lag3*-deficient Tregs have enhanced suppression toward autoreactive T cell proliferation, effector cytokine production, and probably viability (as suggested by Bcl2 expression) *in vivo*, perhaps at the population level as a result of their enhanced proliferative and survival capacity.

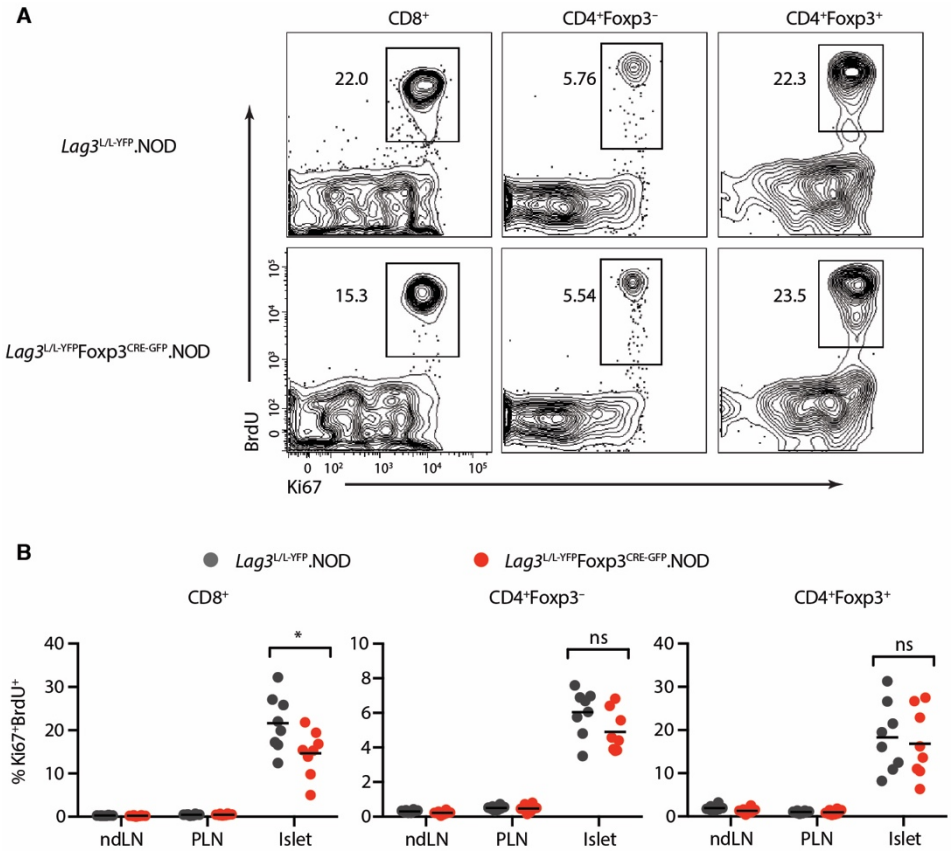

Figure 20. Intrisic and extrinsic impact of Treg-expressed LAG3 on T cell proliferation.

Proliferation of T cells assessed by Ki67 expression and BrdU incorporation (females, 10 weeks of age, n = 8, three independent experiments). Each mouse was injected with 2mg BrdU in PBS intraperitoneally 8 hours ahead of sacrifice. Representative staining plots of intra-islet T cells were shown in (A). Horizontal black bars indicate means. Nonparametric Mann-Whitney test was used. ns, not significant; *$p < 0.05$.

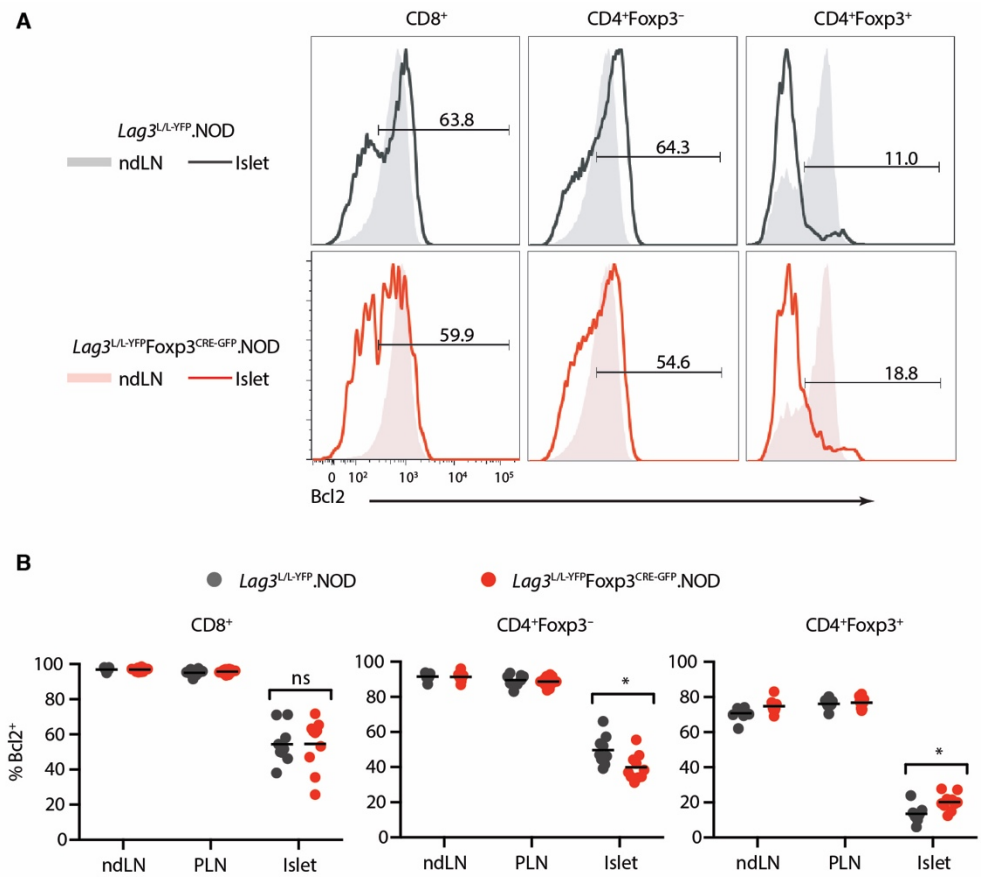

Figure 21. Intrinsic and extrinsic impact of Treg-expressed LAG3 on Bcl2 expression in T cells.

Expression of anti-apoptotic factor Bcl2 in T cells (females, 10 weeks of age, n = 9 to 10, three independent experiments). Representative histograms were shown in (A). Horizontal black bars indicate means. Nonparametric Mann-Whitney test was used. ns, not significant; *$p < 0.05$.

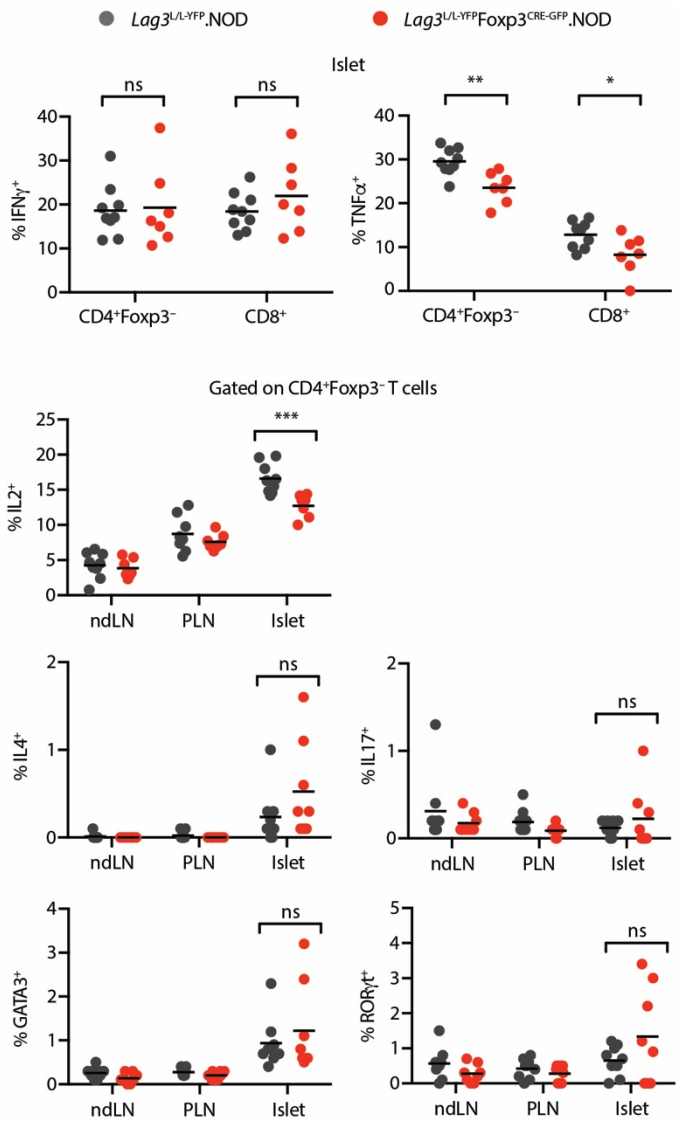

Figure 22. Effector cytokine production in the absence of LAG3 on Tregs.

Flow cytometric analysis of cytokines in Tconvs shown (n = 7 to 9, three independent experiments, 10 weeks of age; all female mice). Cells were *ex vivo* stimulated with PMA and ionomycin for 5 hours before staining. Horizontal black bars indicate means. Nonparametric Mann-Whitney test was used. ns, not significant; *$p < 0.05$, **$p < 0.01$.

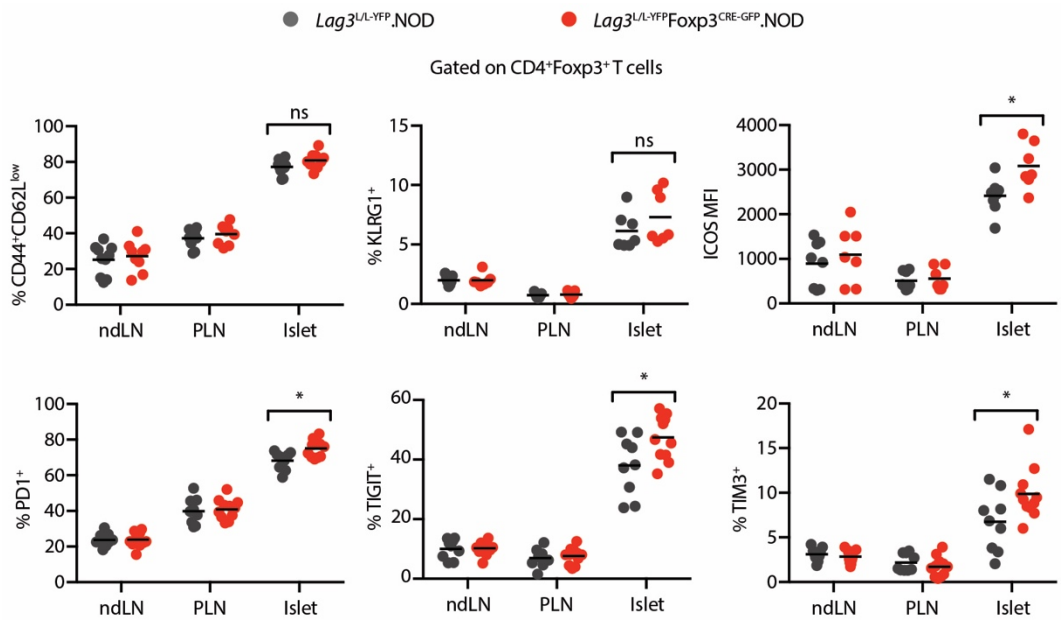

Figure 23. Phenotypic analysis on *Lag3*-deficient Tregs.

Flow cytometric analysis of markers in Tregs (top: n = 7 to 10, three independent experiments, 8 weeks of age; bottom: n = 9 to 11, four independent experiments, 10 weeks of age; all female mice). Horizontal black bars indicate means. Nonparametric Mann-Whitney test was used. ns, not significant; *$p < 0.05$.

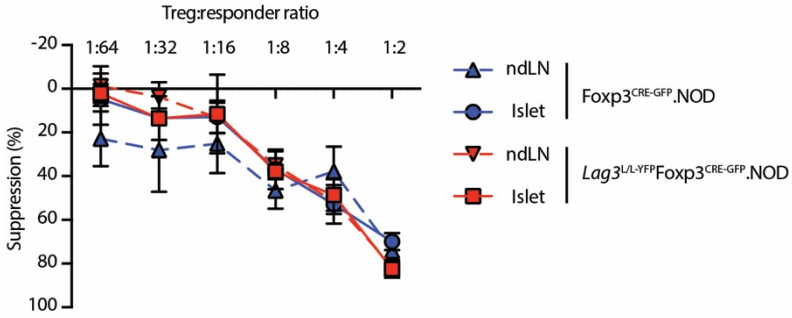

Figure 24. Functional analysis on *Lag3*-deficient Tregs.

Suppressive capability of Tregs assessed by micro-suppression assay *in vitro* (n = 3). Division index of responder cells was measured based on division of the proliferation dye CellTrace Violet. Treg suppression was calculated using the formula %Suppression = (1-DI_{Treg}/DI_{Ctrl}). DI_{Treg} stands for the division index of responder cells with Treg cells, and DI_{Ctrl} stands for the division index of responder cells activated without Treg cells. Data were presented as mean ± SEM. Nonparametric Mann-Whitney test was used. ns, not significant.

4.1.2 LAG3 intrinsically limits Treg proliferation

Note: this sub-chapter is taken from the publication "Zhang Q *et. al. Sci. Imm.* (2017)" [225].

To assess the impact of *Lag3* deletion on the Treg transcriptome, we performed RNA sequencing of WT and *Lag3*-deficient Tregs from the islets and ndLN. A substantial number of genes and pathways were modulated by the loss of LAG3 expression on Tregs in the islets (**Fig. 25A**). Interestingly, a group of genes were down-regulated in intra-islet WT but not *Lag3*-deficient Tregs, compared to peripheral Tregs (**Fig. 25B**), suggesting

that these genes might be required for optimal Treg function or survival, and that LAG3 may limit their expression in intra-islet Tregs.

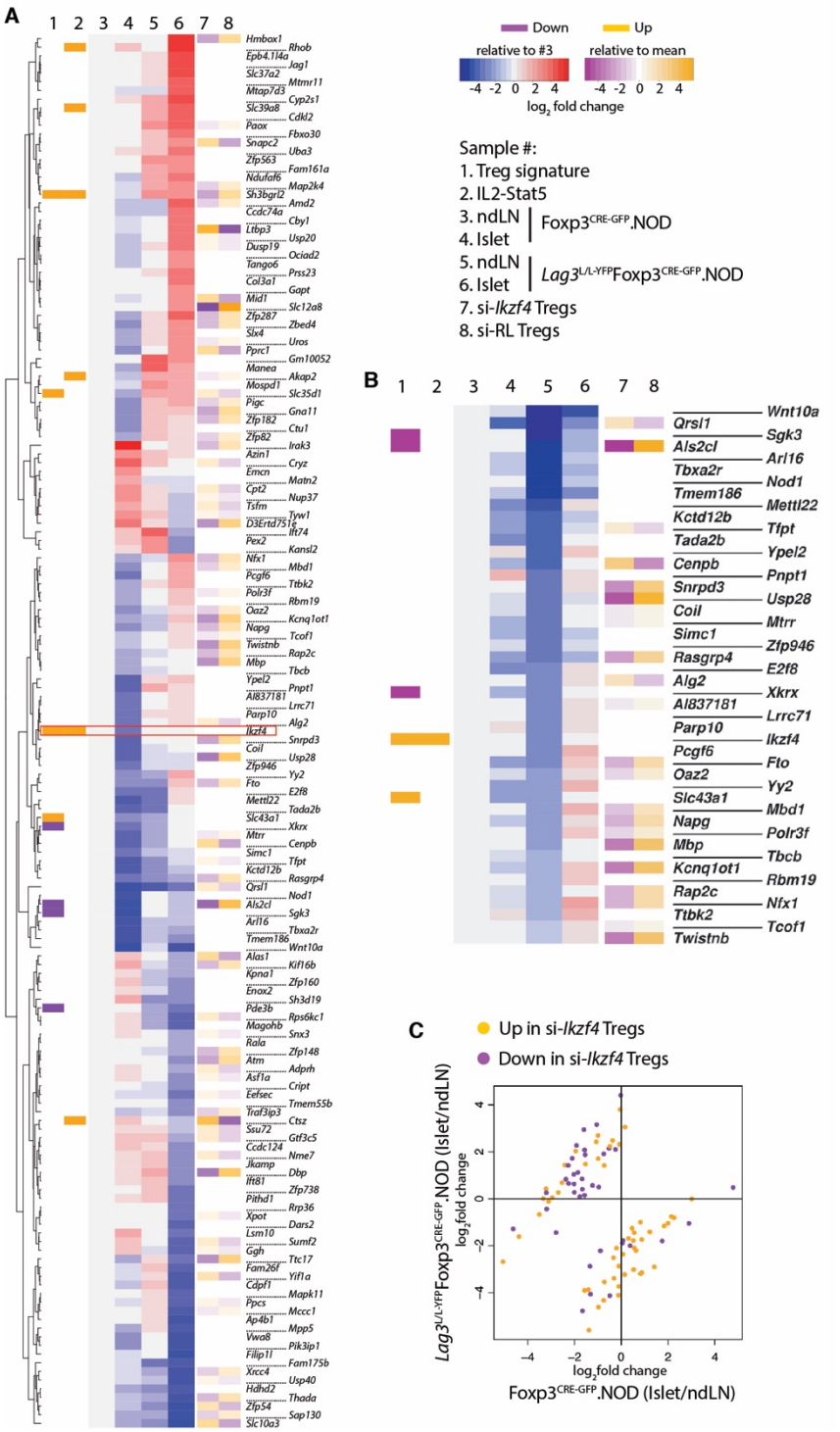

Figure 25. LAG3 alters the Treg transcriptome.

(**A**) Heat map of differentially expressed genes in *Lag3*-deficient versus WT ndLN and intra-islet Tregs. Fold change in gene expression was relative to WT Tregs from ndLN and shown as the mean of independent triplicates (females, 8 weeks of age). The dendrogram was calculated based on standard Euclidean distance mean linkage clustering and rotated to sort the values in intra-islet Tregs of *Lag3*$^{L/L\text{-}YFP}$Foxp3$^{CRE\text{-}GFP}$.NOD mice. (**B**) Heat map of genes that were down-regulated in intra-islet WT Tregs but still maintained in *Lag3*-deficient Tregs. The dendrogram was rotated to sort the values (low to high) in intra-islet Tregs of Foxp3$^{CRE\text{-}GFP}$.NOD mice. si-*Ikzf4*, *Ikzf4* siRNA. RL, Renilla Luciferase (control siRNA). (**C**) Scatterplot of the Eos targeted genes in *Lag3*-deficient versus WT Treg expressional profiles.

One of the enhanced genes in insulitic *Lag3*-deficient Tregs was *Ikzf4* (Eos), a corepressor of Foxp3 that prevents the expression of Tconv genes in Tregs (**Fig. 25**) [21,22,157,245]. Strikingly, the expression profile of intra-islet WT Tregs resembled the previously published transcriptional signature in *Ikzf4*-knockdown Tregs, whereas the expression profile of intra-islet *Lag3*-deficient Tregs resembled the transcriptional signature in mock control Tregs (**Fig. 25**) [21]. These data suggest that LAG3 might limit Eos expression, and thus the function and maintenance of intra-islet Tregs. IL-2 is known to be essential for Treg cell maintenance, and defective IL-2 signaling in Tregs triggers autoimmune islet destruction [17,120,246]. Genes modulated by IL-2–STAT5 signaling were substantively enhanced in the absence of LAG3 on Tregs (**Fig. 26**). Overall, the transcriptome analyses suggest that LAG3 negatively regulates intra-islet Tregs by down-regulating key genes and pathways that are essential for Treg maintenance and function.

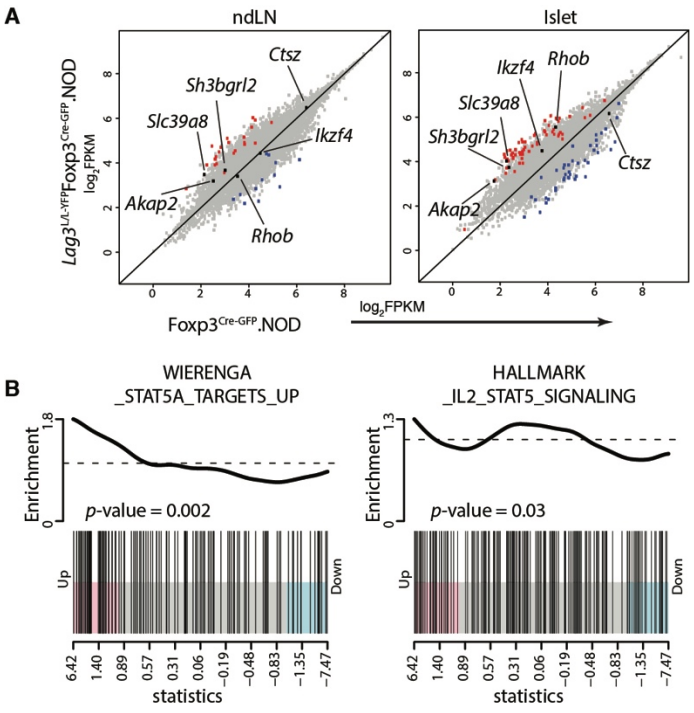

Figure 26. IL-2–Stat5 pathway is modulated by LAG3 expression in Tregs.

(A) Differentially expressed IL-2–Stat5 targeted genes shown in x-y dot plots. Labels denoted genes from mSigDB HALLMARK_IL2_STAT5_SIGNALING that were significantly upregulated (red) or downregulated (blue) in *Lag3*-deficient Tregs compared with WT Tregs. (**B**) Barcode plots depicting the enrichment of genes in the mSigDB WIERENGA_STAT5_TARGETS_UP and HALLMARK_IL2_STAT5_SIGNALING pathways. Statistics denoted the Wald statistic used to test the significance of coefficients in a negative binomial generalized linear model.

To directly assess whether *Lag3*-deficient Tregs had a proliferative advantage over WT Tregs, and to determine whether the pathways identified by transcriptome analysis were intrinsically regulated by LAG3 in Tregs, we co-transferred an equal number of activated congenic marker-mismatched WT (Thy1.1$^+$) and *Lag3*-deficient (Thy1.2$^+$) Tregs into NOD (Thy1.1$^+$Thy1.2$^+$) hosts (**Fig. 27A**). Both WT and *Lag3*-deficient donor Tregs were sorted from mice that expressed the islet antigen-specific BDC2.5 TCR, which facilitated islet entry [216,247]. Foxp3 expression was unaltered in both Treg populations following adoptive transfer (**Fig. 28**), suggesting that LAG3 may not impact Treg stability. Strikingly, *Lag3*-deficient Treg cells out-competed WT Treg cells in the islets (60% vs. 40%, respectively) and in the PLN (54% vs. 46%, respectively) but not in the ndLN (**Fig. 27B** and **27C**).

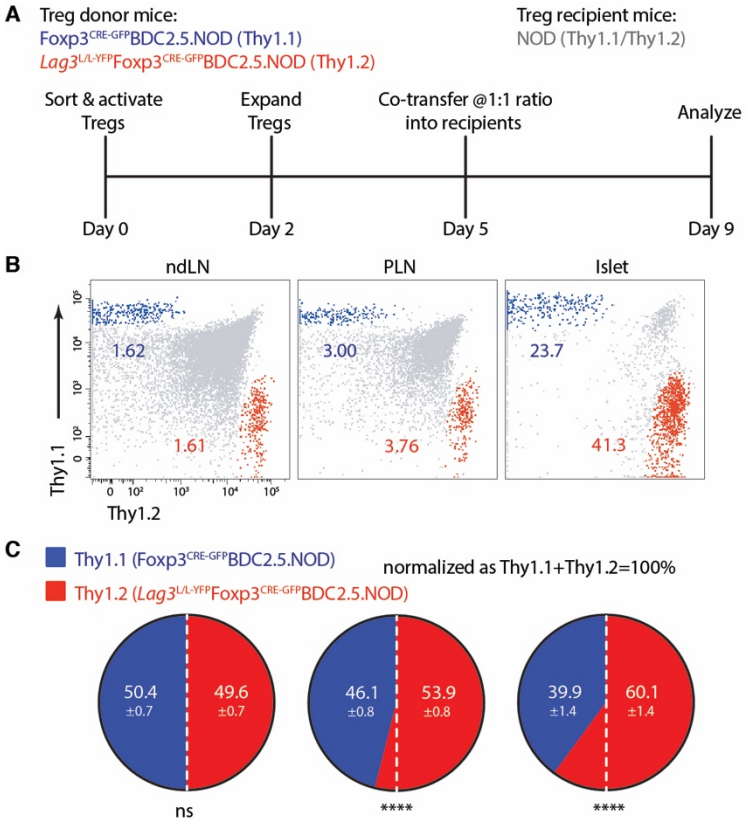

Figure 27. *Lag3*-deficient Tregs out-compete WT Tregs.

(A) Schematic of Treg cotransfer experiment. (**B**) Representative plots of Thy1.1$^+$ (WT, blue) and Thy1.2$^+$ (*Lag3*-deficient, red) Tregs (gated CD4$^+$Vβ4$^+$) in NOD recipients (grey). (**C**) Proportion of WT and *Lag3*-deficient Tregs in the islets and lymph nodes assessed with the percentage of Thy1.1$^+$ and Thy1.2$^+$ in CD4$^+$Vβ4$^+$ cells after transfer (n = 17, three independent experiments; all female mice). Data were presented as mean $\pm$ SEM. Nonparametric Mann-Whitney test was used in (C). ns, not significant; ****$p < 0.0001$.

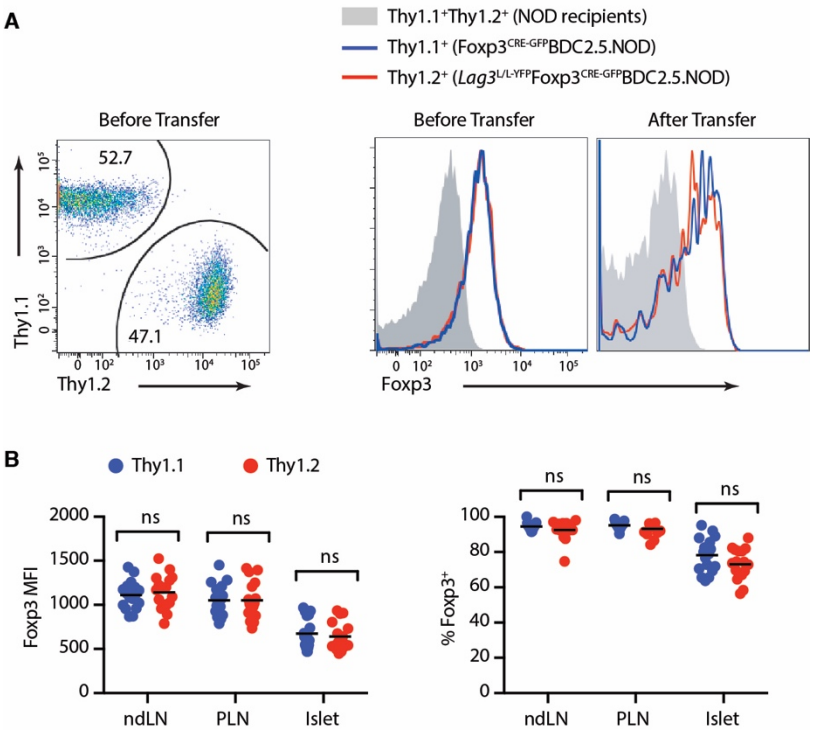

Figure 28. Foxp3 expression is not affected by LAG3 expression in Tregs.

(A) Representative histogram of Foxp3-GFP expression in Tregs before and after transfer. (**B**) Foxp3 expression in co-transferred Tregs (female hosts, n = 17, three independent experiments). Horizontal black bars indicate means. Nonparametric Mann-Whitney test was used in (B). ns, not significant.

Previous studies have shown that reduced CD25 and Bcl2 levels cause a decline in intra-islet Treg viability, while administration of low-dose IL2 promotes Bcl2 expression and Treg survival [17,248,249]. A higher percentage of intra-islet *Lag3*-deficient versus WT Tregs expressed Ki67 and Bcl2 (**Fig. 29**). Although differences were also observed in the periphery in these co-transfer experiments, this is probably due to the activation of Tregs *in vitro* prior to adoptive transfer. Consistent with the transcriptomic analysis, *Lag3*-

deficient Tregs exhibited higher CD25 expression and STAT5 phosphorylation, compared with WT Tregs (**Fig. 29**). Furthermore, Eos (*Ikzf4*) expression was reduced in WT but not *Lag3*-deficient intra-islet Tregs compared with periphery Tregs, whereas another Ikaros family member, Helios (encoded by gene *Ikzf2*), was unaffected by LAG3 expression (**Fig. 29**).

To determine whether LAG3 modulated Eos expression and whether this might impact Treg proliferation, I first assessed Eos levels in WT and *Lag3*-deficient Tregs following stimulation *in vitro*. As anticipated from our transcriptomic analysis, *Lag3*-deficient Tregs exhibited enhanced Eos expression after stimulation, compared to WT Tregs (**Fig. 30**). Likewise, activated *Lag3*-deficient Tregs exhibited increased proliferation, as measured by BrdU incorporation, over WT Tregs. Importantly, knockdown of *Ikzf4* in *Lag3*-deficient Tregs reduced Eos expression and Treg proliferative capacity, whereas overexpression of human *IKZF4* in WT Tregs enhanced Treg proliferation (**Fig. 30**). Taken together, these data support a model in which LAG3 intrinsically limits Treg proliferation and viability by modulating pathways that are critical for Treg function and proliferation, particularly the IL-2/STAT5 and Eos pathways.

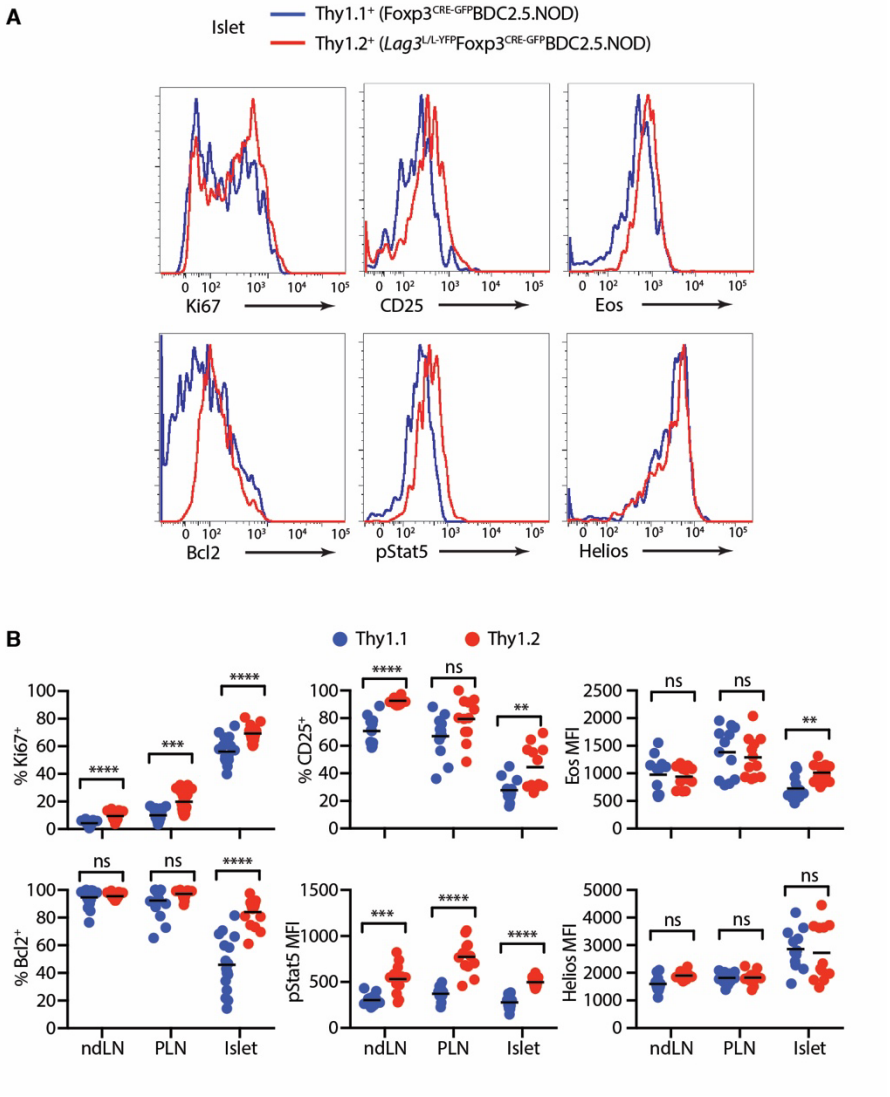

Figure 29. LAG3 intrinsically limits Treg proliferation.

(A) Representative histograms of markers shown in co-transferred intra-islet Tregs. (**B**) Flow cytometric analysis of markers shown. Horizontal black bars indicate the mean (n= 12 to 17, two to three independent experiments; all female mice). Nonparametric Mann-Whitney test was used in (B). ns, not significant; *$p < 0.05$, **$p < 0.01$, ***$p < 0.001$, ****$p < 0.0001$.

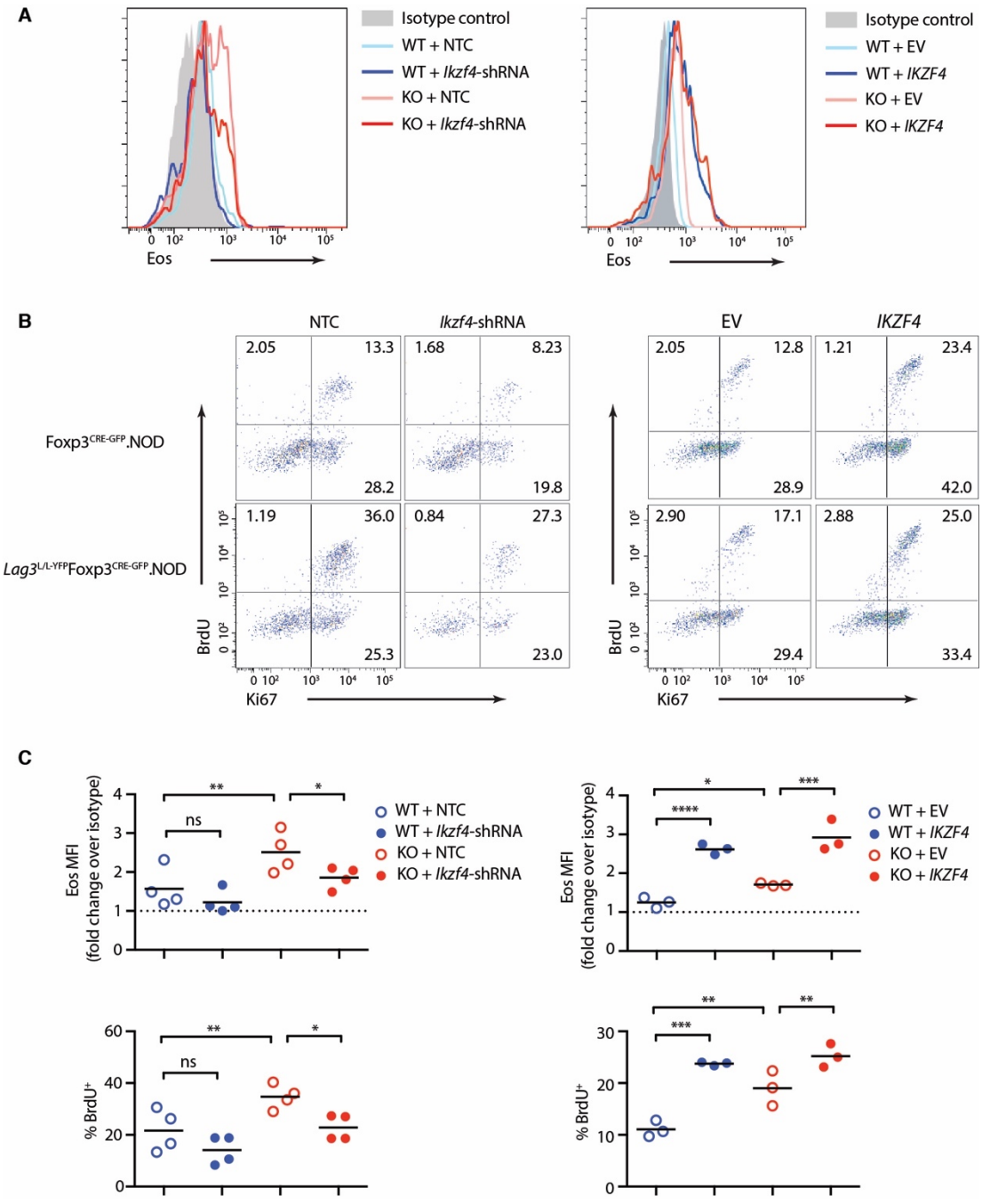

Figure 30. LAG3 limits Treg proliferation through Eos pathway.

Representative flow plots of Eos expression (**A**) and BrdU incorporation (**B**), and statistics (**C**) in Tregs shown. WT, Foxp3$^{CRE-GFP}$.NOD; KO, *Lag3*$^{L/L-YFP}$Foxp3$^{CRE-GFP}$.NOD; NTC, non-targeting control; EV, empty vector pMIA. BrdU was pulsed into Treg culture media 2 hours prior to the staining. Fisher's LSD test was applied to one-way ANOVA to determine the statistical significance. ns, not significant; *p < 0.05, **p < 0.01, ***p < 0.001, ****p < 0.0001.

4.2 Transcription and clonotype differences between *Lag3*$^{+}$ *and Lag3*$^{-}$ Treg subsets

4.2.1 *Lag3* is preferentially expressed in a subset of Tregs but is not necessarily a Treg differentiation factor

Not all intra-islet Tregs express LAG3 (**Fig. 3** and **4**), suggesting that heterogeneity exists among these Tregs. One wonders whether: (1) the signaling through LAG3 receptor drives intra-islet LAG3^{+} Tregs to differentiate into a unique subset; or (2) LAG3 is preferentially expressed on a distinct subset of Tregs in the islet microenvironment, and if so, what cell-intrinsic and cell-extrinsic factors upregulate or maintain LAG3 expression in Tregs. To address these questions, I sorted LAG3^{-} (GFP^{+}YFP^{-} from *Lag3*$^{L/L\text{-}YFP}$*Foxp3*^{GFP}.NOD and *Lag3*$^{L/L\text{-}YFP}$Foxp3$^{CRE\text{-}GFP}$.NOD), LAG3^{+} (GFP^{+}YFP^{+} from *Lag3*$^{L/L\text{-}YFP}$*Foxp3*^{GFP}.NOD), and LAG3-wannabe (GFP^{+}YFP^{+} from *Lag3*$^{L/L\text{-}YFP}$Foxp3$^{CRE\text{-}GFP}$.NOD) Tregs from ndLN and islets at various ages for further bioinformatics analysis (**Fig. 31**). I included Treg subsets from *Lag3*$^{L/L\text{-}YFP}$Foxp3$^{CRE\text{-}GFP}$.NOD mice so that I could ask whether the differences between LAG3^{+} vs. LAG3^{-} Tregs were the cause or consequence of *Lag3* expression in Tregs. I utilized the transcriptional profiling of these Treg subsets to identify the potential “upstream” regulators and “downstream” targets of LAG3.

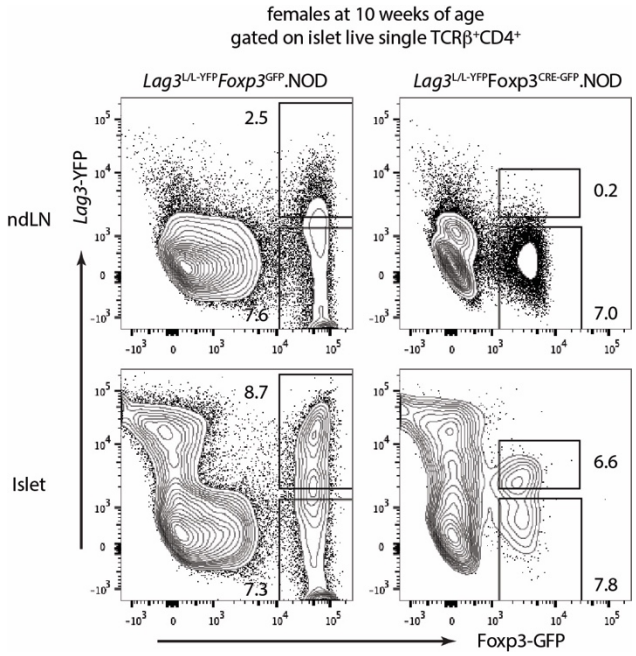

Figure 31. LAG3^{-}, LAG3^{+}, and LAG3-wannabe Tregs.

Representative flow plots of Treg subsets from ndLN and islet of *Lag3*$^{L/L\text{-}YFP}$*Foxp3*^{GFP}.NOD and *Lag3*$^{L/L\text{-}YFP}$Foxp3$^{CRE\text{-}GFP}$.NOD mice (female, 10 weeks of age). Treg subsets were identified based on *Lag3*-YFP and Foxp3-GFP expression.

As expected, Tregs from different stages and tissues exhibited distinct transcriptional profiles (PC dimension 1 and 2) (**Fig. 32**). Although there was a noticeable variability between the duplicates at 6 weeks of age, technical issues were not detected. This may be because the islet microenvironment is being dramatically re-shaped during the initiation stage of insulitis and autoimmune diabetes, and thus the Treg transcriptome is drastically variable between mice to mice at young ages. More biological repeats are needed to clarify the variability. Nevertheless, the YFP^{+} and YFP^{-} Tregs separated into very distinct subsets, whereas the transcriptional differences between LAG3^{+} and LAG3-

wannabe Tregs were relatively small (PC dimensions 2 and 3) (**Fig. 32**). This indicates that *Lag3* is preferentially expressed in a distinct subset of Tregs but may not be a major driving factor for Treg differentiation.

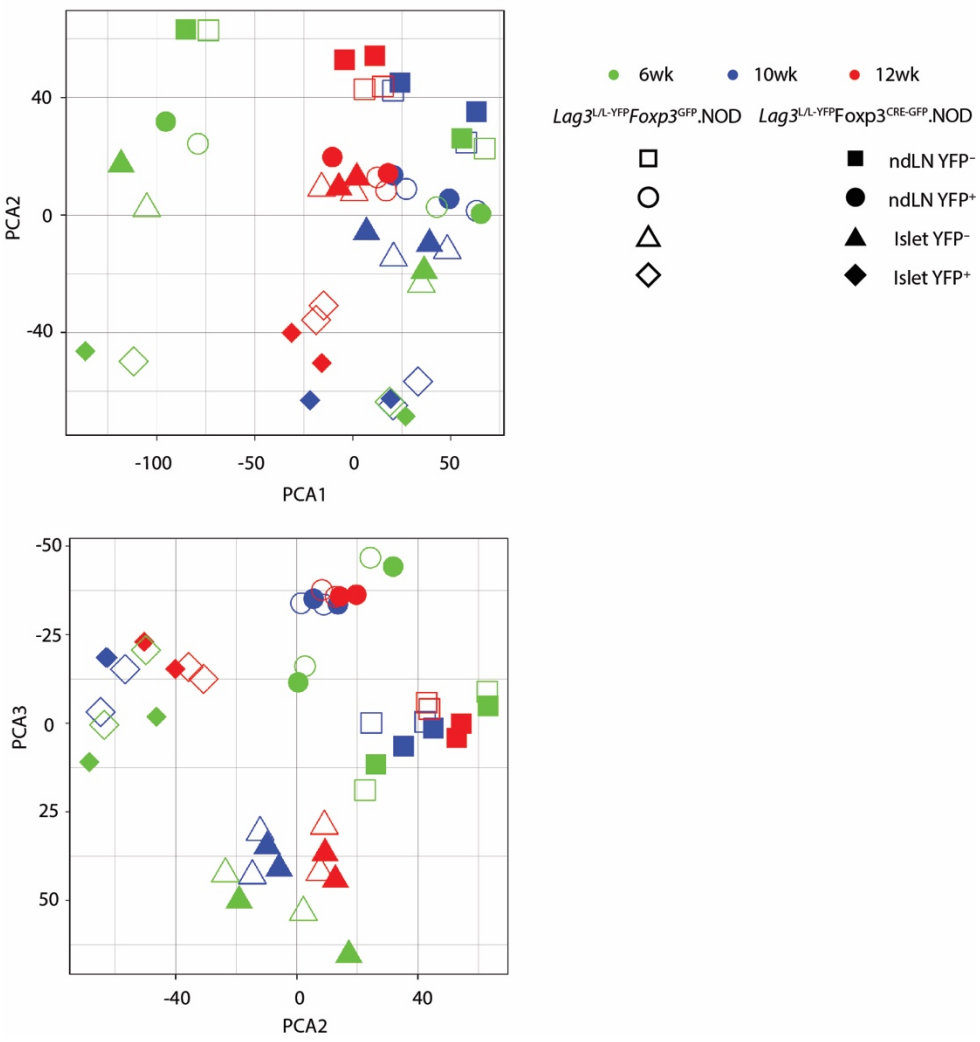

Figure 32. LAG3^{+} and LAG3^{-} Tregs are distinct subsets.

Principle component analysis of RNAseq profiles shown (females; 6, 10, and 14 weeks of age as indicated, two repeats per time point).

4.2.2 *Lag3* is selectively and stably expressed on a proportion of intra-islet Treg clones

Since *Lag3* seemed to be preferentially expressed on a subset of intra-islet Tregs, I asked whether the *Lag3*$^+$ and *Lag3*$^-$ Tregs were derived from the same or distinct Treg clones. To address this question, I performed sequencing of TCRβ chain CDR3 region of islet-infiltrating and ndLN YFP$^+$ vs. YFP$^-$ Treg subsets. Consistent with the transcriptional profiling, intra-islet YFP$^+$ Tregs were more clonally expanded in comparison to YFP$^-$ Tregs, but the lack of *Lag3* did not affect Treg clonality (**Fig. 33A** to **33C**), suggesting that *Lag3* is selectively expressed on some Treg clones and may not have a selective effect on Treg clonal expansion.

Next, I asked whether *Lag3* expression was stable in insulitic Tregs. If LAG3 expression in Tregs were transient or dynamically changing, one would expect to see a large percent of the same clones in both YFP$^+$ and YFP$^-$ Tregs. However, intra-islet YFP$^+$ and YFP$^-$ Tregs only shared ~5% of their TCR repertoires (**Fig. 33D**), indicating that *Lag3* expression in these insulitic Treg clones is stable. Together, these data suggest that LAG3 is preferentially and constitutively expressed on a subset of intra-islet Tregs.

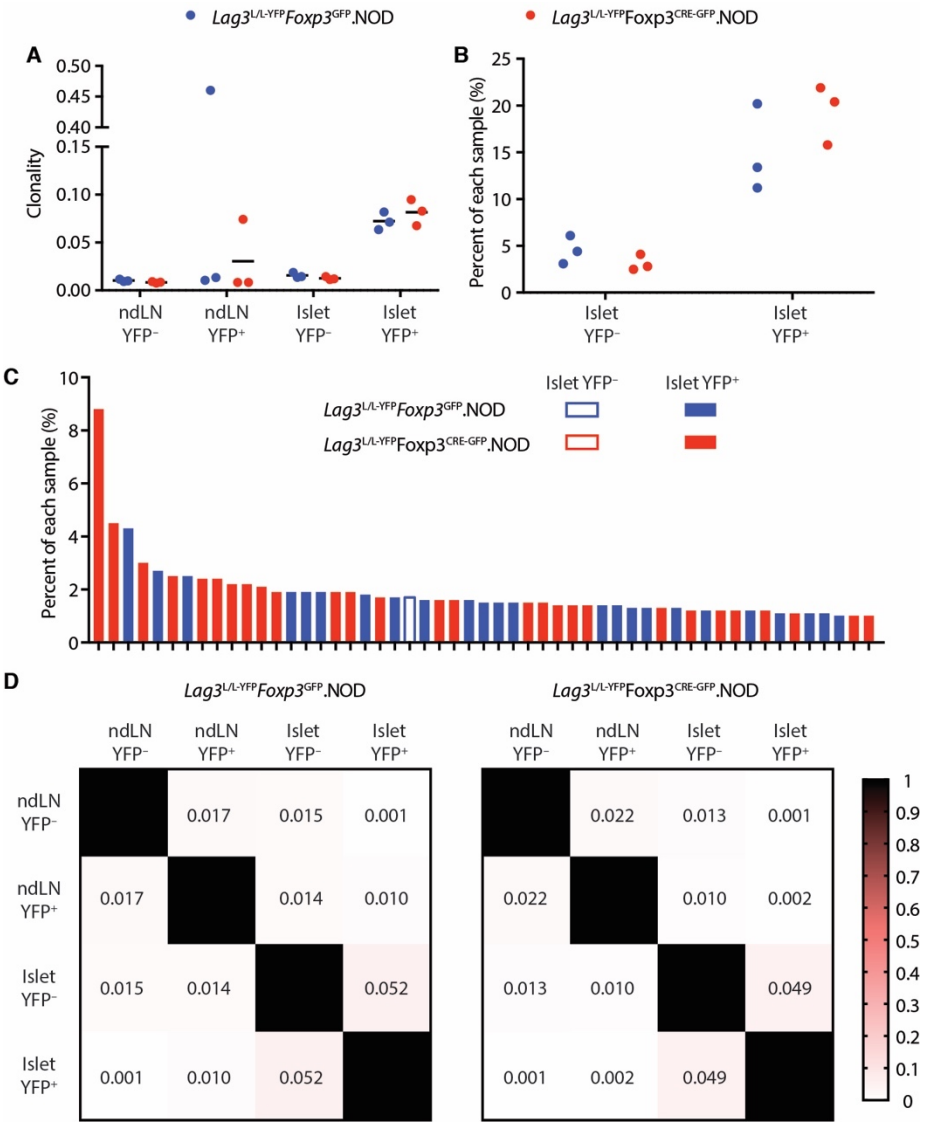

Figure 33. LAG3⁺ and LAG3⁻ Tregs do not share the same TCR β chain usage.

(**A**) Productive clonality (0 to 1) of different Treg subsets shown. A low clonality indicates a relative diverse sample, while a high clonality number indicates that the sample is dominated by a few high-frequency clones. (**B**) Total percentage of top 10 frequent clones in each sample. (**C**) Percentage of most frequent (>1.0%) TCR sequences in each sample. Each column indicates a TCR sequence. (**D**) Repertoire overlap between subsets compared within the same individual mouse. Shown as the mean Morisita overlap index of three individual mice (female, 10 weeks of age). Morisita index is equal to 0 if the samples do not have any shared TCR clones, and it is equal to 1 if the same TCR clones occur in the same frequencies in both samples. See Chapter 2.11 for detailed analysis methods**.**

4.3 Summary and discussion

My study supports a model in which LAG3 is preferentially and constitutively expressed on a subset of Tregs, and intrinsically limits Treg proliferation and functionality by repressing pathways that promote the maintenance of Tregs at inflammatory sites. *Lag3*-deficient Tregs do not appear to have increased suppressive capacity on a per-cell basis. However, they do have an enhanced proliferative and survival advantage that potentiates their suppressive capacity at the population level, endowing them with a critical advantage over time. As disease progresses, subtle changes in *Lag3*-deficient Tregs allow these cells to accumulate over time, leading to a substantial impact on the development of chronic autoimmune diabetes. It is remarkable that this small, Treg-restricted genetic alteration renders male NOD mice resistant to diabetes and substantially limits autoimmune diabetes in female mice, whereas LAG3 deletion in all T cell subsets markedly accelerates the disease. Thus, in an autoimmune environment where chronic inflammation dominates, LAG3 may be constitutively expressed on Tregs, thereby limiting their capacity to block the function of diabetogenic T cells and prevent autoimmune diabetes. This raises the possibility that constitutive co-inhibitory receptor expression on Tregs may underlie their insufficiency in autoimmune disease. It is also possible that increased or constitutive LAG3 expression on Tregs may also limit their suppressive

capacity in inflammatory or infectious diseases where increased tissue damage or pathology is observed.

The impact of co-inhibitory receptors on Treg function and maintenance has been controversial. It was reported that the absence of PD1 on Tregs led to generation of ex-Foxp3 T cells [250]. However, Foxp3 stability was maintained in the absence of LAG3 on Tregs, suggesting distinct pathways are regulated by LAG3 in Tregs. Although my observations here do not preclude a role for LAG3 in promoting Treg suppression [6,146,186,187], my data do point to a dominant role for LAG3 in limiting Treg maintenance and proliferation. This may, in part, be mediated by the Foxp3 corepressor Eos, which is required for Treg maintenance [21,22]. Indeed, there seemed to be a direct correlation between Eos expression and Treg proliferation, as both were higher following stimulation of *Lag3*-deficient Tregs, and the overexpression or knockdown of Eos resulted in analog alterations in Treg proliferation. Furthermore, enhanced IL-2/STAT5 signaling has been clearly shown to promote Treg maintenance and survival [17,120,246,248,249]. LAG3 appears to limit this pathway, thereby having a global impact on Treg function. Future studies may shed light on two further questions: (1) Do other IRs promote or limit Treg function, proliferation and/or survival? (2) Do these IRs affect these Treg parameters using comparable or distinct mechanisms? In **Appendix A**, I show that specific deletion of PD1 in Tregs exhibited similar effect as deletion of LAG3 in Tregs on autoimmune diabetes in the NOD mouse model.

The constitutive expression of LAG3 on some Tregs may be a consequence of chronic TCR stimulation in the islet microenvironment. My observations suggest that LAG3 is preferentially and stably expressed on certain insulitic Treg clones, although

lineage tracing mice (*Rosa26*-reporter x *Lag3*$^{CRE-ERT2}$) will give a more definitive answer. There are two questions to follow up. (1) What are the cell-extrinsic factors that upregulate and maintain LAG3 expression? Even though a small proportion of *Lag3*-YFP$^+$ Tregs were also observed in the periphery, the percent of intra-islet LAG3$^+$ Tregs was two-fold higher than that in the periphery. In addition, levels of LAG3 (MFI of LAG3 staining or *Lag3*-YFP) on insulitc LAG3$^+$ Tregs was at least 3 to 4-fold higher than on peripheral Tregs (**Fig. 3**, **4** and **31**). This indicates that factors within the islet-microenvironment may upregulate and sustain the constitutive LAG3 expression on Tregs. Interestingly, preliminary analysis using the MHC-II tetramer cocktail containing insulin B_{9-23} mimotopes (p8G/E) showed that some of these intra-islet *Lag3*-YFP$^+$ Tregs were reactive to insulin, and this observation was also applicable to *Lag3*-YFP$^+$CD4$^+$Foxp3$^-$ T cells (**Fig. 34**). However, none of these insulin-reactive Tregs or Teffs were *Lag3*-YFP$^-$. Given that all the islet-infiltrating T cells are islet-antigen specific [216], one wonders whether these intra-islet *Lag3*-YFP$^+$ T cells express LAG3 as a consequence of chronic stimulation by those predominant islet-antigens, which may be affected by TCR affinity as well as the availability and amount of islet-antigens. In site immunostaining of intra-islet Tregs may help to determine the localization of intra-islet *Lag3*-YFP$^+$ vs. *Lag3*-YFP$^-$ Tregs in connection with APCs and islet-antigens. (2) What are the transcriptional programs that intrinsically regulate *Lag3* expression in Tregs? The RNA-seq results suggest that *Lag3*-YFP$^+$ and *Lag3*-YFP$^-$ Tregs might be distinct subsets. However, some of these differences may be a consequence of LAG3 expression on the cell surface and the subsequent signaling through LAG3. By comparing *Lag3*-YFP$^+$ with *Lag3*-wannabe Tregs, it may be possible to identify the genes that are affected by LAG3

signaling, and determine the transcriptional programs that regulate *Lag3* expression. Identifying cell-extrinsic and cell-intrinsic factors that regulate *Lag3* expression may provide new approaches to modulate LAG3 in the clinic.

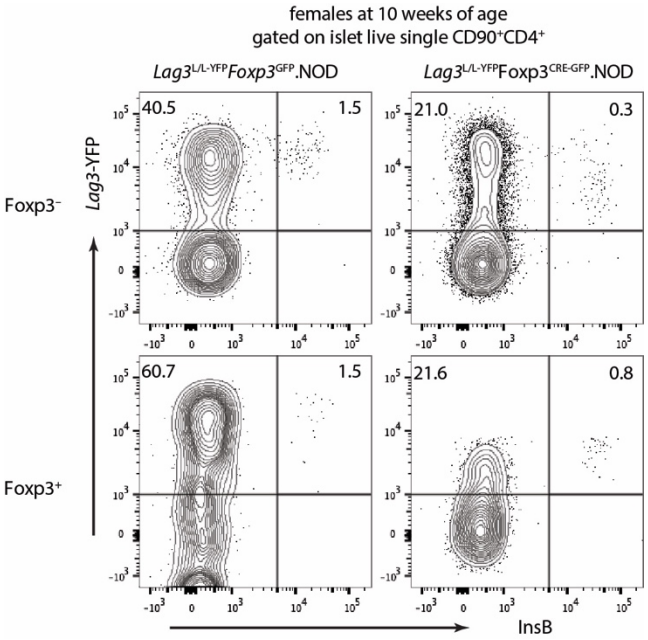

Figure 34. Proportion of LAG3$^+$ Tregs that are reactive to insulin.

Staining of insulin $B_{9\text{-}23}$ tetramers on *Lag3*-YFP$^+$ Tregs and Teffs (females, 10 weeks of age).

5.0 Chapter 5: Hypotheses for future studies

Here, I propose several hypotheses on two topics that are relevant to my PhD study: (1) relative contribution and transcriptional regulation of different co-inhibitory receptors, and (2) a proposal for the revised “two-checkpoint hypothesis”.

5.1 Relative contribution and transcriptional regulation of different co-inhibitory receptors

It has been more than 20 years since the co-inhibitory receptor CTLA4 was shown to negatively regulate T cell activation [210,211]. Several other critical co-inhibitory receptor pathways have also been discovered and characterized since then. These receptors include PD1, which is now being actively targeted in the clinic, and LAG3, TIGIT and TIM3 [251-253]. The success of CTLA4 or PD1 blockade has revolutionized current cancer immunotherapies [251,254]. A better understanding of their modes of action will ultimately help improve the efficacy of targeting these receptors in the clinic. Here, I will speculate some future directions.

5.1.1 The overall impact of co-inhibitory receptors may depend on which immune population(s) play the dominant role

Note: this part of the discussion was taken from the publication "Zhang Q *et. al. Sci. Imm.* (2017)" with slight modifications [225].

My observations (Chapter 3 and Chapter 4) highlight the differential impact of LAG3 modulation on different T cell subsets *in vivo*, where LAG3 modulation alleviates or exacerbates disease, depending on whether Treg or Tconv cells are targeted. The impact of losing LAG3 on Tregs leads to enhanced immune suppression and therefore may offset the effect of blocking the LAG3 pathway in Tconvs. Indeed, one wonders if this might underlie the lack of efficacy observed on tumor growth with LAG3 blockade alone [203]. These findings may also apply to other co-inhibitory receptors [252,253], whose intrinsic effect on Tregs might have been previously overlooked. In Appendix A, I show that deletion of PD1 on Tregs also results in protection from autoimmune diabetes, while anti-PD1 treatment leads to accelerated autoimmune diabetes in NOD mice [112].

My findings may have clinical relevance in that patients who fail to respond to checkpoint blockade immunotherapy may do so because it has a greater impact on promoting Treg function than mitigating Tconv exhaustion. Thus the efficacy of immunotherapy in a particular patient may be modulated by the Tconv:Treg cell ratio and/or co-inhibitory receptor expression on different T cell subsets. Given that anti-LAG3 has entered phase I clinical trials for multiple tumor types with the goal to enhance the efficacy of PD1 blockade, we should consider the differential impact this might have on Treg function and survival versus Tconv exhaustion, as well as the strategies that

specifically target checkpoints on Tconvs or Tregs to boost anti-tumor immunity or mitigate autoimmunity, respectively.

5.1.2 Co-inhibitory receptors may function distinctively but cooperatively to regulate T cell tolerance

It is evident that PD1 and LAG3 act synergistically in several different disease models (introduced in Chapter 1), as the impact is maximized when both pathways are targeted, compared to conditions in which either one is targeted [113,200,201,203,204]. However, it is less clear how these two pathways cooperate with each other to exert downstream effects. It is possible that these two different co-inhibitory receptors function via different modes and mediate distinct signaling pathways to regulate T cell activities, which may lead to differential requirement of these two receptors in T cell tolerance. There are a couple of clues to this speculation.

First, PD1 and LAG3 expression patterns are distinct. While LAG3 surface expression on T cells is more limited to specific tissues in diseased mice, such as pancreas in NOD mice and tumors in tumor-bearing mice, PD1 is readily observed on T cells in peripheral lymphoid compartments (**Fig. 4**). Additionally, $LAG3^+$ T cells are usually also $PD1^+$, which may partially explain why targeting PD1 often results in a greater effect than targeting LAG3 [113,200,201,203]. Several questions remain to be answered: (1) What is the stimulation requirement to induce PD1 vs. LAG3 expression on T cells? Perhaps PD1 expression is induced by tonic stimulation and further enhanced by chronic TCR stimulation, whereas LAG3 expression is induced by strong or chronic TCR stimulation. (2) Is the expression of PD1 or LAG3 stable or dynamically changing?

Lineage tracing mice, such as Rosa26-reporter x *Lag3*$^{CRE\text{-}ERT2}$ or *Pdcd1*$^{CRE\text{-}ERT2}$, will probably provide an answer to this question. (3) Are there any T cell subsets that uniquely express LAG3 but not PD1, and what are their function? LAG3 is highly expressed on CD8$\alpha\alpha^+$ IELs (**Fig. 16**), but it is not clear whether LAG3 is expressed as a consequence of chronic stimulation in the intestine, or whether LAG3 mediates any immunosuppressive activities of these cells. Understanding how expression of PD1 and LAG3 is regulated will help improve the precision of targeting these receptors.

Second, signaling pathways downstream of PD1 and LAG3 may be different. The intracellular domains of PD1 and LAG3 are distinct. PD1 cytoplasmic tail possesses two phosphorylation sites with one located in an ITIM and the other located in an ITSM, which recruit the phosphatases Src homology region 2 domain-containing phosphatase-1 (SHP-1) and SHP-2 that limit TCR signaling [179], whereas LAG3 cytoplasmic tail lacks ITIM or ITSM domains and possesses unique conserved motifs among all known immune receptors [176]. However, there is little understanding of LAG3 signaling pathway. Thus, future studies deciphering the function of conserved domains within LAG3 intracellular tail may advance our understanding of LAG3 signaling. Furthermore, PD1 and LAG3 pathways may regulate the expression of different genes. For instance, genes that are normally affected in *Pdcd1*-deficent CD8$^+$ T cells were not evidently impacted in *Lag3*-defcient CD8$^+$ T cells (**Fig. 12** and **13**). This implies that PD1 and LAG3 may not share the same downstream targets and that LAG3 may mediate distinct function from PD1 in T cell tolerance. This may also provide some clues to why in an autoimmune-prone background, PD1 and LAG3 play non-redundant roles and loss of either pathway leads to catastrophic autoimmune responses; while in anti-tumor or anti-infection immunity, dual

blockade is usually required to maximally reinvigorate T cell responses. However, it should be noted that those observations were taken from different disease models. Studies comparing the relative contribution of PD1 and LAG3 in the same disease settings may help tailor appropriate combinations of checkpoint blockade-mediated immunotherapies, as the differential expression and function of PD1 and LAG3 may affect the timing and dosing of antibody administration.

5.1.3 The expression of co-inhibitory receptors may be coordinated by a core of transcription factors

Most recent studies focus on pathways downstream of co-inhibitory receptors, but little is known about how their expression is regulated at genetic or transcriptional level. PD1 and LAG3, as well as other co-inhibitory receptors, appear to be co-expressed on T cells, albeit to differing degrees [56,113,200-202,204]. This co-expression pattern was also observed in the autoimmune diabetes model (**Fig. 4** and **7**). One may speculate that it would be more economical if the expression of co-inhibitory receptors were coordinated by a "master" transcription factor together with other transcriptional and epigenic "modifiers" (these "modifiers" can either promote or repress receptor expression).

Current technology may help to test this hypothesis. First, to identify transcription factor candidates: single cell RNA-seq profiling may provide a list of potential transcription factors that exist in cells co-expressing multiple different co-inhibitory receptors, but the "master" transcription factor should also exist in cells that may only express one or two receptors. Second, to screen *cis*-regulatory elements in co-inhibitory receptor genes: using bioinformatics, one could identify conserved *cis*-regulatory DNA sequences that

may be shared between different co-inhibitory receptors and that may be bound by transcription factors identified above. Third, to verify that these *cis*-regulatory elements indeed regulate co-inhibitory receptor expression: using DNase I hypersensitivity assays, one could verify *cis*-regulatory elements that are critical in regulating all or most of the co-inhibitory receptors, and *cis*-regulatory elements that may be important for a specific receptor. Fourth, to verify that these transcriptional factors indeed take part in co-inhibitory receptor expression: using Crispr/cas9 technology, one could either overexpress or knockdown/knockout transcription factors in WT and mutant T cells lacking the *cis*-regulatory element that may be bound by the tested transcription factor.

Even if co-inhibitory receptors are not co-regulated by a "master" transcription factor, it is still worthwhile to identify genetic factors that regulate the expression of co-inhibitory receptors, as such regulatory factors may point to new clinical targets to manipulate co-inhibitory pathways.

5.2 A proposal for the revised "two-checkpoint hypothesis"

We have gained significant insight on how autoimmune diabetes is checked at each stage of its pathogenesis since the original "two-checkpoint hypothesis" was proposed 20 years ago [7]. I have summarized most findings based on the original hypothesis in Chapter 1. However, other possible mechanisms have also been raised, which are discussed here.

5.2.1 Checkpoint 0: generation of autoreactive and regulatory T cell repertoires

In Chapter 1, I introduced factors that may affect the generation of islet-antigen reactive T cell repertoire. However, many questions remain to be addressed in regard to Treg repertoire in autoimmune diabetes:

First, how do different Treg repertoire parameters affect their functionality? There are a couple of important parameters: TCR repertoire diversity and antigen specificity. The diversity of Treg repertoire has been shown to be required for optimal immune homeostasis, and *Foxp3* CNS3 enables a higher diversity of Treg repertoire on the B6 background [160,255]. It has been shown that a low diversity Treg repertoire is selected in NOD mice [256], although it remains to be determined how this low diversity repertoire would translate into suppression of islet-antigen reactive T cells. Antigen specificity is likely to be important, as it may affect Treg activation and infiltration into the islet. T cell infiltration into the pancreas is a cell-autonomous process driven by islet-antigen specificity [216]. Islet-antigen seems to be required for Treg-mediated suppression of autoimmune diabetes, as transferring TCR transgenic Tregs into the hosts lacking their cognate antigens resulted in reduced protection from autoimmune diabetes, compared to WT hosts [257]. It would be of interest to see whether diabetes onset and incidence is associated with the frequency of islet-antigen-reactive Tregs. Tetramers, other than insulin $B_{9\text{-}23}$ tetramers shown in Fig. 34, that can detect islet-antigen specific Tregs may provide some clues.

Second, what factors impact Treg selection in autoimmune diabetes? What is less clear is the threshold between negative selection of islet-antigen reactive T cells and

positive selection of Tregs in NOD mice. TCR affinity is crucial for lymphocyte fate determination, as thymocytes that recognize self-ligands at intermediate affinity will be positively selected, but these cells also possess the potential to undergo programmed cell death (negative selection) or develop into Tregs (agonist selection) [258]. In a retrogenic TCR mouse study, frequency of pancreatic Tregs seemed to be positively associated with TCR affinity [259]. Another recent study suggests that both high-affinity and low-affinity Tregs contribute to protection from autoimmune diabetes but via distinct immunosuppressive mechanisms [260]. Treg selection vs. negative selection can also be intrinsically impacted by the survival threshold. BIM is a pro-apoptotic factor that is required for negative selection [261]. BIM deficiency in NOD mice did not result in impaired Teff function but resulted in an increased number of insulin-reactive Tregs and protection from autoimmune diabetes [262]. It is possible that the survival threshold for agonistically selected Tregs is higher in NOD mice than other strains, and deficiency in BIM lowered the survival threshold. In contrast, another study suggested that NOD mice exhibited an enhanced agonistic selection of Tregs compared to other mouse strains, and this trait did not map to *Idd* regions that control clonal deletion [263]. However, in this study, BDC2.5 peptide was used to select the BDC2.5 transgenic TCR, and therefore it remains to be determined how TCR affinity and survival threshold affect negative selection vs. Treg selection in WT NOD mice. Additionally, insulin expression in the thymus could also affect Treg selection. Aire is essential in thymic selection by driving the expression of tissue specific self-antigens in the thymus [264]. While *Ins2*$^{-/-}$.NOD mice develop remarkably accelerated autoimmune diabetes perhaps due to defects in negative selection [23,25,26]; *Aire*$^{-/-}$.NOD mice do not develop autoimmune diabetes, and *Aire*$^{-/-}$.NOD mice die

because of severe systemic autoimmune symptoms [69]. It is possible that selection of islet-antigen-reactive Treg may also be impaired in *Ins2*$^{-/-}$.NOD mice, whereas Aire positively selects Tregs that are protective of other tissues at the expense of islet-antigen-reactive Tregs.

Further studies are warranted to decipher these questions. Recent immunopathological assessment has revealed that Tregs are not frequently seen in pancreas of T1D patients [48], although it remains to be determined whether Treg selection is impaired in T1D patients, thus leading to the failure in regulating T1D pathogenesis.

5.2.2 Checkpoint 1: end of ignorance

Despite many years of study of T1D, it remains unclear what triggers the initiation of insulitis. In NOD mice, insulitis starts at 3 to 4 weeks of age. Interestingly, in BDC2.5 transgenic NOD mice that express TCRs reactive to islet-antigen Chromogranin A, insulitis also starts around 3 weeks of age. This indicates that islet-antigens are likely "ignored" by pre-existing autoreactive T cells before this time point. There are several possible mechanisms of checkpoint 1.

First, functional APCs are not present. A recent study suggests that innate immune infiltration into the NOD pancreas is a tightly regulated process [30]. The death of β cells induces the recruitment and activation of neutrophils, B-1a cells, and pDCs into the islet in a sequential order (neutrophils peak at 2-3 weeks, total B cells increase steadily starting from 3 weeks, and pDCs peak at 4-5 weeks), and depletion of any of these subsets delayed diabetes onset [30]. Classical DCs appeared in islets later (4-6

weeks), slightly proceeding T cells (5-6 weeks). Interestingly, another study also suggests that B1 cells promote T cell infiltration into the pancreas [265]. However, it remains unclear how APCs (cDCs and/or B cells?) are activated. Intra-vital imaging may provide some insight on the real-time interactions of innate immune cells that infiltrate pancreas in the future. Additionally, upregulation of co-stimulatory ligands, such as CD40 and ICOS ligand, on APCs can be critical in the initiation of insulitis. For instance, the CD40:CD40L axis is required for the initiation of insulitis and autoreactive T cell priming in autoimmune diabetes [76,84-86]. *Icos*$^{-/-}$.NOD mice are free of autoimmune diabetes [79,80]. A very recent study showed that *Icosl*$^{-/-}$.NOD mice were free of insulitis, which exhibited a stronger protection than *Icos*$^{-/-}$.NOD mice [266]. It is curious to see how and when CD40 and ICOS ligand expression are induced on APCs.

Second, autoreactive T cells may not be capable of homing to islets yet. This mechanism was proposed in the original hypothesis [7]. There are two possibilities. First, the pancreatic environment has not expressed homing ligands for autoreactive T cell to home. Second, autoreactive T cells have not expressed homing receptors yet. However, both seem unlikely, as peripheral T cells in neonatal NOD mice already express $\alpha 4\beta 7$, and addressins such as MadCAM-1 are PECAM-1 are present in neonatal NOD pancreas as early as two days of age [267,268].

Third, the “autoantigenic” epitopes are not exposed or present. The primacy of insulin in the initiation of autoimmune diabetes has been shown in the NOD mouse model [23,63]. Thus, it is curious to note at what time point insulin becomes antigenic. It was shown that only intra-islet DCs could activate several primary insulin $B_{9\text{-}23}$-reactive T cell lines, while splenic DCs activated these T cell lines when pulsed with β cell secretory granules

[34]. This indicates that circulating insulin is not the source of autoantigens, but rather the insulin peptides generated in β cell secretory granules are autoantigenic. More recently, a new class of islet-autoantigens, consisting of hybrid insulin peptides covalently cross-linked with other peptides from β cell secretory granules, was identified in both NOD mice and T1D patients [46]. Together, these data suggest that β cell secretory granules play a critical role in the generation of autoantigenic insulin peptides to be recognized by autoreactive T cells. However, it is not clear what epitope(s) play primary vs. secondary roles in the initiation of insulitis. Additionally, NOD mice treated with Z-VAD, a pan-caspase inhibitor, exhibited significantly delayed diabetes onset and reduced incidence, indicating a role for β cell death or stress in the generation or exposure of islet-antigens and subsequent initiation of insulitis [30,269]. Many environmental risk factors have been implicated in β cell stress and death, yet further studies are warranted to establish a causal effect [5,269].

Understanding of checkpoint 1 mechanisms will provide insight on regiments that may help prevent early onset of T1D in genetically predisposed individuals.

5.2.3 Checkpoint 2: uncontrolled chaos

We have gained relatively more knowledge on checkpoint 2 mechanisms compared to checkpoint 1. I discussed most recent findings in regard to cell-intrinsic and cell-extrinsic mechanisms in Chapter 1, and here I summarize some of those critical observations and discuss several possible future directions.

Hierarchical usage of co-stimulatory and co-inhibitory pathways in autoimmune diabetes:

Note: This part of the discussion was taken from the review "Zhang Q, Vignali DAA. *Immunity.* (2016)" with slight modifications [70].

First, both "first-line" and "second-line" pathways affect autoimmune diabetes. The CD28 co-stimulation is a "first-line" pathway essential for autoreactive T cell priming, whereas PD1 has a dominant "first-line" inhibitory impact on autoimmune diabetes. However, the relative contributions of their ligands B7.1, B7.2 and PD-L1, PD-L2, respectively, seem to be affected by the timing of ligand expression and interaction, cell types that preferentially express one ligand versus the other. This is probably further complicated by differential interactions between B7 molecules with CTLA4. Studies with antibodies that specifically block CD28:B7.1, CD28:B7.2, CTLA4:B7.1, CTLA4:B7.2, PD1:PD-L1, PD1:PD-L2 and PD-L1:B7.1 interactions would help to clarify the relative contribution of these receptors and ligands. There may also be "second-line" pathways that do not impact autoimmune diabetes all the time. For instance, while many IgSF co-inhibitory receptors are upregulated on autoreactive T cells and reinforce co-inhibitory signals after T cell priming, their contribution may not impact autoimmune diabetes equally.

Second, the use of different co-stimulatory and co-inhibitory pathways has temporal implications. For instance, unlike the CD28:B7 or CD40:CD40L axes, the other TNFRSF co-stimulatory pathways tend to participate at later stages, probably because these receptors are upregulated on activated T cells and/or their corresponding ligands may be restricted to inflamed tissues. It would appear that CTLA4 functions in a more

restricted time window during the priming phase, while TIM3 and B7-H4 play a role in the later stage. This contrasts with PD1 and LAG3 that appear to be involved over a broader time period. Studies using conditional knockout mice in combination with inducible CRE mice will help further dissect the temporal utilization of co-stimulatory and co-inhibitory receptors.

Third, co-stimulation or co-inhibition is essential to regulate both autoreactive T cell and Treg homeostasis and function. For instance, while it is clear that CD28 provides a dominant co-stimulatory contribution in promoting autoimmunity, it can also impact Treg cell development and thereby limit autoimmunity. Additionally, while LAG3 and PD1 are required to limit the pathogenesis of autoimmune diabetes, they also intrinsically limit Treg functions (Chapter 3, Chapter 4, and Appendix A). Studies with cell type-restricted deletion of co-inhibitory molecules may help to clarify their roles and define populations that could be targeted therapeutically.

Are Tregs destined to fail or are they victimized by the islet microenvironment?

As introduced in Chapter 1, Tregs are perhaps the most crucial controller of autoimmune diabetes [74,81,148-150,164-168]. However, they also appear to be very "fragile" in the autoimmune diabetes-prone background [15,16,74,170,171]. For instance, pancreatic Tregs tend to lose IL-2 receptor (CD25) and Foxp3 expression, therefore losing their suppressive capacity [14,17]. Interestingly, insulitic Tregs exhibit very distinct transcriptional profiles compared to peripheral Tregs (**Fig. 32**). It is equally possible that insulitic Tregs are shaped by the islet microenvironment as a consequence of entering the islet, or that insulitic Tregs are intrinsically different from peripheral Tregs so that they are enabled to enter the islet.

It remains unclear whether Tregs are intrinsically prone to lose their functionality or the islet microenvironment is too hostile to maintain Treg identities. For instance, Nrp1 is required to maximize the competitive fitness of Tregs during inflammation *in vivo* [18-20]. *NRP1* (Chr10p11.22, OR 1.1) has been genetically mapped to the T1D-susceptibility regions. Peripheral Tregs from NOD mice express lower level of Nrp1 than those from B6 mice, and Nrp1 expression is further lost on insulitic Tregs (Appendix B). Possibly, the low expression of Nrp1 on Tregs in NOD mice is a consequence of both intrinsic defects of Tregs and inhospitality of the islet microenvironment. Additionally, in the BDC2.5 transgenic NOD mouse model, even though all T cells express TCRs reactive to Chromogranin A, these mice exhibit much lower diabetes incidence (10-20%) than WT NOD mice (70-90%) by 30 weeks of age [165,270]. Further analysis suggests that insulitic Tregs from BDC2.5 NOD mice are capable of repressing autoimmunity [165], raising the question of whether the islet microenvironment alone could drive Treg insufficiency. However, these transgenic Tregs also express TCRs reactive to Chromogranin A, and thus are more capable of infiltrating into the islet than WT Tregs. It is likely that intrinsic defects of Tregs render them more susceptible to microenvironment insults.

Genetic factors may contribute to the intrinsic defects of Tregs in NOD mice or T1D patients. For instance, both *IL2* (Chr4q27, OR 1.2) and *IL2RA* (Chr10p15.1, OR 1.6) are genetically mapped to the T1D-suscepptility regions. Additionally, the ability of Tregs to infiltrate into the pancreas is also intrinsically determined by their TCR usage, as discussed in Chapter 5.2.1 “checkpoint 0”. Perhaps, the frequency of islet-antigen-reactive Tregs is lower in NOD mice that exhibit earlier onset of autoimmune diabetes.

There might be other yet-unknown genetic factors that intrinsically contribute to Treg insufficiency.

It is less clear what factors in the islet microenvironment confer Tregs insufficiency. One speculation is that pro-inflammatory cytokines, such as IFNγ and TNFα, which have been shown to promote Treg instability in other pro-inflammatory disease models [18,271]. Another study suggests that insulin could also promote Treg instability in Type 2 diabetes patients [272]. Thus, further studies are warranted, as these potential extrinsic factors may affect the efficacy of Treg transfer immunotherapy for treating T1D.

APPENDIX A

Role of PD1 in Treg-mediated self-tolerance

This is a collaborative project with Dr. Arlene Sharpe's laboratory, and therefore I will only show and discuss data that I generated in this appendix.

The impact of co-inhibitory receptors on Treg function and maintenance has been controversial. For instance, some early studies suggest that Tregs may mediate suppression of Teffs through LAG3, whereas my own observations (**Chapter 4.1**) show that LAG3 intrinsically limits Treg proliferation and function in the NOD mouse model [146,187,188,209,225]. I questioned whether this cell-intrinsic effect would also apply to other co-inhibitory receptors.

As introduced in Chapter 1, PD1 is also required to maintain self-tolerance in NOD mice, and loss of PD1 signaling resulted in more exacerbated autoimmune diabetes, compared to loss of LAG3 signaling [103,112,113]. PD1 was readily expressed on peripheral Tregs in NOD mice, and its expression was further enhanced on intra-islet Tregs (**Fig. 4**). I therefore asked whether PD1 had a similar or distinct effect as LAG3 on Tregs in regulating autoimmune diabetes.

Pdcd1$^{L/L}$.B6 mice were generated and kindly provided by Dr. Sharpe's lab, and I bred them onto the NOD background at University of Pittsburgh. Microsatellite tests of 20 *Idd* loci covering 144 SNPs revealed that *Pdcd1*$^{L/L}$.NOD mice were 98.5% NOD at the

F9 generation, and there were four heterozygous SNPs located on Chr1 within the *Pdcd1* gene region, inherited upon gene targeting. I crossed *Pdcd1*$^{L/L}$.NOD mice with Foxp3$^{CRE\text{-}GFP}$.NOD mice to specifically delete *Pdcd1* in Tregs.

Interestingly, the loss of PD1 on Tregs abrogated autoimmune diabetes in female mice, indicating that PD1 may also limit Treg function in the NOD mouse model (**Fig. 35**). This impact was even greater than removal of LAG3 on Tregs, probably because PD1 was expressed at a higher level than LAG3 on Tregs (**Fig. 4** and **17**). However, it remains to be tested whether PD1 and LAG3 limit Treg activities via similar or different modes.

Other studies involving PD1 on Tregs also add some complexity. A recent study showed that high PD1 expression marked dysfunctional tumor-infiltrating Tregs in malignant gliomas patients [273]. Another study reported that *Pdcd1*-deficient Tregs were more suppressive but were incapable of maintaining Foxp3 expression in a mouse colitis model [250]. It is probable that PD1 is required for Treg development and stability, but sustained high PD1 expression limits the suppressive capacity of Tregs. Future studies using PD1 conditional knockout as well as inducible T cell subset-specific CRE mice may help elucidate these questions.

Further investigation on parsing the role of PD1 on Tregs vs. CD8$^+$ T cells is also warranted, as PD1 blockade-mediated cancer immunotherapy has shown some promising, but not complete, efficacy in the clinic, and the efficacy varies between tumor types [251]. As shown in a murine B16 transplantable tumor model, PD1 expression on Tregs was much greater than on CD8$^+$ T cells (**Fig. 4**). One possibility is that the ratio of tumor-infiltrating Tregs to CD8$^+$ T cells varies between different tumor patients, and the efficacy of anti-PD1 treatment may depend on which T cell subset is targeted.

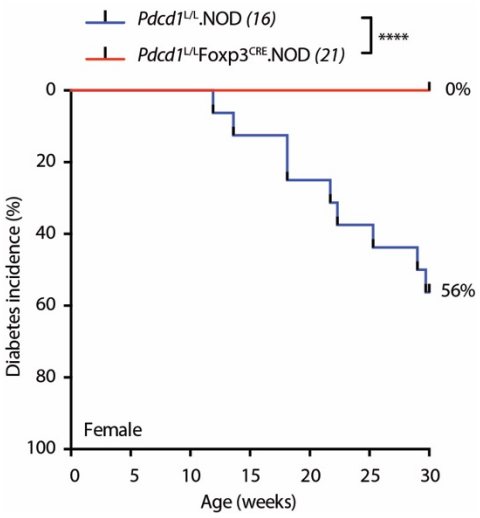

Figure 35. Loss of PD1 on Tregs protects NOD mice from autoimmune diabetes.

Diabetes onset and incidence monitored in *Pdcd1*$^{L/L}$Foxp3$^{CRE\text{-}GFP}$.NOD females together with cohoused littermate controls. The log-rank was applied to Kaplan-Meier survival function estimates to determine the statistical significance. ****$p < 0.0001$.

APPENDIX B

Role of Nrp1 in maintaining Treg function

This is a collaborative project with two former postdocs Drs. Anabelle Visperas and Andres Herrada in the lab. I will introduce their observations with their permission, but only show data that I generated in this appendix.

Nrp1 is a type I transmembrane receptor for vascular endothelial growth factor (VEGF) and semaphorins (Sema3a, Sema4a), and considered a bona fide marker for murine tTregs [19,20,118,119]. Although Nrp1 does not seem to be essential for Treg function or stability at a homeostatic state, it is required to maximize the competitive fitness of Tregs during inflammation *in vivo* [18-20]. In humans, *NRP1* (Chr10p11.22) has been mapped to one of the T1D-susceptibility regions (T1DBase).

Interestingly, specific removal of Nrp1 on Tregs did not further exacerbate autoimmune diabetes onset or incidence in NOD mice (data not shown), possibly because Nrp1 was significantly downregulated on Tregs in NOD mice to begin with (percent of $Nrp1^+$ Tregs in the periphery: B6 mice – > 80%, NOD mice – 50% - 60%, data not shown). Additionally, cell surface Nrp1 seemed to be cleaved by ADAM17 on intra-islet Tregs (data not shown). Based on these preliminary observations, I questioned whether restoration of Nrp1 expression on Tregs would reinvigorate their capacity to regulate autoimmune diabetes.

To address this question, Dr. Andrea Szymczak-Workman generated *Rosa26*$^{LSL\text{-}Ametrine\text{-}Nrp1}$ mice, in which the expression of Nrp1 and Ametrine is driven by the *Rosa26* promoter in CRE^{+} cells (**Fig. 36A**). I bred *Rosa26*$^{LSL\text{-}Ametrine\text{-}Nrp1}$.B6 mice onto the NOD background at University of Pittsburgh. Microsatellite tests of 20 *Idd* loci covering 144 SNPs revealed that *Rosa26*$^{+/LSL\text{-}Ametrine\text{-}Nrp1}$.NOD mice were 98.5% NOD at the F7 generation, and there were one heterozygous SNP located on Chr6 from the targeting construct.

Overexpression of Nrp1 in *Rosa26*$^{+/LSL\text{-}Ametrine\text{-}Nrp1}$Foxp3$^{CRE\text{-}GFP}$.NOD mice restored its expression on peripheral Tregs to the same extent as that in WT B6 mice (**Fig. 36B**). Even though exogenous *Nrp1* expression in Tregs did not rescue the cell surface expression of Nrp1 on insulitic Tregs (**Fig. 36B**), it led to significantly delayed autoimmune diabetes onset in *Rosa26*$^{+/LSL\text{-}Ametrine\text{-}Nrp1}$Foxp3$^{CRE\text{-}GFP}$.NOD mice, compared to littermate controls (**Fig. 36C**). These data suggest that optimal Nrp1 signaling may be required to maintain Treg functionality in an autoimmune-prone environment.

Further investigation regarding the following questions may help improve our understanding on the role of Nrp1 in maintaining Treg function in autoimmune diabetes: (1) What factors promote Nrp1 shedding in the islet microenvironment? The islet microenvironment is enriched with pro-inflammatory cytokines, such as IFNγ and TNFα, which may contribute to the loss of Nrp1 on Tregs. This can be tested by assessing ADAM17 expression and Nrp1 shedding in cytokine-treated WT vs. corresponding receptor knockout Tregs. (2) What are the downstream pathways affected by the loss of Nrp1 signaling in Tregs that may contribute to Treg insufficiency in autoimmune diabetes? Our recent findings suggest that *Nrp1*-difficient Tregs are susceptible to IFNγ-induced

fragility in antitumor immunity [18]. One could assess IFNγ receptor expression on WT, Nrp1-deficient, and Nrp1-overexpressing Tregs, and diabetes incidence in Foxp3$^{CRE-GFP}$, *Ifngr*$^{L/L}$Foxp3$^{CRE-GFP}$, *Nrp1*$^{L/L}$Foxp3$^{CRE-GFP}$, *Ifngr*$^{L/L}$*Nrp1*$^{L/L}$Foxp3$^{CRE-GFP}$.NOD mice. (3) Does modulation of Nrp1 pathway in Tregs have a therapeutic effect on autoimmune diabetes? This can be tested by treating NOD mice with Nrp1 ligands, Sema4a-Ig, for instance [19]. Additionally, one could also use the inducible Foxp3-CRE [274] to temporarily overexpress Nrp1 on Tregs (*Rosa26*$^{+/LSL-Ametrine-Nrp1}$*Foxp3*$^{YFP-CRE-ERT2}$.NOD mice). Understanding these questions will help us identify approaches to reinvigorate Tregs in T1D patients.

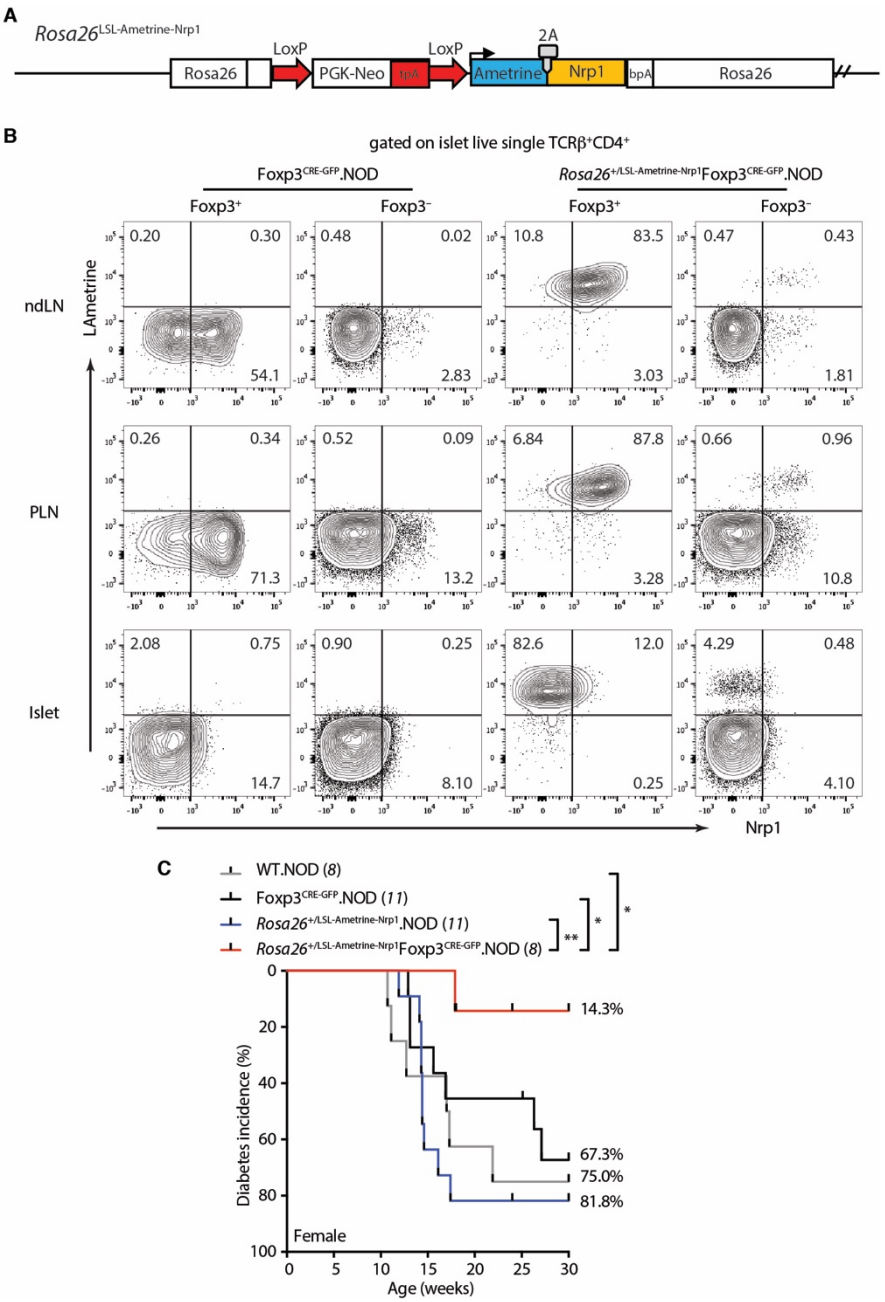

Figure 36. Restoration of Nrp1 expression in Tregs results in delayed autoimmune diabetes

(**A**) Schematic of the *Rosa26*$^{\text{LSL-Ametrine-Nrp1}}$ construct. (**B**) Validation of cell surface Nrp1 expression and Ametrine expression in CD4^{+}Foxp3^{-}, and CD4^{+}Foxp3^{+} T cells in *Rosa26*$^{+/\text{LSL-Ametrine-Nrp1}}$Foxp3$^{\text{CRE-GFP}}$.NOD and cohoused Foxp3$^{\text{CRE-GFP}}$.NOD mice (females, 10 weeks of age). (**C**) Diabetes onset and incidence monitored in female *Rosa26*$^{+/\text{LSL-Ametrine-Nrp1}}$Foxp3$^{\text{CRE-GFP}}$.NOD and cohoused littermate controls. The log-rank was applied to Kaplan-Meier survival function estimates to determine the statistical significance. **p* < 0.05, ***p* < 0.01.

APPENDIX C

Low cell number RNA sequencing

This RNA sequencing protocol is based on the Smart-seq2 technique [220].

Three major advantages of this protocol: (1) As full-length cDNAs are reverse transcribed using the template switching oligo, there is no 3'-bias of sequencing reads, and splicing variants can be distinguished if enough sequencing depth is provided; (2) This protocol is optimized for low cell number (50 – 500 cells) RNA sequencing, but can also be used for purified RNA or single cell RNA sequencing; (3) The cost is relatively lower than any available kits.

C.1 Working Station Setup

Two working areas are needed for the following steps. PCR hoods are considered cleaner than clean stations described below. The clean station can be a bench-top in the general lab that is clean enough but far away from your PCR hoods. ***NO reagents/tubes/plates are allowed to go back and forth between your PCR hood and clean station to avoid any contamination. NO PCR amplification products are allowed in the PCR hood.***

C.2 Reagent Setup

If reagents are ordered in a large volume, make aliquots, avoid using stocks directly, and no used tips are allowed to go back into reagent tubes. If you have a large volume to pipet, it is always better to pipet multiple times with p200 than p1000 to have more accuracy.

1| RT Primer (QZ53): dissolve primers in EB buffer to a final concentration of 100μM, aliquot to 10μl/tube, and store at –20° up to 6 months. Add 90μl water to make final concentration of 10μM when use. – Enough for 100rxn.

RT Primer (QZ53): (PAGE purified, Invitrogen)
AAGCAGTGGTATCAACGCAGAGTACTTTTTTTTTTTTTTTTTTTTTTTTTTTTTVN (V: A/C/G, N: A/T/C/G)

2| TSO (QZ49): dissolve primers in EB buffer to a final concentration of 100μM, aliquot to 10μl/tube, and store at –80° up to 6 months. – Enough for 100rxn. ***Avoid repeated freeze-thaw cycles.***

TSO (QZ49): (RNase-free HPLC purified, Exiqon)
AAGCAGTGGTATCAACGCAGAGTACrGrG+G

3| Amp Primer 1 (QZ50): dissolve primers in EB buffer to a final concentration of 100μM, aliquot to 10μl/tube, and store at –20° up to 6 months. Add 90μl water to make final concentration of 10μM when use. – Enough for 400rxn.

Amp Primer 1 (QZ50): (PAGE purified, Invitrogen) AAGCAGTGGTATCAACGCAGAGT

4| i7 Barcoding Primers (QZ54-77): dissolve primers in EB buffer to a final concentration of 100μM, aliquot to 10μl/tube, and store at –20° up to 6 months. Add 190μl water to make final concentration of 5μM when use. – Enough for 40rxn.

i7 Barcoding Primers: (PAGE purified, Invitrogen)
CAAGCAGAAGACGGCATACGAGATXXXXXXXXGTCTCGTGGGCTCGG (X: barcodes)

Please note that ***N705 cannot be used alone on NextSeq***.

QZ54 (N701): TCGCCTTA	(entry on sample sheet TAAGGCGA)
QZ55 (N702): CTAGTACG	(entry on sample sheet CGTACTAG)
QZ56 (N703): TTCTGCCT	(entry on sample sheet AGGCAGAA)
QZ57 (N704): GCTCAGGA	(entry on sample sheet TCCTGAGC)
QZ58 (N705): AGGAGTCC	(entry on sample sheet GGACTCCT)
QZ59 (N706): CATGCCTA	(entry on sample sheet TAGGCATG)
QZ60 (N707): GTAGAGAG	(entry on sample sheet CTCTCTAC)
QZ61 (N710): CAGCCTCG	(entry on sample sheet CGAGGCTG)

QZ62 (N711): TGCCTCTT (entry on sample sheet AAGAGGCA)
QZ63 (N712): TCCTCTAC (entry on sample sheet GTAGAGGA)
QZ64 (N714): TCATGAGC (entry on sample sheet GCTCATGA)
QZ65 (N715): CCTGAGAT (entry on sample sheet ATCTCAGG)
QZ66 (N716): TAGCGAGT (entry on sample sheet ACTCGCTA)
QZ67 (N718): GTAGCTCC (entry on sample sheet GGAGCTAC)
QZ68 (N719): TACTACGC (entry on sample sheet GCGTAGTA)
QZ69 (N720): AGGCTCCG (entry on sample sheet CGGAGCCT)
QZ70 (N721): GCAGCGTA (entry on sample sheet TACGCTGC)
QZ71 (N722): CTGCGCAT (entry on sample sheet ATGCGCAG)
QZ72 (N723): GAGCGCTA (entry on sample sheet TAGCGCTC)
QZ73 (N724): CGCTCAGT (entry on sample sheet ACTGAGCG)
QZ74 (N726): GTCTTAGG (entry on sample sheet CCTAAGAC)
QZ75 (N727): ACTGATCG (entry on sample sheet CGATCAGT)
QZ76 (N728): TAGCTGCA (entry on sample sheet TGCAGCTA)
QZ77 (N729): GACGTCGA (entry on sample sheet TCGACGTC)

5| i5 Barcoding Primers (QZ78-93): dissolve primers in EB buffer to a final concentration of 100μM, aliquot to 10μl/tube, and store at –20° up to 6 months. Add 190μl water to make final concentration of 5μM when use. – Enough for 40rxn.

i5 Barcoding Primers: (PAGE purified, Invitrogen)
AATGATACGGCGACCACCGAGATCTACACXXXXXXXXTCGTCGGCAGCGTC (X: barcodes)

QZ78 (S502): CTCTCTAT (entry on sample sheet ATAGAGAG)
QZ79 (S503): TATCCTCT (entry on sample sheet AGAGGATA)
QZ80 (S505): GTAAGGAG (entry on sample sheet CTCCTTAC)
QZ81 (S506): ACTGCATA (entry on sample sheet TATGCAGT)
QZ82 (S507): AAGGAGTA (entry on sample sheet TACTCCTT)
QZ83 (S508): CTAAGCCT (entry on sample sheet AGGCTTAG)
QZ84 (S510): CGTCTAAT (entry on sample sheet ATTAGACG)
QZ85 (S511): TCTCTCCG (entry on sample sheet CGGAGAGA)
QZ86 (S513): TCGACTAG (entry on sample sheet CTAGTCGA)
QZ87 (S515): TTCTAGCT (entry on sample sheet AGCTAGAA)
QZ88 (S516): CCTAGAGT (entry on sample sheet ACTCTAGG)
QZ89 (S517): GCGTAAGA (entry on sample sheet TCTTACGC)

QZ90 (S518): CTATTAAG (entry on sample sheet CTTAATAG)

QZ91 (S520): AAGGCTAT (entry on sample sheet ATAGCCTT)

QZ92 (S521): GAGCCTTA (entry on sample sheet TAAGGCTC)

QZ93 (S522): TTATGCGA (entry on sample sheet TCGCATAA)

6| Lysis buffer: dilute Triton X-100 to 2% (vol) in water, and then dilute to 0.2% (vol) right before use.

7| Reagent ordering:

Triton X-100 (molecular grade)	Sigma T8787-50ML
Betaine solution (molecular grade)	Sigma B0300-5VL (3,750 rxn)
$MgCl_2$ solution (molecular grade)	Sigma M1028-100ML
RNase Inhibitor	Clontech 2313B (2,500 rxn)
dNTP mix	Thermo R0193 (5,000 rxn)
SuperScript II RT	Thermo 18064071 (400 rxn)
UltraPure Water	Thermo 10977-015
Hifi HotStart ReadyMix	KAPA KK2602 (500 rxn)
Buffer EB	Qiagen 19086
Agencourt AMPure XP	Beckman Coulter A63881
Hardshell PCR plate	Bio-rad HSP9601
Micro-seal A	Bio-rad MSA5001
Micro-seal B	Bio-rad MSB1001
Nextera XT DNA Library Prep kit	Illumina FC-131-1096 (96 rxn)
Tris-HCl w/ Tween-20	TEKnova T7724
Library Quantification Kit	KAPA KK4854 (1000 rxn)
Library Quantification Standards	KAPA KK4903 (120 rxn)
NextSeq 500/550 High Output v2 (75x)	Illumina FC-404-2005

C.3 Cell Sorting and Lysis

— PCR hood

1| Prepare fresh lysis buffer by adding 1μl of RNase inhibitor (40U/μl) to 19ul of 0.2% Triton X-100 solution, and aliquot 2μl/well into 96-well PCR plate for cell sorting. Seal

with microseal B before and after sorting to avoid evaporation and contamination. – Enough for 10rxn.

2| Cell populations-of-interest will be sorted into eppendorf tubes containing 300μl of sorting buffer first. **Double-sort 500 cells** directly into each well of 96-well plate containing the lysis buffer, gently vortex and spin down the plate at 2,000g for 2min. Additional 500 cells will be sorted into eppendorf tubes for purity check. Any purity <99.5% should be taken notes.

3| Neg Ctrl: add nothing; Pos Ctrl: add 0.3μl of 1ng/μl total RNA.

4| Pre-mix 10μM RT Primers (QZ53) and 10mM dNTPs at 1:1 ratio (vol), and add 2μl of the mixture to each PCR well. – Total volume: 4μl.

5| Seal with microseal B, and spin down the mixture at 2,000g for 2min. ***ALWAYS spin first before you put the plate into a PCR cycler to make sure all reagents are down to the bottom.***

6| Incubate at 72° for 3min, and immediately put the plate on ice. Ideally, the next step should be processed ASAP. **PROGRAM: bprna1**

C.4 Reverse Transcription

— PCR hood

1| Prepare RT mix as below while performing denaturation. ***ALWAYS spin down all the regents down to the bottom of tubes as the concentration may be changed due to the evaporation onto the lid. Due to the low volume for pipetting, pre-mix more rxns of water and $MgCl_2$ first, and then pipet out the total volume you need for the rxns you have planned and mix with other reagents.***

Total volume (μl): 6μl	volume	final
Water	0.56	–
$MgCl_2$ (1M)	0.09	9mM
SuperScript II first-strand buffer (5x)	2	1x
DTT (100mM)	0.5	5mM
Betaine (5M)	2	1M
RNase inhibitors (40U/μl)	0.25	10U
TSO (100μM, QZ49)	0.1	1μM
SuperScript II reverse transcriptase (200U/μl)	0.5	100U

2| Spin down the incubated sample lysates at 2,000g for 2min before opening the seal. ***ALWAYS spin first before you open the seal to avoid any cross-contaminations between samples.***

3| Add 6μl of RT mix to 4μl of sample lysates to make up 10μl in total.

4| Seal with microseal A, and spin down the mixture at 2,000g for 2min.

5| Perform first-strand PCR reactions as below: ***The 10 cycles 50°/42° helps to open up some secondary structure and carry out further reverse transcription.*** **PROGRAM: bprna2**

1x	42°	90min
10x	50°	2min
	42°	2min
1x	70°	15min
1x	4°	hold

C.5 cDNA Amplification

— PCR hood

1| Prepare PCR amplification mix as below.

Total volume (μl): 15μl	volume	final
KAPA HiFi HotStart ReadyMix (2x)	12.5	1x
Water	2.25	–
Amp Primer 1 (10μM, QZ50)	0.25	0.1μM

2| Spin down first-strand product at 2,000g for 2min at room temperature before opening the seal. ***ALWAYS spin at room temperature if the last step has a long or high temperature incubation to avoid condensation of the seal pressure at low temperature.***

3| Add 15μl of PCR amplification mix to 10μl of first-strand product to make 25μl in total.

4| Seal with microseal A, and spin down the mixture at 2,000g for 2min.

5| Perform amplification PCR as below: **PROGRAM: bprna3**

1x	98°	3min
15x	98°	20s
	67°	30s
	72°	6min

1x	72°	5min
1x	4°	hold

C.6 PCR Purification

— Clean Station ***NO PCR amplification products are allowed in PCR hood. All the following steps will be carried out in the clean station.***

1| Equilibrate Ampure XP beads at RT for at least 30min minimize the binding of pollens to beads.

2| Spin down amplified products at 2,000g for 2min at room temperature before opening the seal.

3| Add 15μl of Ampure XP beads (**0.6:1 ratio**) to amplification product, and pipet up and down ten times.

4| Incubate the mixture at room temperature for 5min.

5| Place the plate on magnetic stand for 5min, and carefully remove the clear supernatant.

6| Wash with 200μl of 80% (vol) ethanol solution twice, and pipet out the left ethanol. (ALWAYS make fresh 80% ethanol.)

7| Let the beads dry at room temperature for 5min or until some cracks are seen.

8| Add 17.5μl of EB buffer, and mix ten times to resuspend the beads.

9| Incubate the plate off the magnet for 5min.

10| Place the plate on the magnet for 2min.

11| Collect 15μl of supernatant to a new PCR plate without disturbing the beads. Store cDNA at –80° or –20°.

12| Check the fragment size >500bp with a peak at 1.5-2kb by TapeStation 5000, and quantify by Qubit.

C.7 cDNA Tagmentation

1| Thaw ATM (Amplicon Tagment Mix), TD (Tagment DNA Buffer), and cDNA on ice, and keep NT (Neutralize Tagment Buffer) at room temperature.

2| Dilute cDNA to 0.2ng/μl in water, and add 5μl to each well of 96-well plate (**1ng total input**).

3| Add 10μl TD to each well.

4| Add 5μl ATM to each well, and pipette up and down five times to mix.

5| Seal with microseal B, and spin down the mixture at 2,000g for 2min.

6| Incubate at 55° for 5min, hold at 10°, and immediately proceed to neutralization step. – Total volume: 20μl. **PROGRAM: bplib1**

7| Spin down at 2,000g for 2min at room temperature before opening the seal.

8| Add 5μl NT to the bottom of each well, and pipette up and down five times to mix.

9| Incubate at room temperature for 5min. – Total volume: 25μl.

C.8 Library Amplification

1| Thaw NPM (Nextera PCR Master Mix), and i7/i5 Index primers on ice.

2| Add 15μl NPM to each well.

3| Add 5μl i5 primers to each well.

4| Add 5μl i7 primers to each well.

5| Pipette up and down five times to mix. – Total volume: 50μl.

6| Seal with microseal A, and spin down the mixture at 2,000g for 2min.

7| Perform amplification PCR as below: **PROGRAM: bplib2**

1x	72°	3min
1x	95°	30s
12x	95°	10s
	55°	30s
	72°	30s
1x	72°	5min
1x	10°	hold.

C.9 PCR Purification

1| Equilibrate Ampure XP beads at RT for at least 30min.

2| Spin down amplified product at 2,000g for 2min at room temperature before opening the seal.

3| Add 40μl of Ampure XP beads (**0.8:1 ratio**) to amplification product, and pipet up and down ten times.

4| Incubate the mixture at RT for 5min.

5| Place the plate on magnetic stand for 5min, and carefully remove the clear supernatant.

6| Wash with 200μl of 80% (vol) ethanol solution twice, and pipet out the left ethanol.

7| Let the beads dry at RT for 5min.

8| Add 30μl of EB buffer, and mix ten times to resuspend the beads.

9| Incubate the plate off the magnet for 5min.

10| Place the plate on the magnet for 2min.

11| Collect supernatant to a new PCR plate without disturbing the beads. Store libraries at –80° or –20°.

C.10 Sample Pooling and Sequencing

1| Use KAPA library quantification kit to quantify library concentrations.

A small aliquot of libraries are **diluted 10,000** times (2μl of library products into 198μl H_2O sequentially twice) before setting up the qPCR rxns.

qPCR system: 10μl in total (recommend setting up duplicates)

6μl KAPA buffer + 4μl of diluted libraries/standards/H_2O

qPCR program: **PROGRAM: Vignali Lab quant template**

1x	95°	5min
35x	95°	30s
	60°	45s
1x	65°	melting

Standards Conc.: Std1 (20pM), Std2 (2pM), Std3 (0.2pM), Std4 (0.02pM), Std5 (0.002pM), Std6 (0.0002pM). Std DNAs are 452bp, and have Tm around 86°-87°.

Calculation for library Conc.: **y** x 10,000pM = **y** x 10nM. (**y** is the mean conc. on the qPCR analyzer)

Run the qPCR products on a 1.5% gel, and the size should be 300bp-800bp with a peak at 450bp. Library Tm is around 81°-82°.

2| Dilute libraries to **2nM** in 10mM Tris-HCl w/ 0.1% Tween-20 (pH 8.5).

3| Pool 10μl of each diluted library together.

4| Submit the pooled libraries to Genomic Cores for sequencing on Illumina NextSeq platform. ***Refer to Page 1-3 to input the i5/i7 sequences (S5xx/N7xx entry on sample sheet) on the sample submission form.***

5| Around 10 libraries will be sequenced on the NextSeq 500/550 High Output v2 kit (75 cycles), so one will get about 40M reads per library.

References

1. Eisenbarth, G.S. Type I diabetes mellitus. A chronic autoimmune disease. *The New England journal of medicine* **314**, 1360-1368 (1986).

2. Katsarou, A.*, et al.* Type 1 diabetes mellitus. *Nat Rev Dis Primers* **3**, 17016 (2017).

3. Herold, K.C., Vignali, D.A., Cooke, A. & Bluestone, J.A. Type 1 diabetes: translating mechanistic observations into effective clinical outcomes. *Nature reviews. Immunology* **13**, 243-256 (2013).

4. Pociot, F. & Lernmark, A. Genetic risk factors for type 1 diabetes. *Lancet* **387**, 2331-2339 (2016).

5. Rewers, M. & Ludvigsson, J. Environmental risk factors for type 1 diabetes. *Lancet* **387**, 2340-2348 (2016).

6. Vignali, D.A., Collison, L.W. & Workman, C.J. How regulatory T cells work. *Nature reviews. Immunology* **8**, 523-532 (2008).

7. Andre, I.*, et al.* Checkpoints in the progression of autoimmune disease: lessons from diabetes models. *Proceedings of the National Academy of Sciences of the United States of America* **93**, 2260-2263 (1996).

8. Gepts, W. Pathologic anatomy of the pancreas in juvenile diabetes mellitus. *Diabetes* **14**, 619-633 (1965).

9. American Diabetes, A. 2. Classification and Diagnosis of Diabetes. *Diabetes care* **40**, S11-S24 (2017).

10. Diaz-Valencia, P.A., Bougneres, P. & Valleron, A.J. Global epidemiology of type 1 diabetes in young adults and adults: a systematic review. *BMC Public Health* **15**, 255 (2015).

11. Rawshani, A.*, et al.* The incidence of diabetes among 0-34 year olds in Sweden: new data and better methods. *Diabetologia* **57**, 1375-1381 (2014).

12. Ziegler, A.G.*, et al.* Seroconversion to multiple islet autoantibodies and risk of progression to diabetes in children. *JAMA* **309**, 2473-2479 (2013).

13. Svensson, J., Carstensen, B., Mortensen, H.B., Borch-Johnsen, K. & Danish Study Group of Childhood, D. Early childhood risk factors associated with type 1 diabetes--is gender important? *Eur J Epidemiol* **20**, 429-434 (2005).

14. Dwyer, C.J., *et al.* Altered homeostasis and development of regulatory T cell subsets represent an IL-2R-dependent risk for diabetes in NOD mice. *Sci Signal* **10**(2017).

15. Darce, J., *et al.* An N-terminal mutation of the Foxp3 transcription factor alleviates arthritis but exacerbates diabetes. *Immunity* **36**, 731-741 (2012).

16. Bettini, M.L., *et al.* Loss of epigenetic modification driven by the Foxp3 transcription factor leads to regulatory T cell insufficiency. *Immunity* **36**, 717-730 (2012).

17. Tang, Q., *et al.* Central role of defective interleukin-2 production in the triggering of islet autoimmune destruction. *Immunity* **28**, 687-697 (2008).

18. Overacre-Delgoffe, A.E., *et al.* Interferon-gamma Drives Treg Fragility to Promote Anti-tumor Immunity. *Cell* **169**, 1130-1141 e1111 (2017).

19. Delgoffe, G.M., *et al.* Stability and function of regulatory T cells is maintained by a neuropilin-1-semaphorin-4a axis. *Nature* **501**, 252-256 (2013).

20. Hansen, W., *et al.* Neuropilin 1 deficiency on CD4+Foxp3+ regulatory T cells impairs mouse melanoma growth. *The Journal of experimental medicine* **209**, 2001-2016 (2012).

21. Pan, F., *et al.* Eos mediates Foxp3-dependent gene silencing in CD4+ regulatory T cells. *Science* **325**, 1142-1146 (2009).

22. Sharma, M.D., *et al.* An inherently bifunctional subset of Foxp3+ T helper cells is controlled by the transcription factor eos. *Immunity* **38**, 998-1012 (2013).

23. Nakayama, M., *et al.* Prime role for an insulin epitope in the development of type 1 diabetes in NOD mice. *Nature* **435**, 220-223 (2005).

24. Chentoufi, A.A. & Polychronakos, C. Insulin expression levels in the thymus modulate insulin-specific autoreactive T-cell tolerance: the mechanism by which the IDDM2 locus may predispose to diabetes. *Diabetes* **51**, 1383-1390 (2002).

25. Thebault-Baumont, K., *et al.* Acceleration of type 1 diabetes mellitus in proinsulin 2-deficient NOD mice. *The Journal of clinical investigation* **111**, 851-857 (2003).

26. Moriyama, H., *et al.* Evidence for a primary islet autoantigen (preproinsulin 1) for insulitis and diabetes in the nonobese diabetic mouse. *Proceedings of the National Academy of Sciences of the United States of America* **100**, 10376-10381 (2003).

27. Hu, C.Y., *et al.* Treatment with CD20-specific antibody prevents and reverses autoimmune diabetes in mice. *The Journal of clinical investigation* **117**, 3857-3867 (2007).

28. Pescovitz, M.D.*, et al.* Rituximab, B-lymphocyte depletion, and preservation of beta-cell function. *The New England journal of medicine* **361**, 2143-2152 (2009).

29. Wong, F.S.*, et al.* Investigation of the role of B-cells in type 1 diabetes in the NOD mouse. *Diabetes* **53**, 2581-2587 (2004).

30. Diana, J.*, et al.* Crosstalk between neutrophils, B-1a cells and plasmacytoid dendritic cells initiates autoimmune diabetes. *Nature medicine* **19**, 65-73 (2013).

31. Kawasaki, E. ZnT8 and type 1 diabetes. *Endocr J* **59**, 531-537 (2012).

32. Jun, H.S., Yoon, C.S., Zbytnuik, L., van Rooijen, N. & Yoon, J.W. The role of macrophages in T cell-mediated autoimmune diabetes in nonobese diabetic mice. *The Journal of experimental medicine* **189**, 347-358 (1999).

33. Carrero, J.A.*, et al.* Resident macrophages of pancreatic islets have a seminal role in the initiation of autoimmune diabetes of NOD mice. *Proceedings of the National Academy of Sciences of the United States of America* **114**, E10418-E10427 (2017).

34. Mohan, J.F.*, et al.* Unique autoreactive T cells recognize insulin peptides generated within the islets of Langerhans in autoimmune diabetes. *Nature immunology* **11**, 350-354 (2010).

35. Like, A.A. & Rossini, A.A. Streptozotocin-induced pancreatic insulitis: new model of diabetes mellitus. *Science* **193**, 415-417 (1976).

36. Like, A.A., Rossini, A.A., Guberski, D.L., Appel, M.C. & Williams, R.M. Spontaneous diabetes mellitus: reversal and prevention in the BB/W rat with antiserum to rat lymphocytes. *Science* **206**, 1421-1423 (1979).

37. Ohashi, P.S.*, et al.* Ablation of "tolerance" and induction of diabetes by virus infection in viral antigen transgenic mice. *Cell* **65**, 305-317 (1991).

38. Oldstone, M.B., Nerenberg, M., Southern, P., Price, J. & Lewicki, H. Virus infection triggers insulin-dependent diabetes mellitus in a transgenic model: role of anti-self (virus) immune response. *Cell* **65**, 319-331 (1991).

39. Makino, S.*, et al.* Breeding of a non-obese, diabetic strain of mice. *Jikken dobutsu. Experimental animals* **29**, 1-13 (1980).

40. Pearson, J.A., Wong, F.S. & Wen, L. The importance of the Non Obese Diabetic (NOD) mouse model in autoimmune diabetes. *Journal of autoimmunity* **66**, 76-88 (2016).

41. Markle, J.G.*, et al.* Sex differences in the gut microbiome drive hormone-dependent regulation of autoimmunity. *Science* **339**, 1084-1088 (2013).

42. Yurkovetskiy, L.*, et al.* Gender bias in autoimmunity is influenced by microbiota. *Immunity* **39**, 400-412 (2013).

43. Steward, C.A.*, et al.* The non-obese diabetic mouse sequence, annotation and variation resource: an aid for investigating type 1 diabetes. *Database : the journal of biological databases and curation* **2013**, bat032 (2013).

44. Barrett, J.C.*, et al.* Genome-wide association study and meta-analysis find that over 40 loci affect risk of type 1 diabetes. *Nature genetics* **41**, 703-707 (2009).

45. Onengut-Gumuscu, S.*, et al.* Fine mapping of type 1 diabetes susceptibility loci and evidence for colocalization of causal variants with lymphoid gene enhancers. *Nature genetics* **47**, 381-386 (2015).

46. Delong, T.*, et al.* Pathogenic CD4 T cells in type 1 diabetes recognize epitopes formed by peptide fusion. *Science* **351**, 711-714 (2016).

47. Reed, J.C. & Herold, K.C. Thinking bedside at the bench: the NOD mouse model of T1DM. *Nature reviews. Endocrinology* **11**, 308-314 (2015).

48. Willcox, A., Richardson, S.J., Bone, A.J., Foulis, A.K. & Morgan, N.G. Analysis of islet inflammation in human type 1 diabetes. *Clinical and experimental immunology* **155**, 173-181 (2009).

49. Schwartz, R.H. Acquisition of immunologic self-tolerance. *Cell* **57**, 1073-1081 (1989).

50. Goodnow, C.C., Sprent, J., Fazekas de St Groth, B. & Vinuesa, C.G. Cellular and genetic mechanisms of self tolerance and autoimmunity. *Nature* **435**, 590-597 (2005).

51. Sakaguchi, S., Yamaguchi, T., Nomura, T. & Ono, M. Regulatory T cells and immune tolerance. *Cell* **133**, 775-787 (2008).

52. Starr, T.K., Jameson, S.C. & Hogquist, K.A. Positive and negative selection of T cells. *Annual review of immunology* **21**, 139-176 (2003).

53. Klein, L., Kyewski, B., Allen, P.M. & Hogquist, K.A. Positive and negative selection of the T cell repertoire: what thymocytes see (and don't see). *Nature reviews. Immunology* **14**, 377-391 (2014).

54. McMahan, C.J. & Fink, P.J. RAG reexpression and DNA recombination at T cell receptor loci in peripheral CD4+ T cells. *Immunity* **9**, 637-647 (1998).

55. Schwartz, R.H. T cell anergy. *Annual review of immunology* **21**, 305-334 (2003).

56. Wherry, E.J. & Kurachi, M. Molecular and cellular insights into T cell exhaustion. *Nature reviews. Immunology* **15**, 486-499 (2015).

57. Gabrilovich, D.I. & Nagaraj, S. Myeloid-derived suppressor cells as regulators of the immune system. *Nature reviews. Immunology* **9**, 162-174 (2009).

58. Godfrey, D.I., Stankovic, S. & Baxter, A.G. Raising the NKT cell family. *Nature immunology* **11**, 197-206 (2010).

59. Peng, G.*, et al.* Tumor-infiltrating gammadelta T cells suppress T and dendritic cell function via mechanisms controlled by a unique toll-like receptor signaling pathway. *Immunity* **27**, 334-348 (2007).

60. Hepworth, M.R.*, et al.* Immune tolerance. Group 3 innate lymphoid cells mediate intestinal selection of commensal bacteria-specific CD4(+) T cells. *Science* **348**, 1031-1035 (2015).

61. Cheroutre, H., Lambolez, F. & Mucida, D. The light and dark sides of intestinal intraepithelial lymphocytes. *Nature reviews. Immunology* **11**, 445-456 (2011).

62. Yu, L.*, et al.* Early expression of antiinsulin autoantibodies of humans and the NOD mouse: evidence for early determination of subsequent diabetes. *Proceedings of the National Academy of Sciences of the United States of America* **97**, 1701-1706 (2000).

63. Krishnamurthy, B.*, et al.* Responses against islet antigens in NOD mice are prevented by tolerance to proinsulin but not IGRP. *The Journal of clinical investigation* **116**, 3258-3265 (2006).

64. von Herrath, M., Sanda, S. & Herold, K. Type 1 diabetes as a relapsing-remitting disease? *Nature reviews. Immunology* **7**, 988-994 (2007).

65. Han, S., Donelan, W., Wang, H., Reeves, W. & Yang, L.J. Novel autoantigens in type 1 diabetes. *Am J Transl Res* **5**, 379-392 (2013).

66. Mohan, J.F., Petzold, S.J. & Unanue, E.R. Register shifting of an insulin peptide-MHC complex allows diabetogenic T cells to escape thymic deletion. *The Journal of experimental medicine* **208**, 2375-2383 (2011).

67. Stadinski, B., Kappler, J. & Eisenbarth, G.S. Molecular targeting of islet autoantigens. *Immunity* **32**, 446-456 (2010).

68. Stadinski, B.D.*, et al.* Diabetogenic T cells recognize insulin bound to IAg7 in an unexpected, weakly binding register. *Proceedings of the National Academy of Sciences of the United States of America* **107**, 10978-10983 (2010).

69. Jiang, W., Anderson, M.S., Bronson, R., Mathis, D. & Benoist, C. Modifier loci condition autoimmunity provoked by Aire deficiency. *The Journal of experimental medicine* **202**, 805-815 (2005).

70. Zhang, Q. & Vignali, D.A. Co-stimulatory and Co-inhibitory Pathways in Autoimmunity. *Immunity* **44**, 1034-1051 (2016).

71. Mueller, D.L., Jenkins, M.K. & Schwartz, R.H. Clonal expansion versus functional clonal inactivation: a costimulatory signalling pathway determines the outcome of T cell antigen receptor occupancy. *Annual review of immunology* **7**, 445-480 (1989).

72. Lafferty, K.J. & Cunningham, A.J. A new analysis of allogeneic interactions. *The Australian journal of experimental biology and medical science* **53**, 27-42 (1975).

73. Bretscher, P. & Cohn, M. A theory of self-nonself discrimination. *Science* **169**, 1042-1049 (1970).

74. Salomon, B.*, et al.* B7/CD28 costimulation is essential for the homeostasis of the CD4+CD25+ immunoregulatory T cells that control autoimmune diabetes. *Immunity* **12**, 431-440 (2000).

75. Lenschow, D.J.*, et al.* Differential effects of anti-B7-1 and anti-B7-2 monoclonal antibody treatment on the development of diabetes in the nonobese diabetic mouse. *The Journal of experimental medicine* **181**, 1145-1155 (1995).

76. Bour-Jordan, H.*, et al.* Costimulation controls diabetes by altering the balance of pathogenic and regulatory T cells. *The Journal of clinical investigation* **114**, 979-987 (2004).

77. Butte, M.J., Keir, M.E., Phamduy, T.B., Sharpe, A.H. & Freeman, G.J. Programmed death-1 ligand 1 interacts specifically with the B7-1 costimulatory molecule to inhibit T cell responses. *Immunity* **27**, 111-122 (2007).

78. Paterson, A.M.*, et al.* The programmed death-1 ligand 1:B7-1 pathway restrains diabetogenic effector T cells in vivo. *Journal of immunology* **187**, 1097-1105 (2011).

79. Ansari, M.J.*, et al.* Role of ICOS pathway in autoimmune and alloimmune responses in NOD mice. *Clinical immunology* **126**, 140-147 (2008).

80. Hawiger, D.*, et al.* ICOS mediates the development of insulin-dependent diabetes mellitus in nonobese diabetic mice. *Journal of immunology* **180**, 3140-3147 (2008).

81. Herman, A.E., Freeman, G.J., Mathis, D. & Benoist, C. CD4+CD25+ T regulatory cells dependent on ICOS promote regulation of effector cells in the prediabetic lesion. *The Journal of experimental medicine* **199**, 1479-1489 (2004).

82. Kornete, M., Sgouroudis, E. & Piccirillo, C.A. ICOS-dependent homeostasis and function of Foxp3+ regulatory T cells in islets of nonobese diabetic mice. *Journal of immunology* **188**, 1064-1074 (2012).

83. Kornete, M.*, et al.* Th1-Like ICOS+ Foxp3+ Treg Cells Preferentially Express CXCR3 and Home to beta-Islets during Pre-Diabetes in BDC2.5 NOD Mice. *PloS one* **10**, e0126311 (2015).

84. Balasa, B.*, et al.* CD40 ligand-CD40 interactions are necessary for the initiation of insulitis and diabetes in nonobese diabetic mice. *Journal of immunology* **159**, 4620-4627 (1997).

85. Green, E.A., Wong, F.S., Eshima, K., Mora, C. & Flavell, R.A. Neonatal tumor necrosis factor alpha promotes diabetes in nonobese diabetic mice by CD154-independent antigen presentation to CD8(+) T cells. *The Journal of experimental medicine* **191**, 225-238 (2000).

86. Baker, R.L., Wagner, D.H., Jr. & Haskins, K. CD40 on NOD CD4 T cells contributes to their activation and pathogenicity. *Journal of autoimmunity* **31**, 385-392 (2008).

87. Pakala, S.V., Bansal-Pakala, P., Halteman, B.S. & Croft, M. Prevention of diabetes in NOD mice at a late stage by targeting OX40/OX40 ligand interactions. *European journal of immunology* **34**, 3039-3046 (2004).

88. Martin-Orozco, N.*, et al.* Paradoxical dampening of anti-islet self-reactivity but promotion of diabetes by OX40 ligand. *Journal of immunology* **171**, 6954-6960 (2003).

89. Irie, J., Wu, Y., Kachapati, K., Mittler, R.S. & Ridgway, W.M. Modulating protective and pathogenic CD4+ subsets via CD137 in type 1 diabetes. *Diabetes* **56**, 186-196 (2007).

90. Sytwu, H.K.*, et al.* Anti-4-1BB-based immunotherapy for autoimmune diabetes: lessons from a transgenic non-obese diabetic (NOD) model. *Journal of autoimmunity* **21**, 247-254 (2003).

91. Kachapati, K.*, et al.* Recombinant soluble CD137 prevents type one diabetes in nonobese diabetic mice. *Journal of autoimmunity* **47**, 94-103 (2013).

92. Wicker, L.S.*, et al.* Fine mapping, gene content, comparative sequencing, and expression analyses support Ctla4 and Nramp1 as candidates for Idd5.1 and Idd5.2 in the nonobese diabetic mouse. *Journal of immunology* **173**, 164-173 (2004).

93. Saverino, D., Simone, R., Bagnasco, M. & Pesce, G. The soluble CTLA-4 receptor and its role in autoimmune diseases: an update. *Auto- immunity highlights* **1**, 73-81 (2010).

94. Ueda, H.*, et al.* Association of the T-cell regulatory gene CTLA4 with susceptibility to autoimmune disease. *Nature* **423**, 506-511 (2003).

95. Vijayakrishnan, L.*, et al.* An autoimmune disease-associated CTLA-4 splice variant lacking the B7 binding domain signals negatively in T cells. *Immunity* **20**, 563-575 (2004).

96. Stumpf, M., Zhou, X. & Bluestone, J.A. The B7-independent isoform of CTLA-4 functions to regulate autoimmune diabetes. *Journal of immunology* **190**, 961-969 (2013).

97. Araki, M.*, et al.* Genetic evidence that the differential expression of the ligand-independent isoform of CTLA-4 is the molecular basis of the Idd5.1 type 1 diabetes region in nonobese diabetic mice. *Journal of immunology* **183**, 5146-5157 (2009).

98. Luhder, F., Chambers, C., Allison, J.P., Benoist, C. & Mathis, D. Pinpointing when T cell costimulatory receptor CTLA-4 must be engaged to dampen diabetogenic T cells. *Proceedings of the National Academy of Sciences of the United States of America* **97**, 12204-12209 (2000).

99. Luhder, F., Hoglund, P., Allison, J.P., Benoist, C. & Mathis, D. Cytotoxic T lymphocyte-associated antigen 4 (CTLA-4) regulates the unfolding of autoimmune diabetes. *The Journal of experimental medicine* **187**, 427-432 (1998).

100. Fife, B.T., Griffin, M.D., Abbas, A.K., Locksley, R.M. & Bluestone, J.A. Inhibition of T cell activation and autoimmune diabetes using a B cell surface-linked CTLA-4 agonist. *The Journal of clinical investigation* **116**, 2252-2261 (2006).

101. Dahlen, E., Hedlund, G. & Dawe, K. Low CD86 expression in the nonobese diabetic mouse results in the impairment of both T cell activation and CTLA-4 up-regulation. *Journal of immunology* **164**, 2444-2456 (2000).

102. Okazaki, T. & Honjo, T. PD-1 and PD-1 ligands: from discovery to clinical application. *International immunology* **19**, 813-824 (2007).

103. Wang, J.*, et al.* Establishment of NOD-Pdcd1-/- mice as an efficient animal model of type I diabetes. *Proceedings of the National Academy of Sciences of the United States of America* **102**, 11823-11828 (2005).

104. Ansari, M.J.*, et al.* The programmed death-1 (PD-1) pathway regulates autoimmune diabetes in nonobese diabetic (NOD) mice. *The Journal of experimental medicine* **198**, 63-69 (2003).

105. Fife, B.T.*, et al.* Interactions between PD-1 and PD-L1 promote tolerance by blocking the TCR-induced stop signal. *Nature immunology* **10**, 1185-1192 (2009).

106. Liang, S.C.*, et al.* Regulation of PD-1, PD-L1, and PD-L2 expression during normal and autoimmune responses. *European journal of immunology* **33**, 2706-2716 (2003).

107. Wang, C.J.*, et al.* Protective role of programmed death 1 ligand 1 (PD-L1)in nonobese diabetic mice: the paradox in transgenic models. *Diabetes* **57**, 1861-1869 (2008).

108. Subudhi, S.K.*, et al.* Local expression of B7-H1 promotes organ-specific autoimmunity and transplant rejection. *The Journal of clinical investigation* **113**, 694-700 (2004).

109. Zucchelli, S.*, et al.* Defective central tolerance induction in NOD mice: genomics and genetics. *Immunity* **22**, 385-396 (2005).

110. Sanchez-Fueyo, A.*, et al.* Tim-3 inhibits T helper type 1-mediated auto- and alloimmune responses and promotes immunological tolerance. *Nature immunology* **4**, 1093-1101 (2003).

111. Wang, X.*, et al.* Early treatment of NOD mice with B7-H4 reduces the incidence of autoimmune diabetes. *Diabetes* **60**, 3246-3255 (2011).

112. Bettini, M.*, et al.* Cutting edge: accelerated autoimmune diabetes in the absence of LAG-3. *Journal of immunology* **187**, 3493-3498 (2011).

113. Okazaki, T.*, et al.* PD-1 and LAG-3 inhibitory co-receptors act synergistically to prevent autoimmunity in mice. *The Journal of experimental medicine* **208**, 395-407 (2011).

114. Sakaguchi, S., Takahashi, T. & Nishizuka, Y. Study on cellular events in post-thymectomy autoimmune oophoritis in mice. II. Requirement of Lyt-1 cells in normal female mice for the prevention of oophoritis. *The Journal of experimental medicine* **156**, 1577-1586 (1982).

115. Sakaguchi, S., Fukuma, K., Kuribayashi, K. & Masuda, T. Organ-specific autoimmune diseases induced in mice by elimination of T cell subset. I. Evidence for the active participation of T cells in natural self-tolerance; deficit of a T cell subset as a possible cause of autoimmune disease. *The Journal of experimental medicine* **161**, 72-87 (1985).

116. Abbas, A.K.*, et al.* Regulatory T cells: recommendations to simplify the nomenclature. *Nature immunology* **14**, 307-308 (2013).

117. Sakaguchi, S., Sakaguchi, N., Asano, M., Itoh, M. & Toda, M. Immunologic self-tolerance maintained by activated T cells expressing IL-2 receptor alpha-chains (CD25). Breakdown of a single mechanism of self-tolerance causes various autoimmune diseases. *Journal of immunology* **155**, 1151-1164 (1995).

118. Yadav, M.*, et al.* Neuropilin-1 distinguishes natural and inducible regulatory T cells among regulatory T cell subsets in vivo. *The Journal of experimental medicine* **209**, 1713-1722, S1711-1719 (2012).

119. Weiss, J.M.*, et al.* Neuropilin 1 is expressed on thymus-derived natural regulatory T cells, but not mucosa-generated induced Foxp3+ T reg cells. *The Journal of experimental medicine* **209**, 1723-1742, S1721 (2012).

120. Fontenot, J.D., Rasmussen, J.P., Gavin, M.A. & Rudensky, A.Y. A function for interleukin 2 in Foxp3-expressing regulatory T cells. *Nature immunology* **6**, 1142-1151 (2005).

121. Chinen, T.*, et al.* An essential role for the IL-2 receptor in Treg cell function. *Nature immunology* **17**, 1322-1333 (2016).

122. Hori, S., Nomura, T. & Sakaguchi, S. Control of regulatory T cell development by the transcription factor Foxp3. *Science* **299**, 1057-1061 (2003).

123. Fontenot, J.D., Gavin, M.A. & Rudensky, A.Y. Foxp3 programs the development and function of CD4+CD25+ regulatory T cells. *Nature immunology* **4**, 330-336 (2003).

124. Brunkow, M.E.*, et al.* Disruption of a new forkhead/winged-helix protein, scurfin, results in the fatal lymphoproliferative disorder of the scurfy mouse. *Nature genetics* **27**, 68-73 (2001).

125. Khattri, R., Cox, T., Yasayko, S.A. & Ramsdell, F. An essential role for Scurfin in CD4+CD25+ T regulatory cells. *Nature immunology* **4**, 337-342 (2003).

126. Mucida, D.*, et al.* Reciprocal TH17 and regulatory T cell differentiation mediated by retinoic acid. *Science* **317**, 256-260 (2007).

127. Sujino, T.*, et al.* Tissue adaptation of regulatory and intraepithelial CD4(+) T cells controls gut inflammation. *Science* **352**, 1581-1586 (2016).

128. Sefik, E.*, et al.* MUCOSAL IMMUNOLOGY. Individual intestinal symbionts induce a distinct population of RORgamma(+) regulatory T cells. *Science* **349**, 993-997 (2015).

129. Chen, Y., Kuchroo, V.K., Inobe, J., Hafler, D.A. & Weiner, H.L. Regulatory T cell clones induced by oral tolerance: suppression of autoimmune encephalomyelitis. *Science* **265**, 1237-1240 (1994).

130. Collison, L.W.*, et al.* IL-35-mediated induction of a potent regulatory T cell population. *Nature immunology* **11**, 1093-1101 (2010).

131. Rubtsov, Y.P.*, et al.* Regulatory T cell-derived interleukin-10 limits inflammation at environmental interfaces. *Immunity* **28**, 546-558 (2008).

132. Asseman, C., Mauze, S., Leach, M.W., Coffman, R.L. & Powrie, F. An essential role for interleukin 10 in the function of regulatory T cells that inhibit intestinal inflammation. *The Journal of experimental medicine* **190**, 995-1004 (1999).

133. Nakamura, K., Kitani, A. & Strober, W. Cell contact-dependent immunosuppression by CD4(+)CD25(+) regulatory T cells is mediated by cell surface-bound transforming growth factor beta. *The Journal of experimental medicine* **194**, 629-644 (2001).

134. Collison, L.W.*, et al.* The inhibitory cytokine IL-35 contributes to regulatory T-cell function. *Nature* **450**, 566-569 (2007).

135. Gondek, D.C., Lu, L.F., Quezada, S.A., Sakaguchi, S. & Noelle, R.J. Cutting edge: contact-mediated suppression by CD4+CD25+ regulatory cells involves a granzyme B-dependent, perforin-independent mechanism. *Journal of immunology* **174**, 1783-1786 (2005).

136. Cao, X.*, et al.* Granzyme B and perforin are important for regulatory T cell-mediated suppression of tumor clearance. *Immunity* **27**, 635-646 (2007).

137. Ren, X.*, et al.* Involvement of cellular death in TRAIL/DR5-dependent suppression induced by CD4(+)CD25(+) regulatory T cells. *Cell Death Differ* **14**, 2076-2084 (2007).

138. Pillai, M.R.*, et al.* The plasticity of regulatory T cell function. *Journal of immunology* **187**, 4987-4997 (2011).

139. Bopp, T.*, et al.* Cyclic adenosine monophosphate is a key component of regulatory T cell-mediated suppression. *The Journal of experimental medicine* **204**, 1303-1310 (2007).

140. Pandiyan, P., Zheng, L., Ishihara, S., Reed, J. & Lenardo, M.J. CD4+CD25+Foxp3+ regulatory T cells induce cytokine deprivation-mediated apoptosis of effector CD4+ T cells. *Nature immunology* **8**, 1353-1362 (2007).

141. Deaglio, S.*, et al.* Adenosine generation catalyzed by CD39 and CD73 expressed on regulatory T cells mediates immune suppression. *The Journal of experimental medicine* **204**, 1257-1265 (2007).

142. Tang, Q.*, et al.* Visualizing regulatory T cell control of autoimmune responses in nonobese diabetic mice. *Nature immunology* **7**, 83-92 (2006).

143. Tadokoro, C.E.*, et al.* Regulatory T cells inhibit stable contacts between CD4+ T cells and dendritic cells in vivo. *The Journal of experimental medicine* **203**, 505-511 (2006).

144. Matheu, M.P.*, et al.* Imaging regulatory T cell dynamics and CTLA4-mediated suppression of T cell priming. *Nat Commun* **6**, 6219 (2015).

145. Fallarino, F.*, et al.* Modulation of tryptophan catabolism by regulatory T cells. *Nature immunology* **4**, 1206-1212 (2003).

146. Liang, B.*, et al.* Regulatory T cells inhibit dendritic cells by lymphocyte activation gene-3 engagement of MHC class II. *Journal of immunology* **180**, 5916-5926 (2008).

147. Kim, J.M., Rasmussen, J.P. & Rudensky, A.Y. Regulatory T cells prevent catastrophic autoimmunity throughout the lifespan of mice. *Nature immunology* **8**, 191-197 (2007).

148. Ziegler, S.F. FOXP3: of mice and men. *Annual review of immunology* **24**, 209-226 (2006).

149. Wildin, R.S.*, et al.* X-linked neonatal diabetes mellitus, enteropathy and endocrinopathy syndrome is the human equivalent of mouse scurfy. *Nature genetics* **27**, 18-20 (2001).

150. Bennett, C.L.*, et al.* The immune dysregulation, polyendocrinopathy, enteropathy, X-linked syndrome (IPEX) is caused by mutations of FOXP3. *Nature genetics* **27**, 20-21 (2001).

151. Allan, S.E.*, et al.* Activation-induced FOXP3 in human T effector cells does not suppress proliferation or cytokine production. *International immunology* **19**, 345-354 (2007).

152. Tran, D.Q., Ramsey, H. & Shevach, E.M. Induction of FOXP3 expression in naive human CD4+FOXP3 T cells by T-cell receptor stimulation is transforming growth factor-beta dependent but does not confer a regulatory phenotype. *Blood* **110**, 2983-2990 (2007).

153. Lu, L., Barbi, J. & Pan, F. The regulation of immune tolerance by FOXP3. *Nature reviews. Immunology* **17**, 703-717 (2017).

154. Rudra, D.*, et al.* Transcription factor Foxp3 and its protein partners form a complex regulatory network. *Nature immunology* **13**, 1010-1019 (2012).

155. Hori, S. The Foxp3 interactome: a network perspective of T(reg) cells. *Nature immunology* **13**, 943-945 (2012).

156. Kwon, H.K., Chen, H.M., Mathis, D. & Benoist, C. Different molecular complexes that mediate transcriptional induction and repression by FoxP3. *Nature immunology* **18**, 1238-1248 (2017).

157. Fu, W.*, et al.* A multiply redundant genetic switch 'locks in' the transcriptional signature of regulatory T cells. *Nature immunology* **13**, 972-980 (2012).

158. Zheng, Y.*, et al.* Role of conserved non-coding DNA elements in the Foxp3 gene in regulatory T-cell fate. *Nature* **463**, 808-812 (2010).

159. Feng, Y.*, et al.* Control of the inheritance of regulatory T cell identity by a cis element in the Foxp3 locus. *Cell* **158**, 749-763 (2014).

160. Feng, Y.*, et al.* A mechanism for expansion of regulatory T-cell repertoire and its role in self-tolerance. *Nature* **528**, 132-136 (2015).

161. Arpaia, N.*, et al.* Metabolites produced by commensal bacteria promote peripheral regulatory T-cell generation. *Nature* **504**, 451-455 (2013).

162. Smith, P.M.*, et al.* The microbial metabolites, short-chain fatty acids, regulate colonic Treg cell homeostasis. *Science* **341**, 569-573 (2013).

163. Marino, E.*, et al.* Gut microbial metabolites limit the frequency of autoimmune T cells and protect against type 1 diabetes. *Nature immunology* **18**, 552-562 (2017).

164. Chen, Z., Herman, A.E., Matos, M., Mathis, D. & Benoist, C. Where CD4+CD25+ T reg cells impinge on autoimmune diabetes. *The Journal of experimental medicine* **202**, 1387-1397 (2005).

165. Feuerer, M., Shen, Y., Littman, D.R., Benoist, C. & Mathis, D. How punctual ablation of regulatory T cells unleashes an autoimmune lesion within the pancreatic islets. *Immunity* **31**, 654-664 (2009).

166. Tarbell, K.V., Yamazaki, S., Olson, K., Toy, P. & Steinman, R.M. CD25+ CD4+ T cells, expanded with dendritic cells presenting a single autoantigenic peptide, suppress autoimmune diabetes. *The Journal of experimental medicine* **199**, 1467-1477 (2004).

167. Tarbell, K.V.*, et al.* Dendritic cell-expanded, islet-specific CD4+ CD25+ CD62L+ regulatory T cells restore normoglycemia in diabetic NOD mice. *The Journal of experimental medicine* **204**, 191-201 (2007).

168. Tang, Q.*, et al.* In vitro-expanded antigen-specific regulatory T cells suppress autoimmune diabetes. *The Journal of experimental medicine* **199**, 1455-1465 (2004).

169. Bluestone, J.A.*, et al.* Type 1 diabetes immunotherapy using polyclonal regulatory T cells. *Science translational medicine* **7**, 315ra189 (2015).

170. Zhou, X.*, et al.* Instability of the transcription factor Foxp3 leads to the generation of pathogenic memory T cells in vivo. *Nature immunology* **10**, 1000-1007 (2009).

171. Lenschow, D.J.*, et al.* CD28/B7 regulation of Th1 and Th2 subsets in the development of autoimmune diabetes. *Immunity* **5**, 285-293 (1996).

172. Triebel, F.*, et al.* LAG-3, a novel lymphocyte activation gene closely related to CD4. *The Journal of experimental medicine* **171**, 1393-1405 (1990).

173. Huard, B.*, et al.* Characterization of the major histocompatibility complex class II binding site on LAG-3 protein. *Proceedings of the National Academy of Sciences of the United States of America* **94**, 5744-5749 (1997).

174. Huard, B., Prigent, P., Tournier, M., Bruniquel, D. & Triebel, F. CD4/major histocompatibility complex class II interaction analyzed with CD4- and lymphocyte activation gene-3 (LAG-3)-Ig fusion proteins. *European journal of immunology* **25**, 2718-2721 (1995).

175. Baixeras, E.*, et al.* Characterization of the lymphocyte activation gene 3-encoded protein. A new ligand for human leukocyte antigen class II antigens. *The Journal of experimental medicine* **176**, 327-337 (1992).

176. Andrews, L.P., Marciscano, A.E., Drake, C.G. & Vignali, D.A. LAG3 (CD223) as a cancer immunotherapy target. *Immunological reviews* **276**, 80-96 (2017).

177. Li, N.*, et al.* Metalloproteases regulate T-cell proliferation and effector function via LAG-3. *The EMBO journal* **26**, 494-504 (2007).

178. Mastrangeli, R., Micangeli, E. & Donini, S. Cloning of murine LAG-3 by magnetic bead bound homologous probes and PCR (gene-capture PCR). *Anal Biochem* **241**, 93-102 (1996).

179. Chemnitz, J.M., Parry, R.V., Nichols, K.E., June, C.H. & Riley, J.L. SHP-1 and SHP-2 associate with immunoreceptor tyrosine-based switch motif of programmed death 1 upon primary human T cell stimulation, but only receptor ligation prevents T cell activation. *Journal of immunology* **173**, 945-954 (2004).

180. Xu, F.*, et al.* LSECtin expressed on melanoma cells promotes tumor progression by inhibiting antitumor T-cell responses. *Cancer research* **74**, 3418-3428 (2014).

181. Kouo, T.*, et al.* Galectin-3 Shapes Antitumor Immune Responses by Suppressing CD8+ T Cells via LAG-3 and Inhibiting Expansion of Plasmacytoid Dendritic Cells. *Cancer Immunol Res* **3**, 412-423 (2015).

182. Mao, X.*, et al.* Pathological alpha-synuclein transmission initiated by binding lymphocyte-activation gene 3. *Science* **353**(2016).

183. Workman, C.J., Dugger, K.J. & Vignali, D.A. Cutting edge: molecular analysis of the negative regulatory function of lymphocyte activation gene-3. *Journal of immunology* **169**, 5392-5395 (2002).

184. Iouzalen, N., Andreae, S., Hannier, S. & Triebel, F. LAP, a lymphocyte activation gene-3 (LAG-3)-associated protein that binds to a repeated EP motif in the intracellular region of LAG-3, may participate in the down-regulation of the CD3/TCR activation pathway. *European journal of immunology* **31**, 2885-2891 (2001).

185. Workman, C.J., Rice, D.S., Dugger, K.J., Kurschner, C. & Vignali, D.A. Phenotypic analysis of the murine CD4-related glycoprotein, CD223 (LAG-3). *European journal of immunology* **32**, 2255-2263 (2002).

186. Huang, C.T.*, et al.* Role of LAG-3 in regulatory T cells. *Immunity* **21**, 503-513 (2004).

187. Gagliani, N.*, et al.* Coexpression of CD49b and LAG-3 identifies human and mouse T regulatory type 1 cells. *Nature medicine* **19**, 739-746 (2013).

188. Workman, C.J. & Vignali, D.A. Negative regulation of T cell homeostasis by lymphocyte activation gene-3 (CD223). *Journal of immunology* **174**, 688-695 (2005).

189. Workman, C.J.*, et al.* LAG-3 regulates plasmacytoid dendritic cell homeostasis. *Journal of immunology* **182**, 1885-1891 (2009).

190. Li, N., Workman, C.J., Martin, S.M. & Vignali, D.A. Biochemical analysis of the regulatory T cell protein lymphocyte activation gene-3 (LAG-3; CD223). *Journal of immunology* **173**, 6806-6812 (2004).

191. Lienhardt, C.*, et al.* Active tuberculosis in Africa is associated with reduced Th1 and increased Th2 activity in vivo. *European journal of immunology* **32**, 1605-1613 (2002).

192. Delmastro, M.M.*, et al.* Modulation of redox balance leaves murine diabetogenic TH1 T cells "LAG-3-ing" behind. *Diabetes* **61**, 1760-1768 (2012).

193. Triebel, F., Hacene, K. & Pichon, M.F. A soluble lymphocyte activation gene-3 (sLAG-3) protein as a prognostic factor in human breast cancer expressing estrogen or progesterone receptors. *Cancer Lett* **235**, 147-153 (2006).

194. Buisson, S. & Triebel, F. LAG-3 (CD223) reduces macrophage and dendritic cell differentiation from monocyte precursors. *Immunology* **114**, 369-374 (2005).

195. Andreae, S., Piras, F., Burdin, N. & Triebel, F. Maturation and activation of dendritic cells induced by lymphocyte activation gene-3 (CD223). *Journal of immunology* **168**, 3874-3880 (2002).

196. Avice, M.N., Sarfati, M., Triebel, F., Delespesse, G. & Demeure, C.E. Lymphocyte activation gene-3, a MHC class II ligand expressed on activated T cells, stimulates TNF-alpha and IL-12 production by monocytes and dendritic cells. *Journal of immunology* **162**, 2748-2753 (1999).

197. Buisson, S. & Triebel, F. MHC class II engagement by its ligand LAG-3 (CD223) leads to a distinct pattern of chemokine and chemokine receptor expression by human dendritic cells. *Vaccine* **21**, 862-868 (2003).

198. Bae, J., Lee, S.J., Park, C.G., Lee, Y.S. & Chun, T. Trafficking of LAG-3 to the surface on activated T cells via its cytoplasmic domain and protein kinase C signaling. *Journal of immunology* **193**, 3101-3112 (2014).

199. Woo, S.R.*, et al.* Differential subcellular localization of the regulatory T-cell protein LAG-3 and the coreceptor CD4. *European journal of immunology* **40**, 1768-1777 (2010).

200. Blackburn, S.D.*, et al.* Coregulation of CD8+ T cell exhaustion by multiple inhibitory receptors during chronic viral infection. *Nature immunology* **10**, 29-37 (2009).

201. Richter, K., Agnellini, P. & Oxenius, A. On the role of the inhibitory receptor LAG-3 in acute and chronic LCMV infection. *International immunology* **22**, 13-23 (2010).

202. Butler, N.S.*, et al.* Therapeutic blockade of PD-L1 and LAG-3 rapidly clears established blood-stage Plasmodium infection. *Nature immunology* **13**, 188-195 (2011).

203. Woo, S.R.*, et al.* Immune inhibitory molecules LAG-3 and PD-1 synergistically regulate T-cell function to promote tumoral immune escape. *Cancer research* **72**, 917-927 (2012).

204. Matsuzaki, J.*, et al.* Tumor-infiltrating NY-ESO-1-specific CD8+ T cells are negatively regulated by LAG-3 and PD-1 in human ovarian cancer. *Proceedings of the National Academy of Sciences of the United States of America* **107**, 7875-7880 (2010).

205. Garber, K. Industry 'road tests' new wave of immune checkpoints. *Nature biotechnology* **35**, 487-488 (2017).

206. Camisaschi, C.*, et al.* LAG-3 expression defines a subset of CD4(+)CD25(high)Foxp3(+) regulatory T cells that are expanded at tumor sites. *Journal of immunology* **184**, 6545-6551 (2010).

207. Chen, J. & Chen, Z. The effect of immune microenvironment on the progression and prognosis of colorectal cancer. *Med Oncol* **31**, 82 (2014).

208. Grosso, J.F.*, et al.* LAG-3 regulates CD8+ T cell accumulation and effector function in murine self- and tumor-tolerance systems. *The Journal of clinical investigation* **117**, 3383-3392 (2007).

209. Workman, C.J.*, et al.* Lymphocyte activation gene-3 (CD223) regulates the size of the expanding T cell population following antigen activation in vivo. *Journal of immunology* **172**, 5450-5455 (2004).

210. Tivol, E.A.*, et al.* Loss of CTLA-4 leads to massive lymphoproliferation and fatal multiorgan tissue destruction, revealing a critical negative regulatory role of CTLA-4. *Immunity* **3**, 541-547 (1995).

211. Waterhouse, P.*, et al.* Lymphoproliferative disorders with early lethality in mice deficient in Ctla-4. *Science* **270**, 985-988 (1995).

212. Jha, V.*, et al.* Lymphocyte Activation Gene-3 (LAG-3) negatively regulates environmentally-induced autoimmunity. *PloS one* **9**, e104484 (2014).

213. Zhou, X.*, et al.* Selective miRNA disruption in T reg cells leads to uncontrolled autoimmunity. *The Journal of experimental medicine* **205**, 1983-1991 (2008).

214. Miyazaki, T., Dierich, A., Benoist, C. & Mathis, D. Independent modes of natural killing distinguished in mice lacking Lag3. *Science* **272**, 405-408 (1996).

215. Leiter, E.H. The NOD mouse: a model for insulin-dependent diabetes mellitus. *Current protocols in immunology / edited by John E. Coligan ... [et al.]* **Chapter 15**, Unit 15 19 (2001).

216. Lennon, G.P.*, et al.* T cell islet accumulation in type 1 diabetes is a tightly regulated, cell-autonomous event. *Immunity* **31**, 643-653 (2009).

217. McMurchy, A.N. & Levings, M.K. Suppression assays with human T regulatory cells: a technical guide. *European journal of immunology* **42**, 27-34 (2012).

218. Amir el, A.D.*, et al.* viSNE enables visualization of high dimensional single-cell data and reveals phenotypic heterogeneity of leukemia. *Nature biotechnology* **31**, 545-552 (2013).

219. Emerson, R.O.*, et al.* High-throughput sequencing of T-cell receptors reveals a homogeneous repertoire of tumour-infiltrating lymphocytes in ovarian cancer. *J Pathol* **231**, 433-440 (2013).

220. Picelli, S.*, et al.* Smart-seq2 for sensitive full-length transcriptome profiling in single cells. *Nature methods* **10**, 1096-1098 (2013).

221. Trapnell, C., Pachter, L. & Salzberg, S.L. TopHat: discovering splice junctions with RNA-Seq. *Bioinformatics* **25**, 1105-1111 (2009).

222. Trapnell, C.*, et al.* Transcript assembly and quantification by RNA-Seq reveals unannotated transcripts and isoform switching during cell differentiation. *Nature biotechnology* **28**, 511-515 (2010).

223. Love, M.I., Huber, W. & Anders, S. Moderated estimation of fold change and dispersion for RNA-seq data with DESeq2. *Genome biology* **15**, 550 (2014).

224. Hansen, K.D., Irizarry, R.A. & Wu, Z. Removing technical variability in RNA-seq data using conditional quantile normalization. *Biostatistics* **13**, 204-216 (2012).

225. Zhang, Q.*, et al.* LAG3 limits regulatory T cell proliferation and function in autoimmune diabetes. *Sci Immunol* **2**(2017).

226. Lee, P.P., *et al.* A critical role for Dnmt1 and DNA methylation in T cell development, function, and survival. *Immunity* **15**, 763-774 (2001).

227. Maekawa, Y., *et al.* Notch2 integrates signaling by the transcription factors RBP-J and CREB1 to promote T cell cytotoxicity. *Nature immunology* **9**, 1140-1147 (2008).

228. Long, S.A., *et al.* Partial exhaustion of CD8 T cells and clinical response to teplizumab in new-onset type 1 diabetes. *Sci Immunol* **1**(2016).

229. Marrack, P. & Kappler, J. Control of T cell viability. *Annual review of immunology* **22**, 765-787 (2004).

230. Trudeau, J.D., *et al.* Prediction of spontaneous autoimmune diabetes in NOD mice by quantification of autoreactive T cells in peripheral blood. *The Journal of clinical investigation* **111**, 217-223 (2003).

231. Zhang, N. & Bevan, M.J. CD8(+) T cells: foot soldiers of the immune system. *Immunity* **35**, 161-168 (2011).

232. Scholzen, T. & Gerdes, J. The Ki-67 protein: from the known and the unknown. *J Cell Physiol* **182**, 311-322 (2000).

233. Kaech, S.M. & Cui, W. Transcriptional control of effector and memory CD8+ T cell differentiation. *Nature reviews. Immunology* **12**, 749-761 (2012).

234. Lieberman, S.M., *et al.* Identification of the beta cell antigen targeted by a prevalent population of pathogenic CD8+ T cells in autoimmune diabetes. *Proceedings of the National Academy of Sciences of the United States of America* **100**, 8384-8388 (2003).

235. Prasad, S., Kohm, A.P., McMahon, J.S., Luo, X. & Miller, S.D. Pathogenesis of NOD diabetes is initiated by reactivity to the insulin B chain 9-23 epitope and involves functional epitope spreading. *Journal of autoimmunity* **39**, 347-353 (2012).

236. Amrani, A., *et al.* Progression of autoimmune diabetes driven by avidity maturation of a T-cell population. *Nature* **406**, 739-742 (2000).

237. Han, B., *et al.* Developmental control of CD8 T cell-avidity maturation in autoimmune diabetes. *The Journal of clinical investigation* **115**, 1879-1887 (2005).

238. Tai, N., *et al.* Microbial antigen mimics activate diabetogenic CD8 T cells in NOD mice. *The Journal of experimental medicine* **213**, 2129-2146 (2016).

239. Hebbandi Nanjundappa, R., *et al.* A Gut Microbial Mimic that Hijacks Diabetogenic Autoreactivity to Suppress Colitis. *Cell* **171**, 655-667 e617 (2017).

240. Martinuzzi, E.*, et al.* The frequency and immunodominance of islet-specific CD8+ T-cell responses change after type 1 diabetes diagnosis and treatment. *Diabetes* **57**, 1312-1320 (2008).

241. Coppieters, K.T.*, et al.* Demonstration of islet-autoreactive CD8 T cells in insulitic lesions from recent onset and long-term type 1 diabetes patients. *The Journal of experimental medicine* **209**, 51-60 (2012).

242. Jarchum, I., Nichol, L., Trucco, M., Santamaria, P. & DiLorenzo, T.P. Identification of novel IGRP epitopes targeted in type 1 diabetes patients. *Clinical immunology* **127**, 359-365 (2008).

243. Haribhai, D.*, et al.* Regulatory T cells dynamically control the primary immune response to foreign antigen. *Journal of immunology* **178**, 2961-2972 (2007).

244. Tauro, S., Nguyen, P., Li, B. & Geiger, T.L. Diversification and senescence of Foxp3+ regulatory T cells during experimental autoimmune encephalomyelitis. *European journal of immunology* **43**, 1195-1207 (2013).

245. Ohkura, N.*, et al.* T cell receptor stimulation-induced epigenetic changes and Foxp3 expression are independent and complementary events required for Treg cell development. *Immunity* **37**, 785-799 (2012).

246. D'Cruz, L.M. & Klein, L. Development and function of agonist-induced CD25+Foxp3+ regulatory T cells in the absence of interleukin 2 signaling. *Nature immunology* **6**, 1152-1159 (2005).

247. Gonzalez, A.*, et al.* Genetic control of diabetes progression. *Immunity* **7**, 873-883 (1997).

248. Johnson, M.C.*, et al.* beta-cell-specific IL-2 therapy increases islet Foxp3+Treg and suppresses type 1 diabetes in NOD mice. *Diabetes* **62**, 3775-3784 (2013).

249. Grinberg-Bleyer, Y.*, et al.* IL-2 reverses established type 1 diabetes in NOD mice by a local effect on pancreatic regulatory T cells. *The Journal of experimental medicine* **207**, 1871-1878 (2010).

250. Zhang, B., Chikuma, S., Hori, S., Fagarasan, S. & Honjo, T. Nonoverlapping roles of PD-1 and FoxP3 in maintaining immune tolerance in a novel autoimmune pancreatitis mouse model. *Proceedings of the National Academy of Sciences of the United States of America* **113**, 8490-8495 (2016).

251. Callahan, M.K., Postow, M.A. & Wolchok, J.D. Targeting T Cell Co-receptors for Cancer Therapy. *Immunity* **44**, 1069-1078 (2016).

252. Schildberg, F.A., Klein, S.R., Freeman, G.J. & Sharpe, A.H. Coinhibitory Pathways in the B7-CD28 Ligand-Receptor Family. *Immunity* **44**, 955-972 (2016).

253. Anderson, A.C., Joller, N. & Kuchroo, V.K. Lag-3, Tim-3, and TIGIT: Co-inhibitory Receptors with Specialized Functions in Immune Regulation. *Immunity* **44**, 989-1004 (2016).

254. Leach, D.R., Krummel, M.F. & Allison, J.P. Enhancement of antitumor immunity by CTLA-4 blockade. *Science* **271**, 1734-1736 (1996).

255. Levine, A.G.*, et al.* Suppression of lethal autoimmunity by regulatory T cells with a single TCR specificity. *The Journal of experimental medicine* **214**, 609-622 (2017).

256. Ferreira, C.*, et al.* Non-obese diabetic mice select a low-diversity repertoire of natural regulatory T cells. *Proceedings of the National Academy of Sciences of the United States of America* **106**, 8320-8325 (2009).

257. Tonkin, D.R., He, J., Barbour, G. & Haskins, K. Regulatory T cells prevent transfer of type 1 diabetes in NOD mice only when their antigen is present in vivo. *Journal of immunology* **181**, 4516-4522 (2008).

258. Moran, A.E. & Hogquist, K.A. T-cell receptor affinity in thymic development. *Immunology* **135**, 261-267 (2012).

259. Bettini, M.*, et al.* TCR affinity and tolerance mechanisms converge to shape T cell diabetogenic potential. *Journal of immunology* **193**, 571-579 (2014).

260. Sprouse, M.L.*, et al.* Cutting Edge: Low-Affinity TCRs Support Regulatory T Cell Function in Autoimmunity. *Journal of immunology* (2017).

261. Bouillet, P.*, et al.* BH3-only Bcl-2 family member Bim is required for apoptosis of autoreactive thymocytes. *Nature* **415**, 922-926 (2002).

262. Krishnamurthy, B.*, et al.* BIM Deficiency Protects NOD Mice From Diabetes by Diverting Thymocytes to Regulatory T Cells. *Diabetes* **64**, 3229-3238 (2015).

263. Feuerer, M.*, et al.* Enhanced thymic selection of FoxP3+ regulatory T cells in the NOD mouse model of autoimmune diabetes. *Proceedings of the National Academy of Sciences of the United States of America* **104**, 18181-18186 (2007).

264. Anderson, M.S.*, et al.* Projection of an immunological self shadow within the thymus by the aire protein. *Science* **298**, 1395-1401 (2002).

265. Ryan, G.A.*, et al.* B1 cells promote pancreas infiltration by autoreactive T cells. *Journal of immunology* **185**, 2800-2807 (2010).

266. Briet, C.*, et al.* The Spontaneous Autoimmune Neuromyopathy in ICOSL(-/-) NOD Mice Is CD4(+) T-Cell and Interferon-gamma Dependent. *Frontiers in immunology* **8**, 287 (2017).

267. Phillips, J.M., Haskins, K. & Cooke, A. MAdCAM-1 is needed for diabetes development mediated by the T cell clone, BDC-2.5. *Immunology* **116**, 525-531 (2005).

268. Hanninen, A., Salmi, M., Simell, O. & Jalkanen, S. Mucosa-associated (beta 7-integrinhigh) lymphocytes accumulate early in the pancreas of NOD mice and show aberrant recirculation behavior. *Diabetes* **45**, 1173-1180 (1996).

269. Marre, M.L. & Piganelli, J.D. Environmental Factors Contribute to beta Cell Endoplasmic Reticulum Stress and Neo-Antigen Formation in Type 1 Diabetes. *Front Endocrinol (Lausanne)* **8**, 262 (2017).

270. Katz, J.D., Wang, B., Haskins, K., Benoist, C. & Mathis, D. Following a diabetogenic T cell from genesis through pathogenesis. *Cell* **74**, 1089-1100 (1993).

271. Nie, H.*, et al.* Phosphorylation of FOXP3 controls regulatory T cell function and is inhibited by TNF-alpha in rheumatoid arthritis. *Nature medicine* **19**, 322-328 (2013).

272. Han, J.M., Patterson, S.J., Speck, M., Ehses, J.A. & Levings, M.K. Insulin inhibits IL-10-mediated regulatory T cell function: implications for obesity. *Journal of immunology* **192**, 623-629 (2014).

273. Lowther, D.E.*, et al.* PD-1 marks dysfunctional regulatory T cells in malignant gliomas. *JCI Insight* **1**(2016).

274. Rubtsov, Y.P.*, et al.* Stability of the regulatory T cell lineage in vivo. *Science* **329**, 1667-1671 (2010).